Finite Element Analysis of Damped Vibrations

of

Laminated Composite Plates

By

BAOGANG HU, M.Eng.

A Thesis
Submitted to the School of Graduate Studies
in Partial Fulfilment of the Requirements
for the Degree
Doctor of Philosophy

McMaster University

Damped Vibrations of Composite Plates

DOCTOR OF PHILOSOPHY (1992) McMASTER UNIVERSITY

(Mechanical Engineering) Hamilton, Ontario

TITLE: Finite Element Analysis of Damped Vibrations of Laminated Composite Plates

AUTHOR: Baogang Hu

M.Eng. (Beijing University of Science and Technology)

SUPERVISOR: Professor M.A. Dokainish

NUMBER OF PAGES: xix, 157, Ref. T-6, Ref. D-5

ABSTRACT

In this thesis, the damped free vibrations of composites are treated from the viewpoint of macromechanical analysis. Two damping models are developed, namely: the Viscoelastic Damping (**VED**) model and the Specific Damping Capacity (**SDC**) model. The important symmetry property of the damping matrix is retained in both models.

A Modified Modal Strain Energy method is proposed for the evaluation of modal damping in the VED model using a real, instead of a complex, eigenvalue problem solution. Numerical studies of multi degree-of-freedom systems are conducted to illustrate the better accuracy of the method compared to the Modal Strain Energy method.

The experimental data reported in the literature for damped free vibrations, in both polymer-matrix and metal-matrix composites, were used in the finite element analysis to test and compare the damping models. The natural frequencies and modal damping were obtained using both the VED and the SDC models. It was shown that the results from both models are in satisfactory agreement with the experimental data. Both models were found to be reasonably accurate for systems with low damping. Parametric studies were conducted to study the

effects on damping of the side-to-thickness ratio, the principal moduli ratio, the total number of layers, the ply-angle and boundary conditions.

ACKNOWLEDGMENTS

I would like to express my sincere thanks to my supervisor, Professor M.A. Dokainish, for his understanding and acceptation of my application to pursuing such an exciting research program, and for his continuous support, guidance and encouragement throughout the project.

I am grateful to Professor D.S. Weaver for his understanding and support of my transfer to this program.

Special thanks are due to Professor W.K. Tso, Professor M.A. ElBestawi, and Professor G.F. Round, the members of my Ph.D. supervisory committee, for their continuous interesting and helpful suggestions during the course of the study.

For their friendship and advice, I would like to thank my mechanical engineering colleagues and graduate students, with whom I have shared a pleasant experience. I would particularly like to thank Professor W. Roy C. Underhill, who showed a great interest in this work and provided useful suggestions. Thanks are also due to Mr. Bruce Tole, Dr. Sohail A. Umar-Khitab and Dr. Slavimor Krucinski for their assistance in computer simulation.

I am grateful to Dr. V.K. Kinra of Texas A & M

University, for his prompt provision of several valuable references for the calculation of metal-matrix composites.

I wish to thank Professor W.M. Mansour who made careful review and constructive criticisms for the manuscript of this thesis. I would also like to express my thanks to Mr. G. Harper for his kindly help in correcting the English of the manuscript of the thesis.

I acknowledge, with gratitude, the scholarship which I received from the Department of Mechanical Engineering of McMaster University.

I am indebted to my parents and grandparents, for their love and patience. It was my father who encouraged me to pursue professional studies. I would like to dedicate this thesis to my dear grandfather, who passed away during my writing of the thesis.

Finally, I would like to express my gratitude to my dear wife Wenzheng for her encouragement, help and patience, which were essential for the completion of this work.

TABLE OF CONTENT

Page

ABSTRACT.....iii

ACKNOWLEDGEMENTS.....iv

TABLE OF CONTENT.....vii

LIST OF FIGURES.....x

LIST OF TABLES.....xiii

LIST OF SYMBOLS.....xv

1. GENERAL INTRODUCTION.....1

1.1 Why study damped vibrations of composites?.....1

1.2 Methodology of approach.....3

1.3 Objectives of the thesis.....4

1.4 Thesis organization.. 5

2. LITERATURE REVIEWS.....7

2.1 Theories of laminated composite plates.....7

2.1.1 Introduction.....7

2.1.2 Kinematic modelling.....9

2.1.3 Macromechanical analysis.....25

2.2 Damped vibration analysis of layered fibre-reinforced composites.....32

Page

2.2.1 Introduction.....32
2.2.2 Material Damping.....33
2.2.3 The mathematical treatment of damping in macromechanical analysis.....40
2.2.4 Solutions of viscoelastically damped systems.....50

3. THEORETICAL FORMULATIONS.....56
3.1 Basic assumptions.....56
3.2 Theoretical foundation for undamped vibration analysis.....57
3.3 Modelling of damping for laminated composite plates.....66
3.3.1 Scope of the study.....66
3.3.2 Viscoelastic Damping (VED) model.....68
3.3.3 Specific Damping Capacity (SDC) model.....72
3.3.4 Comments on the modelling methods.....76

4. THE MODIFIED MODAL STRAIN ENERGY METHOD AND ITS APPLICATION TO VISCOELASTICALLY DAMPED SYSTEMS.....79
4.1 Statement of problem.....79
4.2 The Modified Modal Strain Energy method.....83
4.3 Proposed indices.....85

Page

4.3.1. Indices for classifying systems.....85
4.3.2. Overall Error Index.....89
4.4 Typical examples.....90
4.5 Comments.....105

5. NUMERICAL STUDIES.....107
5.1 Undamped free vibrations.....108
5.2 Damped free vibrations.....131
5.2.1 Application of damping models to polymer-matrix composites.....131
5.2.2 Application of damping models to metal-matrix composites.....136
5.2.3 Comments on selection of damping models...144
5.2.4 Parametric studies.....145

6. SUMMARY 152
6.1 Summary and conclusions.....152
6.2 Suggestions for future work.....156

REFERENCES (Theories of laminated plates).....Ref.T-1

REFERENCES (Damping of composites).....Ref.D-1

LIST OF FIGURES

Page

Figure 2.1 Some classes of composites.....8

Figure 2.2 Typical fibre-reinforced laminated composite.....8

Figure 2.3 Hysteresis loop.....35

Figure 2.4 Definition of energies.....43

Figure 2.5 Band-width of response curve.....43

Figure 2.6 Concept of complex modulus and loss angle....44

Figure 2.7 Decay of damped vibration system.....44

Figure 3.1 Laminated plate geometry and the coordinate system.....61

Figure 3.2 Input and output data of material damping study for laminated composites.....67

Figure 3.3 "η - ω_b/ω" and "ξ - ω_b/ω" curves.....71

Figure 4.1 Three-degree-of-freedom system.....92

Figure 4.2 Six-degree-of-freedom system.....92

Figure 4.3 "DLI - OEI(η)" curves.....102

Figure 5.1 Boundary conditions of plates.....109

Figure 5.2 Mode shapes of an isotropic plate, BC-S1....112

Figure 5.3 Mode shapes of an isotropic plate, BC-S2....113

Figure 5.4 Mode shapes of an orthotropic plate, BC-S1..114

Page

Figure 5.5 Mode shapes of an orthotropic plate, BC-S2..115

Figure 5.6 Mode shapes of a [0°/90°/90°/0°], BC-S1.....116

Figure 5.7 Mode shapes of a [0°/90°/90°/0°], BC-S2.....117

Figure 5.8 Mode shapes of a [0°/90°/0°/90°], BC-S1.....118

Figure 5.9 Mode shapes of a [0°/90°/0°/90°], BC-S2.....119

Figure 5.10 Mode shapes of a [45°/-45°/45°/-45°], BC-S1...120

Figure 5.11 Mode shapes of a [45°/-45°/45°/-45°], BC-S2...121

Figure 5.12 Mode shapes of an isotropic plate, BC-Clamped.....122

Figure 5.13 Mode shapes of an orthotropic plate, BC-clamped.....123

Figure 5.14 Mode shapes of a [0°/90°/90°/0°], BC-Clamped.....124

Figure 5.15 Mode shapes of a [0°/90°/0°/90°], BC-Clamped.....125

Figure 5.16 Mode shapes of a [45°/-45°/45°/-45°], BC-Clamped.....126

Figure 5.17 Contours of a 4-layer [θ/-θ], free-free rectangular plate of the first mode.....130

Figure 5.18 Modal damping of the first mode vs. the ply-angle for a cantilever beam.....142

Page

Figure 5.19 The fundamental frequency of the first mode vs. the ply-angle for a cantilever beam.....143

Figure 5.20 Nondimensional frequency of the first mode vs. the side-to-thickness ratio.....148

Figure 5.21 Damping of the first mode vs. the side-to-thickness ratio.....148

Figure 5.22 Nondimensional frequency of the first mode vs. the principal moduli ratio.....149

Figure 5.23 Damping of the first mode vs. the principal moduli ratio.....149

Figure 5.24 Nondimensional frequency of the first mode vs. the total number of layer.....150

Figure 5.25 Damping of the first mode vs. the total number of layer.....150

Figure 5.26 Nondimensional frequency of the first mode vs. the ply-angle.....151

Figure 5.27 Damping of the first mode vs. the ply-angle.....151

LIST OF TABLES

Page

Table 2.1 The differences of modelling approaches.....24

Table 3.1 Damping coefficients corresponding to elastic constants of lamina.....78

Table 4.1 Data of multi degree-of-freedom systems.....93

Table 4.2 Simulation results of Case 31.....94

Table 4.3 Comparison of Overall Error Index (Case 31).....96

Table 4.4 Comparison of Overall Error Index (Case 32).....97

Table 4.5 Comparison of Overall Error Index (Case 33).....98

Table 4.6 Comparison of Overall Error Index (Case 61).....99

Table 4.7 Comparison of Overall Error Index (Case 62).....100

Table 4.8 Comparison of Overall Error Index (Case 63).....101

Table 5.1 Dimensionless fundamental frequencies of a simply supported square plate, [45°/-45°/45°/-45°], BC-S1.....111

Page

Table 5.2 The data of polymer-based composite plates.....133

Table 5.3 Comparisons of natural frequencies and damping of an orthotropic $[0^\circ]_8$ square plate.....134

Table 5.4 Comparisons of natural frequencies and damping of a 8-layer $[0^\circ/90^\circ]_{2s}$ square plate.....135

Table 5.5 Comparisons of modal damping (ψ, %) of a $[\theta/-\theta/\theta/-\theta]$ rectangular (GFRP) plate at the first mode.....137

Table 5.6 Comparisons of modal damping (ψ, %) of a $[\theta/-\theta/\theta/-\theta]$ rectangular (CFRP) plate at the first mode.....138

Table 5.7 Comparisons of modal damping (ψ, %) of a $[\theta/-\theta]_s$ cantilever beam at the first mode.....141

List of Symbols

The following symbols represent the most commonly used notation in the thesis. Occasionally, the same symbol is used to denote another quantity. They are, however, properly identified when first introduced.

a	width of plate
a/h	side-to-thickness ratio
$[A]$	in-plane stiffness matrix
b	height of plate
B^*_{ijkl}	components of complex moduli tensor
$[B]$	coupled bending-stretching stiffness matrix
C_1-C_5	segments of boundary
C_{ijkl}	components of relaxation moduli tensor
DLI	Damping Level Index
$[D_b]$	bending stiffness matrix
$[D_s]$	shear stiffness matrix
E	complex modulus of elasticity
$\{E\}$	error vector
E_L, E_1	elastic modulus along the longitudinal direction
E_L/E_T	principal moduli ratio
$E^{(r)}$	error of modal parameter to the rth mode
E_T, E_2	elastic modulus along the transverse direction
f	fundamental frequency
$\{f\}$	load vector
$\{F(\omega)\}$	load vector in frequency domain
FSI	Frequency Separation Index
G_{LT}, G_{12}, G_{13}	shear modulus relative to L-T (1-2) plane
G_{TT}, G_{23}	shear modulus relative to T-Z (2-3) plane
h	thickness of plate or beam

$H(\omega)$	frequency response function
i	$= \sqrt{(-1)}$
I_1	normal inertia coefficient
I_2	coupled normal-rotary inertia coefficient
I_3	rotary inertia coefficient
j	integer, j=1,2,3,....
K	kinetic energies
K_i	shear correction coefficients
k_i	stiffness of the ith spring
$[K]$	stiffness matrix
$[K^*]$	complex stiffness matrix
$[K_D]$	damping stiffness matrix in the SDC model
$[K^e]$	element stiffness matrix
$[K_R]$	storage stiffness matrix
$[K_I]$	damping stiffness matrix in the VED model
l	beam length
l/h	length-to-thickness ratio
L	Lagrangian function
m	$= \cos\theta$
m_i	the ith mass
$[M]$	mass matrix
$\{M\}$	moment resultant vector
$\check{M}_n$, $\check{M}_t$	moment resultants normal and tangent to the boundary, respectively
n	$= \sin\theta$. Also the nodal number per element
N	total number of layers
$\{N\}$	in-plane resultant force vector
N_i	interpolation functions
$\check{N}_n$, $\check{N}_t$	in-plane resultants normal and tangent to the boundary, respectively
$[NP]$	nonproportional matrix
NPI	Non-Proportionality Index
OEI	Overall Error Index

$[Q]$	reduced stiffness matrix in the material axes (123)
$[\bar{Q}]$	reduced stiffness matrix in the global coordinate system (xyz)
$\{Q\}$	shear force resultant vector
$[Q_D]$	reduced damping stiffness matrix
$\breve{Q}_n$	shear force resultant on the boundary
$RE^{(r)}$	relative error to the rth modal parameter
t	time
T	temperature
u, v, w	displacement components in X, Y, and Z directions
u^o, v^o, w^o	displacement components of the middle plane
U	strain energy
ΔU	dissipated energy
$\{x\}, \{\ddot{x}\}$	vectors of nodal displacements, and accelerations,
$\{X(\omega)\}$	displacement vector in frequency domain
(xyz)	global Cartesian coordinate system
y	modal parameter
w	beam width
$W^{(r)}(y)$	the weight to the rth modal parameter
α, β	constants
$\gamma_{xy}, \gamma_{yz}, \gamma_{zx}$	shear strain components
γ^o_{xy}	shear strain components of the middle plane
δ	the first variational operator
$\varepsilon_x, \varepsilon_y$	strain (normal) components
$\varepsilon^o_x, \varepsilon^o_y$	strain (normal) components of the middle plane
η	loss factor
η_i	loss factor of the ith spring
η_L	damping loss along the longitudinal direction
η_T	damping loss along the transverse direction
η_{GLT}	shear damping loss relative to L-T (1-2) plane

$\eta_{G_{TT}}$	shear damping loss relative to T-Z (2-3) plane
$\eta_{\mu_{LT}}$	damping loss of Poisson's ratio
θ	angle between X axis and 1 axis
κ_x, κ_y	bending curvatures
κ_{xy}	twisting
λ	incremental factor
μ_{LT}, μ_{12}	major Poisson's ratio
Π	total potential energy
ρ	mass density
σ	stress tensor
σ_x, σ_y, σ_z	components of normal stress
τ_{xy}, τ_{yz}, τ_{zx}	components of shear stress
$\{\phi\}$	eigenvector for a real eigenvalue problem
$\{\phi^*\}$	complex eigenvector
ψ	specific damping capacity (SDC)
ψ_L	SDC along the longitudinal direction
ψ_T	SDC along the transverse direction
$\psi_{G_{LT}}$	SDC relative to L-T (1-2) plane
$\psi_{G_{TT}}$	SDC relative to T-Z (2-3) plane
$\psi_{\mu_{LT}}$	SDC of Poisson's ratio
ψ_x, ψ_y	components of shear rotation
ω	natural frequency
ω_o	undamped natural frequency
ω^*	complex frequency factor
$\bar{\omega}$	nondimensional frequency
ω_D	generalized damped natural frequency
(123)	material axes coordinate system
$\|\{\}\|_1$	the first norm of a vector
$\|[]\|_f$	the Frobenius norm of a matrix

Subscripts

,	the first differential
1, or L	longitudinal direction of the fibre
2, or T	transverse direction of the fibre
3, or Z	transverse direction of the fibre
i, j	indices(1,2,3,...)
I	imaginary part
m	index of layer
n	normal component
R	real part
t	tangential component

Superscripts

·	the first differential
··	the second differential
*	complex
+	augmented
-	estimation by the Modified MSE method
^	estimation by the MSE method
ˇ	force resultants on the boundary
H	Hermitian transpose, or conjugate transpose
(m)	index of layer
(r)	index of modal
T	transpose

CHAPTER 1

GENERAL INTRODUCTION

1.1. Why study damped vibrations of composites?

In recent years composites, especially fibre-reinforced laminates, have found increasing application in many engineering structures. This was mainly due to two desirable features of fibre-reinforced composites: a high ratio of stiffness and strength to weight, and the anisotropic material property that can be controlled by varying the fibre orientation and the stacking sequence of the lamina. The last feature provides the structural designer with more flexibility to optimally synthesize the characteristics of the designed structures.

Consider, for example, the design of robotic manipulators. Most of industrial robots today are built with heavy links and consequently they can only handle a small percent of their own weight as a payload. The reason is mainly due to an inherent design requirement to minimize structural vibrations by increasing the mechanical stiffness of each component. This massive structural design makes the robot slow and leads to high energy consumptions. For the next generation of high-performance robots, materials with lighter weight and higher stiffness will be used for their construction. Several

benefits can be achieved from the use of lightweight arms. One can attain higher motion speeds, better energy efficiency and improved mobility. Composites are ideally suited to such purposes. Furthermore, composite materials generally exhibit higher damping properties compared to structural metallic materials. This feature provides composite materials with another advantage in limiting the resonant or near-resonant amplitudes of vibration.

In applications of robotics with flexible arms, material damping can play an important role to obtain highly controlled performance regarding efficiency, accuracy, and stability. As one of many sources of energy dissipation, damping in materials can be a dominant contributor to the overall damping in aerospace systems. Although damping is mainly effective in the range of resonance, it is usually only when resonance occurs that structural vibration becomes a problem. Excessive amplitudes of vibration can cause failure of components through fatigue, malfunction of instruments, radiation of noise, and customer's discomfort.

Therefore, a knowledge of the damping properties of composite materials is important. Though many of the analyses have been devoted to the study of the dynamics of laminated composite plates, investigations of the damping effect are rather limited. There is a need for more systematic and in-depth analytical research to be performed on the damping aspects of composite plates.

1.2. Methodology of approach

Since a fibre laminated composite contains at least two layers, its mechanical behaviour is a function of the lamination arrangement. It is unfeasible to experimentally determine the mechanical behaviour of all possible combinations that may be used in structural design. However, few analytical solutions seem to be available in the literature. They are restricted to cases of simple loading, boundary conditions and geometries. In this regard, Finite Element Methods (FEM) are especially useful and versatile tools in the prediction of mechanical behaviour of laminated composites.

This thesis makes use of the Finite Element approach to perform the analysis of damped vibrations of laminated composite plates. Various finite element models have been developed to improve the accuracy, simplicity of formulation, numerical stability, convergence and cost effectiveness of computation. The C^0-type plate element method is applied on the basis of the First-order Shear Deformation Theory. This theory uses Hamilton's principle to derive the governing equations of the plate. It includes the effects of transverse shear deformation, rotary, and coupled normal-rotary inertias.

1.3. Objectives of the thesis

The objectives of this thesis are:

a) to formulate two macromechanical damping models corresponding to the First-order Shear Deformation Theory;

b) to verify the damping models for polymer-matrix and metal-matrix composites using the experimental results available in the literature;

c) to identify the differences of the two damping models;

d) to conduct parametric studies on the modal frequencies and damping due to variations of:

   i) the side-to-thickness ratio,

   ii) the principal moduli ratio,

   iii) the total number of layers,

   iv) the ply-angle,

   The following configurations are considered:

   - simply supported or clamped boundary conditions,

- symmetrically or antisymmetrically laminated,
- angle-ply or cross-ply.

e) to investigate the error arising from the use of the Modal Strain Energy (MSE) method in obtaining the modal damping;

f) to develop a Modified Modal Strain Energy approach to improve the accuracy;

g) to compare the results of the MSE and the Modified MSE methods with the exact solution;

h) to develop the numerical indices to examine the validity of the approximation methods.

1.4. Thesis organization

This thesis contains six chapters. The first chapter is the Introduction. It justifies the present study and highlights its engineering applications.

Chapter 2 reviews the previous work done on laminated plates and the damped vibrations of composites. Various solutions are presented with their advantages and disadvantages.

The formulations of the two macromechanical damping models, namely, Viscoelastic Damping (VED) model, and Specific Damping Capacity (SDC) model, are derived in Chapter 3.

The Modified Modal Strain Energy method is proposed in Chapter 4 for a better evaluation of modal damping. The numerical studies show that the numerical indices proposed in this chapter provide an effective measure to assess the accuracy of the approximations.

Chapter 5 reports the numerical studies on the free vibration systems. The verifications of damping models for both polymer-matrix and metal-matrix composites are conducted by comparing the analytical findings with the experimental results in the literature. The parametric studies on the modal frequencies and damping are also investigated in this chapter.

A summary of the thesis and recommendations for future work are provided in Chapter 6. Chapters 3, 4 and 5 contain new contributions to the area of the dynamics of composite materials.

CHAPTER 2

LITERATURE REVIEWS

2.1. Theories of laminated composite plates

2.1.1. Introduction

Composites can be classified into five types: particulate, fibre, laminated (or layered), flake, and filled as shown in Figure 2.1. Among them the laminated composites are by far most widely used. The present work is concerned with the fibre-reinforced laminated composite plates.

A fibre-reinforced laminated composite is constructed of a number of plies of unidirectional fabric composites stacked at various angles relative to the x axis of the laminate as shown in Figure 2.2. The basic building block of layered composites is a single lamina of unidirectional fibre composite, in which all the fibres are set to be parallel and embedded in a matrix. Fibres which are currently in use are glass, carbon, and boron. Typical matrices are polymeric (polymer-matrix), such as epoxy, and light metallic (metal-matrix), primarily aluminum alloys.

The practical analysis of the mechanical response of composite bodies involves analytical studies on one of two levels of abstraction. These areas of studies are known as micromechanics and macromechanics as reported by Mallick (1988):

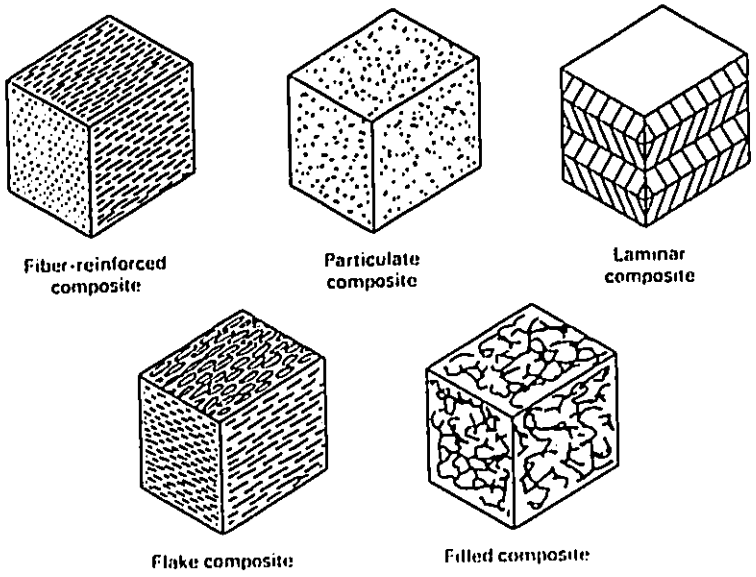

Figure 2.1 Some classes of composites (After Weeton, et.al., 1987)

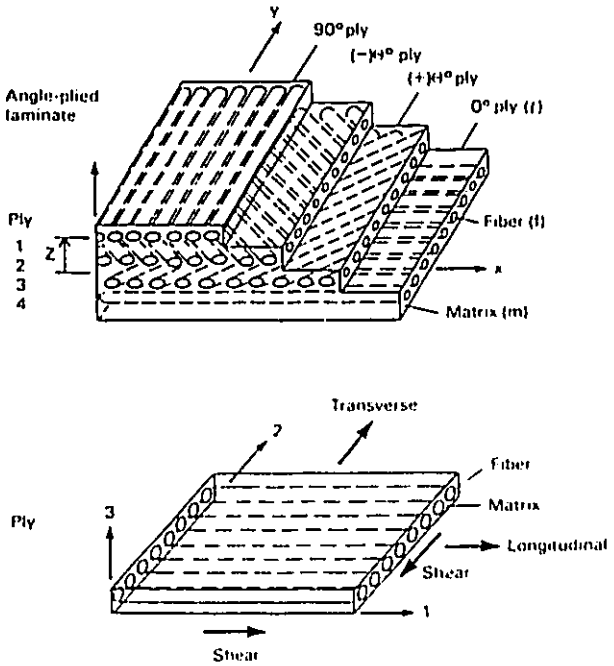

Figure 2.2 Typical fibre-reinforced laminated composite (After Weeton, et.al., 1987)

a) Micromechanics is a study of the mechanical properties of unidirectional composites in terms of constituent materials (fibre and matrix). The heterogeneity and anisotropy of each ply are recognized and accounted for in the analysis.

b) Macromechanics studies the overall mechanical properties of a fibre-reinforced composite material, which leads to the development of laminated plate theory. The material is assumed to be homogeneous.

We will present a brief review of literature on the different theories applied to laminated plates in view of macromechanical analysis. There exists a large number of publications on the subject. The emphases in this review will be on the kinematic modelling of the plates and solution methods. This will serve as a basis for selection of an appropriate theory in the present work.

2.1.2. Kinematic modelling

Composite laminates contain two or more layers of different materials that are bonded together to achieve the best properties of the constituent layers. Because of the different material properties of the layers, the resulting laminate is in general anisotropic along the thickness direction and presents different kinematic modelling

requirements in comparison with monolithic plates. The need for more accurate computational models of laminated plates has led to the development of a variety of theories in this regard.

In early studies, the Classical Laminated Plate Theory (**CLPT**, or **CPT**), which was based on the Kirchhoff's hypothesis, was applied in modelling laminated plates. This theory assumes that the linear elements perpendicular to the middle surface of the plate do not change in length and remain straight and normal to the deflected middle surface after deformation. This assumption is equivalent to neglecting transverse shearing deformation γ_{xz} and γ_{yz}, and the normal strain ε_z in the thickness direction as reported by Whitney (1987). The displacement components of a plate in this case are given by:

$$\begin{aligned} u(x,y,z) &= u^o(x,y) - z w^o_{,x}(x,y) \ , \\ v(x,y,z) &= v^o(x,y) - z w^o_{,y}(x,y) \ , \\ w(x,y,z) &= w^o(x,y) \ , \end{aligned} \tag{2.1}$$

where u, v, and w are the displacement components in the x-, y-, and z-directions, respectively; u^o and v^o are the in-plane (stretching) displacements of the middle plane.

Due to the neglected transverse shear deformations, this theory will result in big errors when applied to plates with thick cross sections. In addition, the discrepancy will increase as the magnitude of the in-plane stiffness increases

relative to the transverse stiffness of the material. It has been noted by Whitney and Sun (1973), and Reddy (1990) that the Classical Laminated Plate Theory underestimates the deflections and overestimates the natural frequencies and the buckling loads. Further, because the Classical Plate Theory accounts for second-order derivatives of the transverse deflection in the energy expression, it is computationally inefficient (requirement of C^1 continuous shape functions).

Using a stress formulation, Reissner (1945) was the first to develop a shear-deformation theory for static analysis. Mindlin (1951) proposed the First-order Shear Deformation Theory (**FSDT**), which is a displacement-based theory, for the dynamic analysis of homogeneous isotropic plates. This was extended to the laminated anisotropic plates by Yang, Norris and Stavsky (1966). In this theory linear displacements were assumed across the entire laminate thickness. The transverse shear deformation, however, was not neglected. The displacement field of Yang-Norris-Stavsky (**YNS**, or **FSDT**) was taken as follows:

$$\begin{aligned} u(x,y,z) &= u^o(x,y) - z\psi_x(x,y) , \\ v(x,y,z) &= v^o(x,y) - z\psi_y(x,y) , \\ w(x,y,z) &= w^o(x,y) , \end{aligned} \tag{2.2}$$

where ψ_x and ψ_y are the shear rotations.

In this theory any line which is originally normal to

the plate median surface is assumed to remain straight during deformation but not generally normal to the median surface.

This theory works much better than the Classical Laminated Plate Theory for thick plates. Further, in this theory only the first derivatives appear in the energy functional and therefore only the C^0 continuity is required for the shape functions. Moreover, the shape functions from plane elasticity elements can be used for the plate bending and the elements can be mapped isoparametrically.

Since the transverse shear strains are assumed to be constant through the thickness of the plate, correction factors have to be used in the First-order Shear Deformation Theory. The shear correction factors are dimensionless quantities introduced to account for the discrepancy between the constant state of shear strains in the First-order theory and the parabolic distribution of shear strain in the elasticity theory.

Several approaches by Chow (1971) and Whitney (1973) were proposed for calculating the shear correction factors for different laminates. Most of these approaches are based on matching certain gross response characteristics, as predicted by the First-order Shear Deformation Theory, with the corresponding characteristics of the three-dimensional elasticity theory.

Numerical studies have shown that the First-order Shear Deformation Theory is adequate in presenting the global

behaviour of laminated plates. These include deflection and vibration analyses by Whitney and Pagano (1970), Reddy and Chao (1981), and the buckling analysis by Noor (1975). However, such a theory is inadequate for the analysis of the through-the-thickness stress response in the localized regions of geometric, load, and material discontinuities. The theory suffers from the following drawbacks:

a) The in-plane normal strain is distributed linearly through the thickness, rather than nonlinearly.

b) The transverse normal strain is neglected.

c) The transverse strains are constant through the thickness. Consequently the theory does not satisfy the conditions of zero transverse shear stresses on the top and bottom surfaces.

In an early attempt to overcome these drawbacks, a three-dimensional elasticity theory was tried for laminated composite plates by Pagano (1969, 1970) and Srinivas *et al.* (1970 a, b). This theory treats each layer as an elastic continuum with possible distinct material properties from adjacent layers. The number of governing differential equations is thus 3N; with N being the number of layers in the laminate. Continuity displacements and stresses at the interface of two layers give rise to additional relationships.

Theoretically, it is possible to account for the stress field of the structure by considering each layer as a

three-dimensional solid. However, the equations become intractable as the number of layers becomes large. In practical applications, numerous layers may be present (the use of 20 layers in aircraft structures is not unusual). In addition, the element aspect ratio is also restricted to the application of three-dimensional models in the finite element analysis.

Alternatively, several two-dimensional refined theories have been proposed. These include

a) High-order Shear Deformation Theories (**HSDT**),

b) Layer-wise Shear Angle Theories (**LSAT**).

Many different High-order Shear Deformation Theories have been proposed which are based on nonlinear displacement and/or stress assumptions through the thickness of the plates.

In Whitney and Sun's model (1973) the displacement field in parabolic form is assumed to be given by:

$$\begin{aligned} u(x,y,z) &= u^o(x,y) + z\psi_x(x,y) + \frac{z^2}{2}\phi_x(x,y) \ , \\ v(x,y,z) &= v^o(x,y) + z\psi_y(x,y) + \frac{z^2}{2}\phi_y(x,y) \ , \\ w(x,y,z) &= w^o(x,y) + z\psi_z(x,y) \ . \end{aligned} \tag{2.3}$$

Lo *et al.* (1977) pointed out that the inclusion of the quadratic terms in the in-plane displacement does not provide a significant advantage over the First-order Shear Deformation Theory because they can not represent the parabolic form of transverse shear strains. They presented a theory using the

following displacement form:

$$u(x,y,z) = u^o(x,y) + z\psi_x(x,y) + \frac{z^2}{2}\phi_x(x,y) + z^3\xi_x(x,y) ,$$

$$v(x,y,z) = v^o(x,y) + z\psi_y(x,y) + \frac{z^2}{2}\phi_y(x,y) + z^3\xi_y(x,y) ,$$

$$w(x,y,z) = w^o(x,y) + z\psi_z(x,y) + z^2\phi_z(x,y) , \tag{2.4}$$

where ϕ_x, ϕ_y and ϕ_z, ξ_x and ξ_y are the corresponding higher-order terms in the Taylor's series expansion and are also defined at the middle plane. The total number of displacement parameters is eleven in this theory, which makes the application of the resulting theory rather expensive.

Reddy (1984) proposed a three-order theory on the basis of equation (2.4), by neglecting the transverse normal stress effect and satisfying the zero transverse shear stress conditions on the plate surface. The displacement field then took the following form:

$$u(x,y,z) = u^o + z\left[\psi_x - \frac{4}{3}\left(\frac{z}{h}\right)^2(\psi_x + w^o_{,x})\right] ,$$

$$v(x,y,z) = v^o + z\left[\psi_y - \frac{4}{3}\left(\frac{z}{h}\right)^2(\psi_y + w^o_{,y})\right] , \tag{2.5}$$

$$w(x,y,z) = w^o(x,y) .$$

Although the in-plane displacements in this model were assumed to be cubic functions of the thickness coordinate, the total number of displacement parameters is five which is equal to that in the First-order Shear Deformation Theory. This

theory, however, yields a C^1 continuous finite element formulation.

Ren and Hinton (1986) slightly modified the degrees of freedom used in equation (2.5) and defined new variables as:

$$\begin{aligned} \chi_x &= \psi_x + w^o_{,x} \ , \\ \chi_y &= \psi_y + w^o_{,y} \ . \end{aligned} \tag{2.6}$$

They studied a four-layer, cross-ply [0°/90°/90°/0°] square plate subjected to a sinusoidal transverse load and found that the model gave results better than those of Reddy's.

Krishna Murty (1987) found out that the transverse shear strains in the Reddy's model vanish at points in the plate where displacements are constrained to be zero, such as those on the fixed edge. Obviously this does not represent the true situation. This limitation has been overcome by the following displacement model:

$$\begin{aligned} u(x,y,z) &= u^o - w^o_{b,x} - \frac{4z^2}{3h^2}\psi_x(x,y) \ , \\ v(x,y,z) &= v^o - w^o_{b,y} - \frac{4z^2}{3h^2}\psi_y(x,y) \ , \\ w(x,y,z) &= w^o_b(x,y) + w^o_s(x,y) \ , \end{aligned} \tag{2.7}$$

where w_b and w_s are bending and shear partial deflections, respectively. Note that the transverse deflection contains two parts. The model also adds one more variable to the Reddy's three-order model.

Senthilnathan *et al.* (1988) proposed a displacement field similar to that of the Krishna Murty's by assigning

$$\psi_x = w^o_{s,x} \ , \qquad \psi_y = w^o_{s,y} \ . \tag{2.8}$$

The resulting model is shown to have one variable less than that in the Reddy's, yet it accounts for a parabolic variation of the transverse shear stresses with zero value at the free surfaces.

With the increasing interest in the use of composite materials in high technology areas, it is important for the composite-structure designer to be able to predict with high degree of confidence the failure/fracture mode of composites. One of the most critical failure modes is recognised as the delamination mode. The initiation and growth of this failure mode is due to the appearance of interlaminar stresses τ_{xz}, τ_{yz} and σ_z. Several refined models have been developed to include higher order terms in the transverse displacement w. The displacement field in the Kwon and Akin's model (1987) is given by:

$$\begin{aligned} u(x,y,z) &= u^o(x,y) + z\psi_x(x,y) \ , \\ v(x,y,z) &= u^o(x,y) + z\psi_y(x,y) \ , \\ w(x,y,z) &= w^o(x,y) + z\psi_z(x,y) + z^2\phi_z(x,y) \ . \end{aligned} \tag{2.9}$$

Seven variables appear in this model. However, ψ_z and

ϕ_z can be eliminated using the assumption of quadratic distributions of transverse shear strains through the thickness. Thus the model has properties similar to the Reddy's three-order model on the parabolic distribution of the transverse shear strains with five variables. One of the significant differences is that the linear transverse normal strain ε_z was introduced in this model, while it is zero in Reddy's model.

Unlike the commonly used algebraic through-the-thickness terms in most theories, Stein (1986) developed a displacement field in terms of trigonometric functions in the following form:

$$\begin{aligned} u &= u^o + \psi_x \frac{z}{h} + \phi_x \sin\frac{\pi z}{h} \ , \\ v &= v^o + \psi_y \frac{z}{h} + \phi_y \sin\frac{\pi z}{h} \ , \\ w &= w^o + \phi_z \cos\frac{\pi z}{h} \ . \end{aligned} \tag{2.10}$$

This model gives a three-dimensional description of the stresses. It was reported that the trigonometric through-the-thickness terms would give more accurate results in comparison with the algebraic ones.

One of advantages of applying higher-order shear deformation theory is that there is no need to use shear correction coefficients in computing the shear stresses if a parabolic term in the transverse shear strains through thickness is included (Reddy, 1984).

Both of the First-order Shear Deformation Theory and the High-order Shear Deformation Theory are called single-layer theories because they are based on a single displacement expansion through the laminate thickness. Consequently, the transverse shear angle is continuous in the form of a smooth curve through the thickness, rather than varying from layer to layer. Such theories cannot accurately model laminates made of dissimilar material layers. For example, a sandwich plate with a soft core usually has zig-zag shaped in-plane displacements through the thickness. These types of displacements are difficult to present by a single-layer theory.

The Layer-wise Shear Angle Theories (**LSAT**) assume independent displacement/stress approximations for each layer. For this reason, they are also called multi-layer theories. These theories can guarantee the continuity of the transverse shear stresses at the interfaces.

Sun and Whitney (1973) assumed the displacement field in the *m*th layer to be of the form:

$$\begin{aligned} \overline{u}_m(x,y,z) &= u^o_m(x,y) - \overline{z}_m(\psi_x)_m(x,y) \ , \\ \overline{v}_m(x,y,z) &= v^o_m(x,y) - \overline{z}_m(\psi_y)_m(x,y) \ , \\ \overline{w}_m(x,y,z) &= w^o(x,y) \ , \end{aligned} \tag{2.11}$$

where $\bar{z}_m$ is the thickness-coordinate with the origin located at the midplane of the *m*th layer; u^o_m and v^o_m are the displacements at the midplane of the *m*th layer. Distinct

transverse shear deformations are allowed to exist within each layer in this theory.

In fact, this theory is an application of the First-order Shear Deformation Theory with layer-wise definition of the generalized displacements. It has been noted by Sun and Whitney (1973) that there are certain constraint conditions at the interfaces of the layers which have to be satisfied. Consequently, not all the displacement components and rotations in the layers are independent kinematically. These constraint conditions must be taken into account before the variational principle is employed.

For plates consisting of layers perfectly bonded together (the layers conjunct concurrently without slippage), we know from elasticity theory that at the interface (z=a) of the mth and the $(m+1)$th layers the following two sets of continuity conditions must hold :

$$\begin{aligned} \bar{u}_m(z=a) &= \bar{u}_{m+1}(z=a) \ , \\ \bar{v}_m(z=a) &= \bar{v}_{m+1}(z=a) \ , \\ \bar{w}_m(z=a) &= \bar{w}_{m+1}(z=a) \ , \end{aligned} \tag{2.12}$$

and

$$\begin{aligned} (\bar{\tau}_{xz})_m(z=a) &= (\bar{\tau}_{xz})_{m+1}(z=a) \ , \\ (\bar{\tau}_{yz})_m(z=a) &= (\bar{\tau}_{yz})_{m+1}(z=a) \ , \\ (\bar{\sigma}_z)_m(z=a) &= (\bar{\sigma}_z)_{m+1}(z=a) \ . \end{aligned} \tag{2.13}$$

Mau (1973) introduced the interlaminar shear stresses as Lagrange multipliers to satisfy the continuity of displacements at the interfaces of the layers. The governing

equations were obtained by minimizing the modified potential energy functional.

On the basis of equation (2.11), Mawenya and Davies (1974) imposed the constraints on the deformations so that the shear stresses are guaranteed to be continuous at the interface of the layers. As a result, the independent variables are u^o, v^o, w^o, $(\psi_x)_m$ and $(\psi_y)_m$ for the mth layer. Therefore, the total number of parameters is (2N+3) for an N-layer composite plate.

The theory, based on equation (2.11), is termed the Layer-wise Constant Shear Angle Theory because the shear rotations are uniform for any one particular layer but vary from layer to layer. The high-order shear deformation assumption with layer-wise definition of the generalized displacements was proposed by Taledano and Murakami (1987), in which the parabolic variations of transverse shear strains for each individual layer are obtained.

Noting the computational expense in the Layer-wise Shear Angle Theories, Di Sciuva (1986) proposed a simplified layer-wise model, in which the displacement field was assumed to be of the form

$$
\begin{aligned}
u(x,y,z) &= u^o + z(\psi_x - w^o_{,x}) + \sum_{m=1}^{N-1} (\phi_x)_m (z - z_m) H(z-z_m) \,, \\
v(x,y,z) &= v^o + z(\psi_y - w^o_{,y}) + \sum_{m=1}^{N-1} (\phi_y)_m (z - z_m) H(z-z_m) \,, \\
w(x,y,z) &= w^o(x,y) \,,
\end{aligned}
\tag{2.14}
$$

where $(\phi_x)_m$ and $(\phi_y)_m$ are the shear rotations of the mth layer in the x-z and y-z planes, respectively. $H(z-z_m)$ is the Heaviside unit function. This theory accounts for piecewise linear distribution across the thickness of the in-plane displacements and constant transverse displacement. By imposing the contact conditions on the transverse shearing stresses, all terms of $(\phi_x)_m$ and $(\phi_y)_m$ will vanish. Consequently, the total number of variables will be reduced from (2N+3) to 5.

Apparently, the greater accuracy of prediction for laminated plates is achieved on the expense of the complexity of formulation and elevated cost of computation.

As a compromise between accuracy and efficiency, Noor and Burton (1989 a) proposed an elegant method. They applied a two-phase computational procedure for the accurate determination of the vibration frequencies, stresses and deformations in multilayered composite plates. In the first phase a simple two-dimensional First-order Shear Deformation Theory is used to predict the global response characteristics of the plate (vibration frequencies, average through-the-thickness displacements and rotations), as well as in-plane stresses and strains. In the second phase, the equilibrium equations and constitutive relations of the three dimensional theory of elasticity are used to calculate the transverse stresses and strains, to obtain better estimates for the composite shear correction factors, and to calculate corrected

values for the frequencies, displacements and in-plane stresses in the thickness direction.

Numerous theories of laminated plates have been documented in the literature. Table 2.1 gives a compact review of the most common theories for laminated structures (Noor and Burton, 1989 b).

The first important step in developing an adequate mathematical model for a laminated composite material is to select a proper structural theory (*i* e., kinematics) for the problem. Reddy (1989, 1990) suggested the following guidelines:

a) The First-order Shear Deformation Theory represents the best compromise between accuracy and computational efficiency. It yields, with sufficient accuracy, the global response characteristics, such as the maximum deflection, the fundamental frequency and the critical buckling load.

b) The Higher-order Shear Deformation Theories yields improved in-plane and interlaminar stress distributions.

c) The Layer-wise Shear Angle Theories are the best alternative to three-dimensional theories to evaluate local effects such as interlaminar stresses, edge effects, and delamination in composites.

Table 2.1. The differences of modelling approaches (After Noor and Burton, 1989 b)

Type	Displacement assumptions	Constraints on stresses	References
First-order shear deformation theory (5 parameters)	Linear u,v, constant w.	$\sigma_z = 0$.	Yang, Norris, and Stavsky (1966); Reddy (1979, 1980).
Higher-order shear deformation theory (11 parameters)	Cubic u,v, quadratic w.	None.	Lo, Christensen, and Wu (1978); Kant *et al.* (1988)
Simplified higher-order theory (5 parameters)	Cubic u,v, constant w.	$\sigma_z = 0$, $\tau_{xz}=\tau_{yz}=0$ at top and bottom surfaces.	Reddy (1984 a); Bhimaraddi and Stevens(1984).
Layer-wise theory ((2*N+3) parameters)	Piecewise linear u,v, constant w.	$\sigma_z = 0$.	Mau (1973); Srinivas (1973); Bert (1984).
Simplified layer-wise theory (5 parameters)	Piecewise linear u,v, constant w.	$\sigma_z = 0$, continuity of τ_{xz}, τ_{yz} at layer interfaces.	Di Sciuva (1986); Murakami (1986).
Predictor-corrector approach (5 parameters)	Predictor phase: linear u,v, constant w. Corrector phase: by three-dimensional equilibrium.	Predictor phase: $\sigma_z = 0$.	Noor and Burton (1989 a).

2.1.3. Macromechanical analysis

In the analysis of the response of composite materials, it is desirable to seek an exact (or closed-form) solution. An exact solution provides a basis for comparisons of the various improved theories. Pagano (1969) achieved an exact solution to the cylindrical bending of a simply supported laminate under a sinusoidal distributed normal pressure loading. In 1970, Srinivas *et al*. applied a three-dimensional, linear, small deformation theory in the evaluation of the bending, vibration and buckling of simply supported rectangular laminates. The vibration of a circular plate of cylindrically orthotropic material has been studied by Fan and Ye (1990). There appears to be rather few analytical solutions available in the literature for the study of laminated composites of limited types of geometry and boundary conditions.

Two numerical techniques are basically used in this research area, namely, Rayleigh-Ritz method (**RRM**) and Finite Element method (**FEM**).

The Rayleigh-Ritz procedure specifies a "guessed at" form of the displacement solution. In this case the resulting governing equations are exchanged for a system of algebraic equations. The "guessed at" displacement solutions are more formally termed admissible functions. These are defined as those which at least satisfy all geometric boundary

conditions, displacement constraints and rotation constraints. Better yet are those functions which, in addition, satisfy part or all of the stress boundary conditions, *i* e., stress couples, in-plane and shear resultants.

A number of studies, which used RRM, have appeared in the literature. The analysis of natural frequencies of lateral vibration for square laminated plates with clamped edges was presented by Bert and Mayberry (1969), for rectangular plates with simply supported or free boundaries by Kamal and Durvasula (1986), and for circular plates by Sivakvomaran (1989). The buckling analysis was reported by Dawe and Craig (1986). Rayleigh-Ritz method, similar to analytical solutions, usually has its limitations regarding loading, boundary conditions, laminations and geometries.

The Finite Element method is the most attractive method for dealing with complicated problems of composite laminated plates. It is possible to incorporate various finite element models which improve the accuracy of the solution, simplify the formulation, introduce numerical stability and guarantee convergence, and cost-effectiveness of computation.

The displacement-based element method is widely used in the formulation of the C^0-type elements. This type uses the variational principle to derive the governing equations of the plate.

Following the procedures of finite element technique, one usually obtains the element stiffness matrix $[K^e]$ in the

following form:

$$[K^e] = \int_V [B]^T[D][B]\, dV$$
$$= \int_{-1}^{1}\int_{-1}^{1}\int_{-1}^{1} [B]^T[D][B]|J|\, d\xi d\eta d\zeta \ . \qquad (2.15)$$

The elasticity matrix [D] differs from layer to layer and is not a continuous function of ζ. Panda and Natarajan (1976, 1979) introduced "the thickness concept" to overcome this difficulty. The variable ζ in any mth layer is replaced by ζ_m which varies from -1 to 1 in the mth layer. The stiffness matrix can be written as:

$$[K^e] = \sum_{m=1}^{N} \int_{-1}^{1}\int_{-1}^{1}\int_{-1}^{1} [B]^T[D^{(m)}][B]|J|\, \frac{h_m}{h}\, d\xi d\eta d\zeta_m \ . \qquad (2.16)$$

Reddy (1980) commented that this concept is essentially identical to the First-order Shear Deformation Theory in which [D] is obtained from the relations between the resultant forces and the associated strains.

In the three-dimensional finite element formulation, Barker *et al.* (1972) applied 24-node isoparametric brick elements for each layer of the plate. The analysis becomes intractable when the number of layers is increased. Noting this difficulty, Jones *et al.* (1984) and Hoa *et al.* (1985) used super-element schemes in which one element may contain several layers. The thickness concept was used in the

integration procedure. This scheme can reduce substantially the computational cost compared with a ply-by-ply element scheme.

In applications involving the First-order Shear Deformation Theory, unreasonable results are obtained regarding the transverse (interlaminar) shear stresses. However, highly accurate results have been obtained from the equilibrium equations of the three-dimensional theory of elasticity. Pryor and Barker (1971), Chaudhuri (1986), and Lajczok (1986) obtained:

$$\tau_{xz} = \int_{-\frac{h}{2}}^{z} (\sigma_{x,x} + \tau_{xy,y})\, dz \ ,$$
$$\tau_{yz} = \int_{-\frac{h}{2}}^{z} (\tau_{xy,x} + \sigma_{y,y})\, dz \ . \qquad (2.17)$$

Furthermore, the variation in transverse normal stress is determined through the equation by Engblom and Ochoa (1986) as:

$$\sigma_z = \int_{-\frac{h}{2}}^{z} (\tau_{xz,x} + \tau_{yz,y})\, dz \ . \qquad (2.18)$$

This scheme was even adopted when using the High-order Shear Deformation Theory by Kant and Pandya (1988) in the bending analysis of the plates.

In the finite element formulation which includes the independent variable of transverse shear rotation, a problem

known as "shear locking" is encountered when the side-to-thickness ratio is large. In the limit, as the thickness decreases, the shear terms become dominant in the stiffness matrix and the deflections tend to zero.

There exists a number of techniques to alleviate the problem. The most simple and effective method is the selective reduced integration introduced by Zienkiewicz *et al.* (1971) and Hughes *et al.* (1978). In this technique, bending energies are integrated using the normal rule, while the shear terms are computed using the reduced integration rule.

It is known that the construction of an C^1 element is algebraically complicated and computationally inefficient. In the early studies of composite plates, the hybrid and mixed element methods were introduced to avoid the continuity problem.

Two different approaches are utilized when applying the variational principles. The "hybrid" formulation is used when one set of unknowns can be eliminated at the element level. The "generalized mixed" formulation is used when both sets of unknowns, displacements and stresses, appear in the global governing equations.

Mau *et al.* (1972, 1973) first applied the hybrid stress method and the layer-wise constant shear angle assumption to the laminated thick plate. This method is based on an assumed stress field in the element and an assumed displacement field along the inter-element boundary. The

chosen element is a quadrilateral plate element with four corner nodes. The continuity conditions on the interlaminar stresses are satisfied in this theory. The resulting formulation requires interpolation functions with only C^0 continuity.

A mixed shear flexible finite element was developed by Putcha and Reddy (1986) for the nonlinear analysis of laminated plates. The displacement field of Reddy's three-order theory was used with five displacement components as in equation (2.5), including six additional components (M_1, M_2, M_6, N_1, N_2, and N_6) as the primary variables. This method leads to a C^0 element.

The numerical studies on static and dynamic analyses as reported by Tsay and Reddy (1978), Spiker and Munir (1980), Spiker (1984), and Murakami (1986) have shown that both hybrid and mixed methods can achieve excellent accuracy in predicting the displacements and the stresses.

For plate structures having regular geometric planes, a full finite element analysis may be unnecessary. The finite strip method offers an alternative approach which reduces the problem size, yet maintains some versatility. Unlike the standard finite element method which describes the displacements using polynomial functions, the finite strip method uses a combination of polynomial and harmonic functions. The harmonic functions satisfy, *a priori*, the boundary conditions at the ends of the strips and have the

advantage of greatly reducing the number of equations to be solved. The finite strip methods have been applied to the flexure problem by Hinton (1977) and to the vibration problem by Crig and Dawe (1986).

In summary, the finite element techniques proved to be powerful and versatile tools in engineering application. The need for finite element analysis is especially high for composite materials and structures with various configurations of lamination.

2.2. Damped vibration analysis of layered fibre-reinforced composites

2.2.1. Introduction

Material damping, referred to as internal damping, is the phenomenon within the material in which energy is dissipated (Bert, 1980). Damping plays an important role in attenuating the response of systems at resonance. Understanding material damping is an important step in the development of the analytical tools that are needed by space engineering designers. The study of material damping falls into two categories:

a) mechanism oriented;

b) application oriented.

The first approach requires a clear understanding and quantification of the physical processes which bring about the damping, and almost without exception leads to nonlinear computational models. The study in this case is mainly based on materials science and is fundamental to the second approach. In some situations, however, this approach is difficult to use because the need for precise laws to describe the energy dissipation will make the model expensive.

The second approach employs simple damping models to represent the system. While the physical origin of the damping may be obscure, the simplicity of the approach provides

qualitative, and under certain conditions, even quantitative merits.

This section presents a comprehensive review of the damping in layered fibre-reinforced composites, its mathematical treatment from an application oriented viewpoint and the solution methods for viscoelastic materials. The objective of this review is to define the basic aspects of damping, in layered composites, which are necessary for the development of adequate models to describe their dynamic response.

2.2.2. Material damping

The dynamic properties of a laminated composite are characterized by:

a) the constituent materials: fibre and matrix (polymer/metal), *etc.*;

b) the construction of each lamina of unidirectional fibre composite: fibre volume, distribution of constituents, the nature of the bond between fibre and matrix, *etc.*;

c) the arrangement of the layers: stacking angles, stacking sequence, total number of layers, *etc.*;

d) the fabrication defects: voids, delamination, residual stresses, *etc.*

Material damping can be caused by a variety of combinations of fundamental physical mechanisms, depending upon the specific material. The damping mechanisms for three classes of materials, namely, fibre, polymer and metal, are examined.

The desired features associated with the use of fibre material, such as carbon, are its high specific strength, high stiffness and its directional properties. In this case, material damping may arise due to the inhomogeneous strain in fibrous materials as reported by Goodman (1988). Generally, such materials have extremely low damping capacities and their contribution to the damping of the composites is negligible as noted by Adams *et al.* (1969). In some cases, however, fibre damping has to be considered in the analysis. An effort has been made by Lesieutre *et al.* (1991) to improve damping of composite material using bromine-intercalated graphite fibres.

For metals, the mechanisms of damping were reported by Bert (1973), Wolfenden and Wolla (1991). The studies covered the following aspects:

a) the dislocations,

b) the point defects,

c) the grain boundary,

d) the thermoelastic coupling,

e) the eddy-current effects,

f) the stress-induced ordering,

g) the electronic effects.

It is difficult to establish a comprehensive model for the damping of a specific metal in terms of the variables listed previously. One approach towards quantifying the internal damping behaviour is through the use of the hysteresis loop, presumed to be obtained from experimental measurements on a material sample. Figure 2.3 (a) illustrates a type of hysteresis loop which is believed to be representative of typical constructional metal alloys and even of some high damping alloys as reported by Nashif *et al.* (1985). The shape of the loop depends on the operative damping mechanism. Significant nonlinearity characterizes metallic materials, particularly at high levels of stress. Adams (1972) showed that damping in metals is hysteretic and not viscous by nature and that it is strongly dependent on the amplitude of vibration, except at very low strain levels.

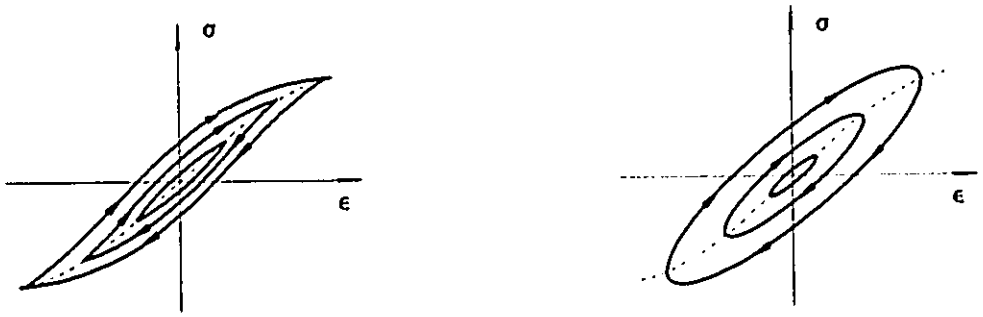

(a) Metallic material (b) Viscoelastic material

Figure 2.3 Hysteresis loop (after Nashif *et al.*, 1985)

Due to the long-range molecular order associated with their giant molecules, polymers exhibit a rheological behaviour which is intermediate between that of a crystalline solid and that of a simple liquid as reported by Bert (1973). Damping arises from relaxation and recovery of the polymer network after it has been deformed. Damping exhibits a strong dependence on the frequency of loading and the temperature of the composite because of the direct relationship between material temperature and molecular motion as reported by Nashif *et al.* (1985).

According to Lazan (1959, 1965), the various damping phenomena and mechanisms may be classified under one of two headings:

a) dynamic hysteresis (known as the rate-dependent damping),

b) static hysteresis (known as the rate-independent damping).

Viscoelastic materials, such as polymers, are associated with dynamic hysteresis which depends on the rate of cyclic load or displacement. Dynamic hysteresis yields damping that is frequency-dependent and amplitude-independent. In contrast with dynamic hysteresis, static hysteresis involves strain laws which are insensitive to time, strain rate, stress rate or other derivatives. The two principal mechanisms which lead to static hysteresis are magneto elasticity and plastic strain.

The hysteresis loop associated with viscoelastic materials tends to be elliptic in shape (Figure 2.3 b), and the loop area is dependent on frequency. On the other hand, metallic materials generally display static hysteresis loop with sharp corners at both ends and are nearly linear in the low-stress, the low-strain region as shown in Figure 2.3 a. The loop area is independent of frequency but is dependent on the stress level.

The "linearity" of damping is usually checked by the model relating damping energy ΔU to stress σ:

$$\Delta U = J \sigma^n , \qquad (2.19)$$

where J and n are the damping constant and the damping exponent, respectively. Linear damping is characterized by the following two aspects:

a) damping exponent n = 2;

b) the hysteretic loop is elliptical in form.

If the hysteresis loop is of non-elliptical shape, the operative mechanism is non-linear. It is reported by Singh *et al.* (1991) that linear damping can occur up to a strain amplitude of 10^{-3} for polymer-matrix, and 10^{-6} for metal-matrix composites.

One of the attractive characteristics of composites is the possibility of introducing additional sources of damping by controlling the nature of the fibre and matrix interface. This interface can provide significant enhancement of material

damping through the following mechanisms:

a) the energy loss at the interface;

b) the friction at the interface caused by relative motion between the matrix and the fibre.

Studies reported by McLean and Read (1975), and Gibson *et al.* (1982) indicate that the vibration damping properties of polymer-matrix composites may be significantly improved and optimized by using discontinuous fibres rather than continuous fibres. One possible explanation for this phenomenon, given by Nelson and Hancock (1979), is the presence of shear stress concentrations at the numerous fibre ends in a discontinuous fibre composite and the resulting shear stress transfer to the viscoelastic matrix. When a short-fibre composite is subjected to a cyclic strain, the matrix at the fibre interface near the ends of the fibre undergoes a high cyclic shear strain, which in turn produces significant viscoelastic energy losses. It was reported that most of the energy dissipation in polymers is due to shear strain and very little is caused by dilatational strains.

The shear stress concentration may also induce plastic effects as well as partially debonding at the fibre-matrix interface. This will result in slip between the fibre and the matrix and induce frictional losses. The effect of interfacial slip on damping was investigated by McLean and Read (1975), Nelson and Hancock (1979). However, such a fibre-matrix debonding would adversely affect the strength and stiffness of

the composite. Therefore it is desirable to have a strong interfacial bond where slip at the interface can be avoided.

For metal-matrix composites, the application of whisker and particulate composites could lead to increased damping via an increased dislocation density near the interfaces as reported by Wolfenden and Wolla (1991). Another way to achieve high damping in a metal-matrix composite is to subject it to sufficiently high loads to cause the matrix to deform plastically as noted by Bert (1980).

The important parameters which affect damping are identified as: the stiffness ratio E_f/E_m, the fibre volume fraction V_f, and the fibre aspect ratio l/d. These were investigated by Adams (1973, 1988), Sun *et al.* (1985 a, b, 1987). The fibre orientation, the stacking sequences and the associated frequencies were studied by Crawley *et al.* (1983) and Crawley (1984). The strain levels were studied by Varschavsky (1972), Weiss (1977) and Deonath and Rohatgi (1981). The environmental influences, such as temperature and moisture, were reported by Roylance (1976), Maymon *et al.* (1977), Rehfield and Briley (1978), and Creama *et al.* (1991). Due to the diversity and complexity of the damping mechanisms it is difficult to realize a complete characterization of the damping capacities even for a single composite material.

Very limited data are available today regarding the dynamic stiffness and damping of the laminated composites. Moreover, the data are extremely sparse and dependent on the

method of measurement applied.

2.2.3. The mathematical treatment of damping in macromechanical analysis

The need for a quantitative description of material damping has led to damping expressions in terms of various experimentally determined parameters. Almost all modes of damping are based on the concepts of a linear single degree of freedom system. A brief description of the commonly used parameters and their relationships were reported by Lazan (1965), Bert (1980), and Rawal *et al.* (1985). These are based on the following aspects:

a) The specific damping energy (ΔU), and the specific damping capacity (ψ).

ΔU is defined as the unit energy absorbed by a microscopically uniform material per unit volume per cycle of loading as shown in Figure 2.4 a, and is given by:

$$\Delta U = \oint \sigma d\varepsilon \ . \tag{2.20}$$

ψ is the ratio of ΔU to the maximum strain energy (U) per unit volume as shown in Figure 2.4 b and is given by:

$$\psi = \frac{\Delta U}{U} \ . \tag{2.21}$$

b) The damping ratio (ξ), and the quality factor (Q).

ξ is defined as the ratio of the natural damping coefficient to the critical one which can be calculated using the half-power bandwidth method as shown in Figure 2.5 and is given by:

$$\xi = \frac{\Delta f}{2f_n} , \tag{2.22}$$

where Δf is the band width at half power points of the resonant peak for the nth mode and f_n is its associated resonant frequency. The quality factor, Q, is defined as

$$Q = \frac{1}{2\xi} = \frac{f_n}{\Delta f} . \tag{2.23}$$

c) The complex modulus (E^*), the loss factor (η), and the loss angle (ϕ).

Applying the complex-stiffness approach to the material stiffness (elastic modulus), one obtains:

$$\begin{aligned} E^* &= E_1 + iE_2 \\ &= E_1(1 + i\eta) \\ &= E_1(1 + i\tan\phi) . \end{aligned} \tag{2.24}$$

Here E^* is the complex modulus of elasticity. E_1 is known as storage modulus, as it is related to storing energy in the volume; and E_2 is defined as the loss modulus or dissipation modulus because it is related to the

dissipation of energy in the volume. η is called the loss factor, and ϕ is the loss angle by which the strain lags behind the load. The relationship between them is as given in Figure 2.6 and is described by:

$$\eta = \tan \phi = \frac{E_2}{E_1} . \qquad (2.25)$$

d) The logarithmic decrement (δ).

It describes the decay of free vibration and is defined as in Figure 2.7. For two successive peaks one can write:

$$\delta = \ln\left(\frac{a_i}{a_{i+1}}\right) . \qquad (2.26)$$

For n peaks one obtains:

$$\delta = \frac{1}{n} \ln\left(\frac{a_i}{a_{i+n}}\right) . \qquad (2.27)$$

The different ways used for the definition of the damping are interrelated provided that the damping is low. Moreover, the simple relationship between damping parameters is independent of the different mechanisms of energy dissipation as reported by Rawal *et al.* (1985) who reported the following relation:

$$\eta = \frac{\psi}{2\pi} = 2\xi = \frac{1}{Q} = \frac{E_2}{E_1} = \frac{\delta}{\pi} = \frac{\Delta U}{2\pi U} = \tan \phi . \qquad (2.28)$$

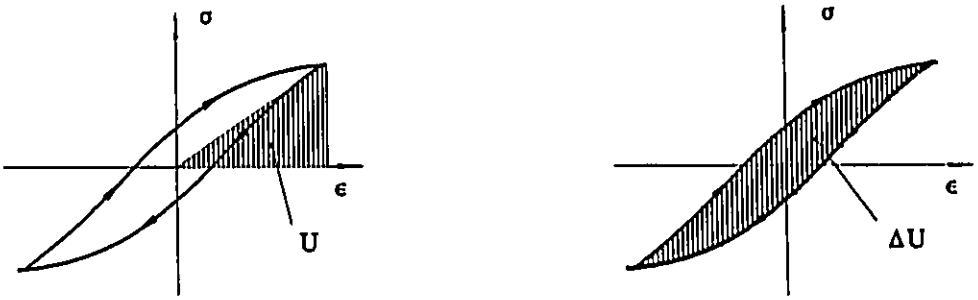

(a) Maximum strain energy U

(b) Specific damping energy D

Figure 2.4 Definition of energies

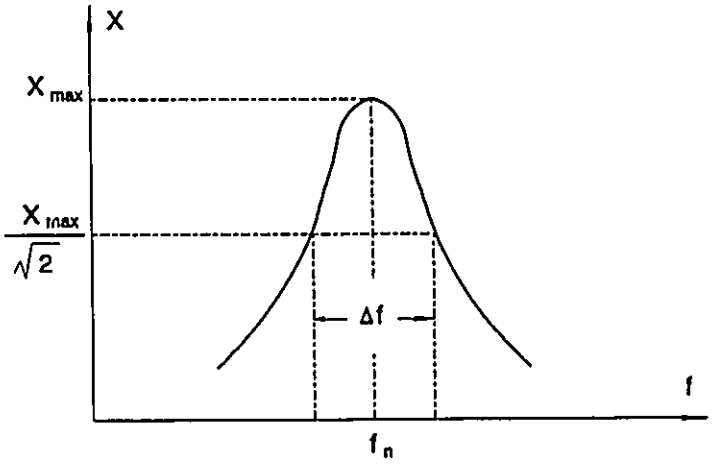

Figure 2.5 Band-width of response curve

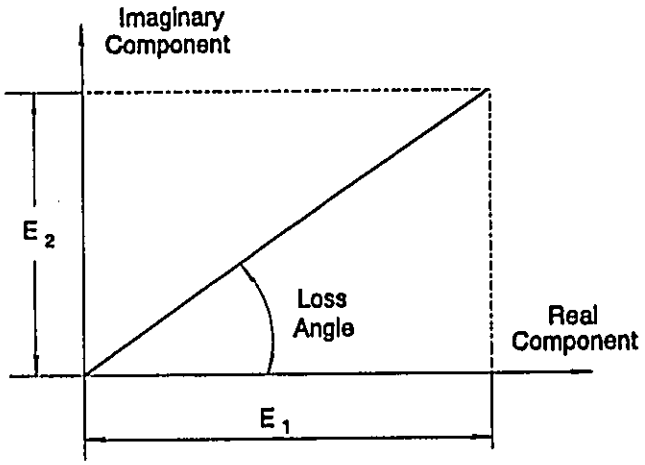

Figure 2.6 Concept of complex modulus and loss angle

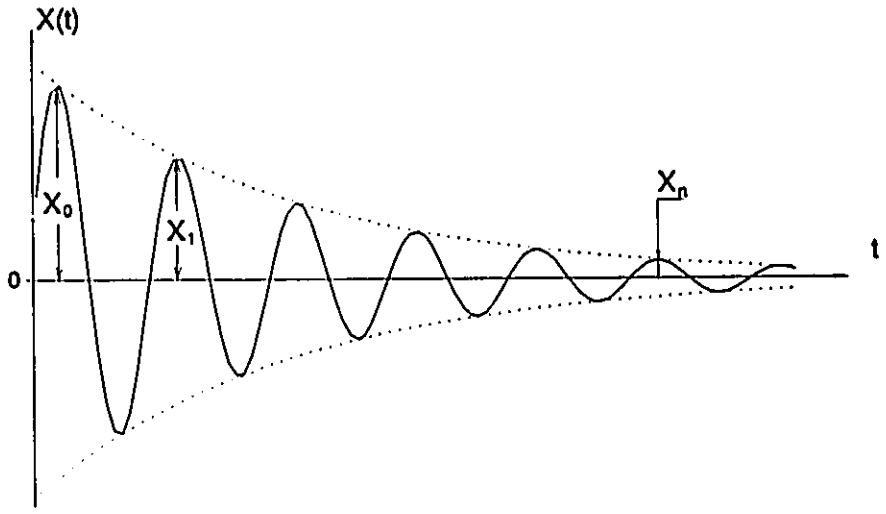

Figure 2.7 Dacay of damped vibration system

The constitutive relation for a viscoeleastic material is generally written in the following form which is reported by Hashin (1970):

$$\sigma_{ij}(t) = \int_{-\infty}^{t} C_{ijkl}(t-\tau) \frac{\partial \varepsilon_{kl}(\tau)}{\partial \tau} d\tau \ , \qquad (2.29)$$

where σ_{ij} and ε_{kl} are the stress and strain tensors, respectively; C_{ijkl} is the relaxation moduli tensor. In the case where the composite is subjected to a sinusoidal strain, one obtains

$$\sigma_{ij} = B^{*}_{ijkl}(\omega) \ \varepsilon_{kl} \ , \qquad (2.30)$$

where $B^{*}_{ijkl}(\omega)$, termed the complex moduli tensor, is generally complex and frequency dependent. It can be written as:

$$B^{*}_{ijkl} = (B_{ijkl})_R + i(B_{ijkl})_I \ . \qquad (2.31)$$

The procedure of replacing the elastic moduli by complex moduli for a viscoelastic material is called by Schapery (1974) the "Correspondence Principle".

In the macromechanical analysis of laminated composites, the success of closely predicting the material damping is obviously dependent upon the underlying assumptions used to build the model. Many investigators have adopted the assumption of viscoelasticity to determine complex moduli of polymer-matrix composites as reported by Gibson *et al.* (1982), Alam and Ashani (1986) and Sun *et al.* (1987,). The dominant

mechanism of damping is the viscoelastic energy dissipation in polymer materials. The complex modulus in equation (2.24) is a concise form to describe the damping properties of viscoelastic materials. The mathematical theory of linear viscoelasticity is reasonably complete. Various aspects, such as, creep, stress-relaxation, relaxation-time spectrum, the complex compliance, *etc.*, can be related to each other by mathematical transformations of varying degrees of complexity.

Sun *et al.* (1985), using micromechanical analysis, studied unidirectionally aligned short fibre composites. They made use of the principle of force-balance, elastic-viscoelastic correspondence and the energy approach. The damping η_L along the longitudinal direction, damping η_T along the transverse direction, shear damping $\eta_{G_{LT}}$, and the damping $\eta_{\mu_{LT}}$ of Poisson's ratio were all derived in terms of E_f/E_m, G_f/G_m, η_f, η_m, fibre volume friction V_f, fibre aspect ratio l/d, and the angle θ between fibre orientation and forcing direction. That work is so significant that one could then use the known damping coefficients as the input data in the macromechanical analysis of laminated composites.

The following aspects of damping should be taken into account when studying the dynamic behaviour of structural systems:

a) There is a growing need to accurately describe the damping properties through mathematical models which are

simple, yet representative of the behaviour of the real material. For metallic materials, however, great difficulty has been encountered in producing a parametric approach comparable to that which was developed for polymeric materials. According to Lazan (1959, 1965), the formulation of the complex modulus in linear viscoelasticity not only provides a basic, minimum and mathematically consistent description, but is also very convenient computationally.

b) The significant features of polymer-matrix composite materials are their dependence, both stiffness and damping, on frequency and temperature, which can be expressed as:

$$E^* = E(\omega, T) \ , \qquad \eta = \eta(\omega, T) \ , \tag{2.32}$$

where ω is the angular frequency; and T is the temperature. The viscoelastic assumption does lead to these effects as demonstrated by Lazan (1959), and Nashif *et al.* (1985).

c) Unlike the viscous damping which is restricted to be linearly proportional to velocity, the loss modulus may be a more generalized and realistic description of material damping as reported by Lee (1987).

However, some of investigators such as, Adams and Bacon (1973), Morison (1982), Lin *et al.* (1984), and Xiao *et*

al. (1988) made use of the definition of specific damping capacity, ψ, to study the damped system of polymer-matrix composites. Low damping was assumed to facilitate the evaluation of damping using the mode shapes of the associated undamped system. According to Adams and Bacon (1973), that approach has the advantages, over viscoelastic or complex modulus models, that materials with stress dependent damping can be accounted for and that the energy dissipation throughout the laminate can be examined in detail.

In the early analyses by Adams and Bacon (1973) and Morison (1982), they considered the input parameters of damping to the analytical models to be given by ψ_L, ψ_T, and ψ_{LT} for each lamina. Three components are involved in the total energy dissipation of the element in the following form:

$$\delta(\Delta U) = \delta(\Delta U_1) + \delta(\Delta U_2) + \delta(\Delta U_{12}) \ . \qquad (2.33)$$

Liao *et al.* (1986) used this model to design symmetric laminated beams with optimal damping and optimal stiffness. This model, however, is not complete because the energy loss due to the shear deformation was not included. Lin *et al.* (1984), and Xiao *et al.* (1988) added to it another damping parameter to account for ψ_{TT}, and the total energy dissipation of the element becomes

$$\delta(\Delta U) = \delta(\Delta U_1) + \delta(\Delta U_2) + \delta(\Delta U_{12}) + \delta(\Delta U_{23}) + \delta(\Delta U_{13}) \ , \qquad (2.34)$$

in which

$$\begin{aligned}
\delta(\Delta U_1) &= \frac{1}{2}\psi_L \varepsilon_{11}\sigma_{11} , \\
\delta(\Delta U_2) &= \frac{1}{2}\psi_T \varepsilon_{22}\sigma_{22} , \\
\delta(\Delta U_{23}) &= \frac{1}{2}\psi_{TT} \varepsilon_{23}\sigma_{23} , \\
\delta(\Delta U_{13}) &= \frac{1}{2}\psi_{LT} \varepsilon_{13}\sigma_{13} , \\
\delta(\Delta U_{12}) &= \frac{1}{2}\psi_{LT} \varepsilon_{12}\sigma_{12} .
\end{aligned} \tag{2.35}$$

In the numerical studies, they found that ψ_{TT} is not important because changing its value by 15% gave no significant difference in the overall theoretical values. Thus, they assigned $\psi_{TT} = \psi_{LT}$ in their prediction of vibrational damping of free laminated plate.

Hwang and Gilbson (1991) used three-dimensional stress components to study the damping of laminates under uniaxial extension. That model accounts for the damping η_z due to the interlaminar normal stress σ_z. This was found to be particularly important for a thick plate.

The majority of the damping studies have been conducted on the polymer-matrix composites. There exist limited investigations on material damping for metal-matrix composites. A significant work in this regard was reported by Kinra *et al.* (1991), where they extended the model of Ni and Adams (1984), to study the flexural and axial damping of metal-matrix composites. A close agreement between theory and experiment was reported.

2.2.4. Solutions of viscoelastically damped systems

The linear viscoelastic assumption was used in modelling damping for composite materials, particularly for a polymer-matrix. In this modelling approach, the discretized equation of motion using finite element method is usually written in the form:

$$[M]\{\ddot{x}\} + [K^*]\{x\} = \{f\}, \tag{2.36}$$

where [M] - mass matrix;

[K*] - complex stiffness matrix;

{x}, {ẍ} - vectors of nodal displacements, and accelerations, respectively;

{f} - vector of applied node loads.

There exist four distinct techniques to study the system in the frequency domain. These are:

a) the Direct Frequency Response method,

b) the Complex Eigenvalue method,

c) the Modal Strain Energy (MSE) method,

d) the Perturbation method.

The direct frequency response method assumes the input in the form of a forced excitation at a given frequency as reported by Johnson and Kienholz (1982) and Brockman (1984). The models take the form:

$$\left([K^*(\omega)] - \omega^2[M]\right)\{X(\omega)\} = \{F(\omega)\}, \tag{2.37}$$

or

$$[H(\omega)]^{-1}\{X(\omega)\} = \{F(\omega)\}, \tag{2.38}$$

The corresponding displacement shapes are obtained by solving a system of complex-valued linear equations. The behaviour of the system over a range of frequencies is defined by evaluating the response at several frequencies, and plotting the resulting amplitude and phase shifts versus the forcing frequency. Sun *et al.* (1990) applied this method to evaluate the loss factor of a sandwich beam.

The two main drawbacks of this method are quite substantial. First, the computational effort is greatly increased since the complex coefficient matrix on the left must be formed, inverted, and stored for each frequency of interest in order to obtain a complete solution. This is generally impractical for any but very small problems as reported by Johnson and Kienholz (1982). Second, numerical errors associated with the inversion of ill-conditioned matrices are also possible in the case of lightly damped systems as noted by Bellos and Inman (1990).

The unforced motion of the system can be derived from relation (2.36) in the following form:

$$([K^*(\omega)] - \omega^2[M])\{X\} = \{0\}. \tag{2.39}$$

This is an algebraic eigenvalue problem with complex eigenvalues and eigenvectors. The general forced response for

any input may then be evaluated as a weighted sum of the free responses. Using this method, Alam and Ashani (1986) investigated the flexural damping of a simply supported rectangular plate.

This method gives an exact solution to the problem. However, its main drawback is the high computational cost. Joseph (1974) reported that the complex eigenvalue method is three times more costly than the corresponding undamped eigensolution. There exist few general purpose finite element packages, such as NASTRAN, which has the capability of solving complex eigenvalue problems.

With much less cost in computation, the Modal Strain Energy approach assumes that the damped structure can be represented in terms of the real normal modes of the associated undamped system if appropriate damping terms are inserted into the uncoupled modal equations of motion. This method was first suggested by Kerwin and Ungar in 1962, and then developed later by Johnson and Kienholz (1982) and Soni (1982). It was used to predict damping in sandwich structures, where the material loss factor was found to be very small compared with that of the viscoelastic core. In this situation, the loss factor can be approximated by

$$\eta^{(r)} = \eta_v \frac{U_v^{(r)}}{U^{(r)}} , \qquad (2.40)$$

where η_v is the material loss factor of viscoelastic core and

$U_v^{(r)}/U^{(r)}$ is the ratio of elastic strain energy attributable to the sandwich core when the structure deforms in the rth mode shape.

Shen and Stevens (1984) applied the first-order perturbation method to study the flexural damping of a viscoelastically coated beam. In that study, they solved a real eigenvalue problem without considering the coat layer. They later augmented [K] and [M] by [ΔK] and [ΔM] due to the coat. This led to a new set of eigenpairs for the system in the following form:

$$\begin{aligned} (\bar{\lambda}^{(i)})^2 &= (\lambda^{(i)})^2 + (\Delta\lambda^{(i)})^2, \\ \{\bar{\phi}\}^{(i)} &= \{\phi\}^{(i)} + \{\Delta\phi\}^{(i)} , \end{aligned} \tag{2.41}$$

where $(\lambda^{(i)})^2$ and $\{\phi\}^{(i)}$ are the eigenpairs of the undamped system in the ith mode. The first-order corrections are given by:

$$\begin{aligned} (\Delta\lambda^{(i)})^2 &= \frac{\{\phi\}^{(i)T}\left[[\Delta K] - (\lambda^{(i)})^2[\Delta M]\right]\{\phi\}^{(i)}}{\{\phi\}^{(i)T}[M]\{\phi\}^{(i)}} , \\ \Delta\{\phi\}^{(i)} &= \sum_{\substack{j=1 \\ j\neq i}}^{n} \alpha_{ij}\{\phi\}^{(i)} , \end{aligned} \tag{2.42}$$

where

$$\alpha_{ij} = \frac{\{\phi\}^{(j)T}\left[[\Delta K] - \lambda^{(i)2}[\Delta M]\right]\{\phi\}^{(i)}}{(\lambda^{(i)2} - \lambda^{(j)2})\left(\{\phi\}^{(i)T}[M]\{\phi\}^{(i)}\right)} . \tag{2.43}$$

The last two methods give approximation solutions to the problem. The greatest advantage of using these two methods is the saving realized in computational cost by solving a real

in place of a complex eigenvalue problem. The perturbation method can account for frequency-dependent material properties, but suffers the drawback of being incapable of solving a system with repeated eigenvalues as seen from equation (2.43). The Modal Strain Energy method is gaining acceptance and is frequently used by investigators for tackling the viscoelastic damping problem. However, no rigorous error analysis is available in the literature regarding this method.

Nashif *et al.* (1985) and Jones (1986) found the noncausality of the form $\{f(t)\} \neq 0$ for $t < 0$ in a single degree of freedom system. The problem arises because $[K^*]$ is assumed to be constant, which is an excessively restrictive idealization of the behaviour of real polymeric materials.

Apart from the frequency-domain methods above, a time-domain realization method has been used to study vibrations of viscoelastic structures. Based on linear system theory, this method enables the analyst to represent a given system by an equivalent system. For the given equation (2.36), Golla and Hughes (1985) developed a symmetrical matrix-second-order realization in viscous damping mechanisms:

$$[M^+]\{\ddot{x}^+\} + [C^+]\{\dot{x}^+\}[K^+]\{x^+\} = \{f^+\}, \qquad (2.44)$$

where $[M^+]$, $[C^+]$, and $[K^+]$ are the augmented mass, damping, and stiffness matrices, respectively. The superscript $^+$ denotes that the system of coordinates has been augmented by

the inclusion of an appropriate set of "dissipation coordinates". Their method can tackle frequency-dependent materials but the computational cost is increased because of the augmentation.

In 1990, Zabaras and Pervez applied an analysis similar to that of Lin *et al.* (1984) to predict specific damping capacity for the first two fundamental modes. Then they obtained the equivalent viscous damping ratio to form a Rayleigh damping matrix [C] for the prediction of damping in laminated plates. The approach can get rid of noncausal behaviour of the response, but needs further experimental verification.

CHAPTER 3

THEORETICAL FORMULATIONS

3.1. Basic assumptions

In studying laminated composites from a viewpoint of macromechanical analysis, the idealization of the problem is an important step. The following assumptions are made:

a) Perfect bonding exists between the fibres and the matrix. Consequently one assumes no slip at the interfaces of the layers.

b) The bonds are presumed to be infinitesimally thin as well as non-shear-deformable otherwise they will be considered as layers.

c) The composites behave in a manner similar to linear materials.

d) Each lamina is treated as a homogeneous and transversely isotropic continuum.

e) The displacements u, v, and w are small compared to the plate thickness.

f) The transverse normal strain ε_z is negligible;

g) Only material damping is considered. Damping due to other sources, *i e.*, air damping and/or joint damping, is neglected.

3.2. Theoretical foundation for undamped vibration analysis

The First-order Shear Deformation Theory is adopted because it is simple in modelling and it is economic and reasonably accurate computationally.

The displacement field is considered to be in the following form:

$$\begin{aligned} u(x,y,z,t) &= u^{o}(x,y,t) - z\psi_x(x,y,t) \ , \\ v(x,y,z,t) &= v^{o}(x,y,t) - z\psi_y(x,y,t) \ , \\ w(x,y,z,t) &= w^{o}(x,y,t) \ . \end{aligned} \tag{3.1}$$

Assuming that the displacements are small, one can write the strain-displacement relations as follows:

$$\begin{aligned} \varepsilon_x &= \varepsilon_x^{o} + z\kappa_x \ , \\ \varepsilon_y &= \varepsilon_y^{o} + z\kappa_y \ , \\ \varepsilon_z &= 0 \ , \\ \gamma_{yz} &= \psi_y + w_{,y} \ , \\ \gamma_{xz} &= \psi_x + w_{,x} \ , \\ \gamma_{xy} &= \gamma_{xy}^{o} + z\kappa_{xy} \ . \end{aligned} \tag{3.2a}$$

In these expressions, one defines

$$\{\varepsilon^{o}\} = \begin{Bmatrix} \varepsilon_x^{o} \\ \varepsilon_y^{o} \\ \gamma_{xy}^{o} \end{Bmatrix} = \begin{Bmatrix} u_{,x}^{o} \\ v_{,y}^{o} \\ u_{,y}^{o} + v_{,x}^{o} \end{Bmatrix} , \tag{3.2b}$$

and

$$(\kappa) = \begin{Bmatrix} \kappa_x \\ \kappa_y \\ \kappa_{xy} \end{Bmatrix} = \begin{Bmatrix} \psi_{x,x} \\ \psi_{y,y} \\ \psi_{x,y} + \psi_{y,x} \end{Bmatrix} . \qquad (3.2c)$$

The quantities ε_x^o, ε_y^o, and γ_{xy}^o represent midsurface strains, while the κ_x and κ_y are bending curvatures and κ_{xy} is the twisting of the plate.

The following notations of stresses and strains are adopted to facilitate the mathematical derivation in what follows:

$$\sigma_1 = \sigma_{11},\ \sigma_2 = \sigma_{22},\ \sigma_3 = \sigma_{33},\ \sigma_4 = \tau_{23},\ \sigma_5 = \tau_{13},\ \sigma_6 = \tau_{12},$$

$$\varepsilon_1 = \varepsilon_{11},\ \varepsilon_2 = \varepsilon_{22},\ \varepsilon_3 = \varepsilon_{33},\ \varepsilon_4 = \gamma_{23},\ \varepsilon_5 = \gamma_{13},\ \varepsilon_6 = \gamma_{12} . \qquad (3.3)$$

Suffix 1 denotes the fibre direction, while 2 and 3 are the two directions transverse to that of the fibre. The constitutive relations for any layer in this fibre-aligned coordinate system are given as

$$\begin{Bmatrix} \sigma_1 \\ \sigma_2 \\ \sigma_4 \\ \sigma_5 \\ \sigma_6 \end{Bmatrix} = \begin{bmatrix} Q_{11} & Q_{12} & 0 & 0 & 0 \\ Q_{12} & Q_{22} & 0 & 0 & 0 \\ 0 & 0 & Q_{44} & 0 & 0 \\ 0 & 0 & 0 & Q_{55} & 0 \\ 0 & 0 & 0 & 0 & Q_{66} \end{bmatrix} \begin{Bmatrix} \varepsilon_1 \\ \varepsilon_2 \\ \varepsilon_4 \\ \varepsilon_5 \\ \varepsilon_6 \end{Bmatrix} , \qquad (3.4)$$

where Q_{ij} are the plane-stress reduced stiffness components in the material axes (123) of the lamina with:

$$Q_{11} = \frac{E_1}{1-\mu_{12}\mu_{21}} = \frac{E_L}{1-(\mu_{LT})^2\frac{E_T}{E_L}} ,$$

$$Q_{12} = \frac{\mu_{12}E_2}{1-\mu_{12}\mu_{21}} = \frac{\mu_{LT}E_T}{1-(\mu_{LT})^2\frac{E_T}{E_L}} ,$$

$$Q_{22} = \frac{E_2}{1-\mu_{12}\mu_{21}} = \frac{E_T}{1-(\mu_{LT})^2\frac{E_T}{E_L}} , \qquad (3.5)$$

$$Q_{44} = G_{23} = G_{TT} ,$$

$$Q_{55} = G_{13} = G_{LT} ,$$

$$Q_{66} = G_{12} = G_{LT} ,$$

where E_L, E_1 = Young's modulus along the longitudinal direction of the fibres;

E_T, E_2 = Young's modulus along the transverse direction of the fibres;

G_{LT}, G_{12}, G_{13} = Shear modulus relative to L-T the plane;

G_{TT}, G_{23} = Interlaminar shear modulus relative to the T-Z plane;

μ_{LT}, μ_{12} = Major Poisson's ratio as measured from the transverse contraction under uniaxial tension parallel to the fibres.

The global relationship between stresses and strains

are given by:

$$\begin{Bmatrix} \sigma_x \\ \sigma_y \\ \sigma_{yz} \\ \sigma_{xz} \\ \sigma_{xy} \end{Bmatrix} = \begin{bmatrix} \overline{Q}_{11} & \overline{Q}_{12} & 0 & 0 & \overline{Q}_{16} \\ \overline{Q}_{12} & \overline{Q}_{22} & 0 & 0 & \overline{Q}_{26} \\ 0 & 0 & \overline{Q}_{44} & \overline{Q}_{45} & 0 \\ 0 & 0 & \overline{Q}_{45} & \overline{Q}_{55} & 0 \\ \overline{Q}_{16} & \overline{Q}_{26} & 0 & 0 & \overline{Q}_{66} \end{bmatrix} \begin{Bmatrix} \varepsilon_x \\ \varepsilon_y \\ \gamma_{yz} \\ \gamma_{xz} \\ \gamma_{xy} \end{Bmatrix} , \qquad (3.6)$$

where

$$\begin{aligned}
\overline{Q}_{11} &= Q_{11}m^4 + 2(Q_{12} + 2Q_{66})m^2n^2 + Q_{22}n^4 , \\
\overline{Q}_{12} &= (Q_{11} + Q_{22} - 4Q_{66})m^2n^2 + Q_{12}(m^4 + n^4) , \\
\overline{Q}_{22} &= Q_{11}n^4 + 2(Q_{12} + 2Q_{66})m^2n^2 + Q_{22}m^4 , \\
\overline{Q}_{16} &= (Q_{11} - Q_{12} - 2Q_{66})m^3n + (Q_{12} - Q_{22} + 2Q_{66})mn^3 , \\
\overline{Q}_{26} &= (Q_{11} - Q_{12} - 2Q_{66})mn^3 + (Q_{12} - Q_{22} + 2Q_{66})m^3n , \qquad (3.7) \\
\overline{Q}_{44} &= Q_{44}m^2 + Q_{55}n^2 , \\
\overline{Q}_{45} &= (Q_{55} - Q_{44})mn , \\
\overline{Q}_{55} &= Q_{55}m^2 + Q_{44}n^2 , \\
\overline{Q}_{66} &= (Q_{11} + Q_{22} - 2Q_{12} - 2Q_{66})m^2n^2 + Q_{66}(m^2 - n^2) ,
\end{aligned}$$

and $m = \cos\theta$, $n = \sin\theta$. The angle θ is as defined in Figure 3.1.

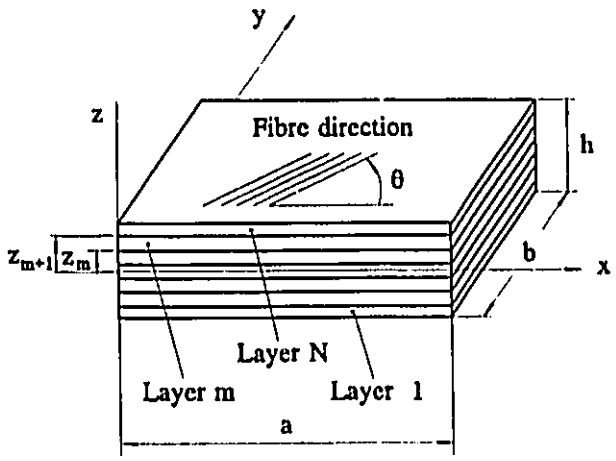

Figure 3.1 Laminated plate geometry and the coordinate system

Introducing the stress and moment resultants per unit length,

$$(N_x,\ N_y,\ N_{xy}) = \int_{-\frac{h}{2}}^{\frac{h}{2}} (\sigma_x,\ \sigma_y,\ \tau_{xy})\ dz\ ,$$

$$(M_x,\ M_y,\ M_{xy}) = \int_{-\frac{h}{2}}^{\frac{h}{2}} (\sigma_x,\ \sigma_y,\ \tau_{xy})\ z dz\ , \qquad (3.8)$$

$$(Q_x,\ Q_y) = \int_{-\frac{h}{2}}^{\frac{h}{2}} (\tau_{xz},\ \tau_{yz})\ dz\ ,$$

one can thus write the plate's constitutive equation in the following compact form:

$$\begin{Bmatrix} \{N\} \\ \{M\} \end{Bmatrix} = \begin{bmatrix} [A] & [B] \\ [B]^T & [D_b] \end{bmatrix} \begin{Bmatrix} \{\varepsilon^0\} \\ \{\kappa\} \end{Bmatrix} , \qquad (3.9a)$$

and

$$\begin{Bmatrix} Q_x \\ Q_y \end{Bmatrix} = [D_s] \begin{Bmatrix} \varepsilon_{xz} \\ \varepsilon_{yz} \end{Bmatrix} . \qquad (3.9b)$$

The components A_{ij}, B_{ij}, D_{bij} (i,j = 1, 2, 6) refer to the in-plane, bending-stretching, and bending stiffness of the plate, respectively. They are defined by:

$$(A_{ij},\ B_{ij},\ D_{bij}) = \sum_{m=1}^{N} \int_{z_m}^{z_{m+1}} \bar{Q}_{ij}^{(m)}(1,\ z,\ z^2)\,dz \qquad (i,j=1,2,6) , \qquad (3.10a)$$

and the components of the shear stiffness D_{sij} (i,j = 4, 5) are defined by:

$$(D_{sij}) = \sum_{m=1}^{N} K_i K_j \int_{z_m}^{z_{m+1}} \bar{Q}_{ij}^{(m)} dz \qquad (i,j=4,5) , \qquad (3.10b)$$

where K_i are the shear correction coefficients.

The equations of motion can then be derived using Hamilton's principle:

$$\int_{t_0}^{t_1} \delta L\ dt = 0 , \qquad (3.11)$$

where δL is the first variation of the Lagrangian and is defined by

$$\delta L = \delta\pi - \delta K$$
$$= \int_R (\delta\varepsilon_1^o N_1 + \delta\varepsilon_2^o N_2 + \delta\varepsilon_6^o N_6 + \delta\kappa_1 M_1 + \delta\kappa_2 M_2 + \delta\kappa_6 M_6$$
$$+ \delta\varepsilon_4 Q_2 + \delta\varepsilon_5 Q_1 + \delta wq)\, dx\, dy - \int \check{N}_n \delta u_n dS$$
$$- \int_{C_i} \check{N}_s \delta u_s dS - \int_{C_i} \check{M}_n \delta\psi_n dS - \int_{C_i} \check{M}_t \delta\psi_s dS - \int_{C_i} \check{Q}_n \delta w dS$$
$$- \int_V \rho (\dot{u}\delta\dot{u} + \dot{v}\delta\dot{v} + \dot{w}\delta\dot{w})\, dV \ , \tag{3.12}$$

where π and K are the total potential and kinetic energies. $\check{N}_n$ $\check{N}_t$, $\check{M}_n$, $\check{M}_t$ and $\check{Q}_n$ are the normal or tangential resultants on the boundary segments C_i. The following contracted notations were also used in writing equation (3.12):

$$N_1 = N_x,\ N_2 = N_y,\ N_6 = N_{xy},\ M_1 = M_x,\ M_2 = M_y,\ M_6 = M_{xy},$$
$$Q_1 = Q_x,\ Q_2 = Q_y,$$
$$\varepsilon_1^o = \varepsilon_x^o,\ \varepsilon_2^o = \varepsilon_y^o,\ \varepsilon_6^o = \varepsilon_{xy}^o,\ \varepsilon_4 = \varepsilon_{yz},\ \varepsilon_5 = \varepsilon_{xz}, \tag{3.13}$$
$$\kappa_1 = \kappa_x,\ \kappa_2 = \kappa_y,\ \kappa_6 = \kappa_{xy}\ .$$

Substituting equation (3.2) in equation (3.12) and integrating by parts with respect to to time and the spatial coordinates (xyz), one obtains the equations of motion as:

$$N_{x,x} + N_{xy,y} = I_1\ddot{u} + I_2\ddot{\psi}_x \ ,$$
$$N_{xy,x} + N_{y,y} = I_1\ddot{v} + I_2\ddot{\psi}_y \ ,$$
$$Q_{x,x} + Q_{y,y} = q + I_1\ddot{w} \ , \tag{3.14}$$
$$M_{x,x} + M_{xy,y} - Q_x = I_3\ddot{\psi}_x + I_2\ddot{u} \ ,$$
$$M_{xy,x} + M_{y,y} - Q_y = I_3\ddot{\psi}_y + I_2\ddot{v} \ .$$

Here I_1, I_2, and I_3 are the normal, coupled normal-rotary and rotary inertia coefficients, respectively. One can thus write:

$$(I_1,\ I_2,\ I_3) = \int_{-\frac{h}{2}}^{\frac{h}{2}} (1, z, z^2)\ \rho dz = \sum_{m=1}^{N} \rho^{(m)} \int_{z_m}^{z_{m+1}} (1,\ z,\ z^2) dz\ . \tag{3.15}$$

The midplane R of the plate is supposed to be subdivided into a finite number of elements, R_e (e=1,2,...). Over each element, R_e, the generalized displacements (u,v,w,ψ_x,ψ_y) are expressed in the following form:

$$u = \sum_{i=1}^{n} u_i N_i, \qquad v = \sum_{i=1}^{n} v_i N_i, \qquad w = \sum_{i=1}^{n} w_i N_i,$$
$$\psi_x = \sum_{i=1}^{n} \psi_{xi} N_i, \qquad \psi_y = \sum_{i=1}^{n} \psi_{yi} N_i, \tag{3.16}$$

where N_i represents the interpolation functions associated with the ith node. The total number of nodes in an element is denoted by n.

The total Lagrangian in equation (3.12) can be expressed in terms of the displacements (u,v,w,ψ_x,ψ_y). Following the conventional finite element procedures, one can obtain the following relation:

$$[M]\ \{\ddot{x}\} + [K]\{x\} = \{f\}, \tag{3.17}$$

where [K] = the global stiffness matrix;

[M] = the global mass matrix;

{x}, {ẍ} = vectors of nodal displacements and accelerations, respectivaly;

{f} = the vector of nodal forces.

For the free vibration problem, equation (3.17) becomes

$$([K] - \omega^2[M])\{\phi\} = \{0\}, \tag{3.18}$$

where ω and $\{\phi\}$ are the natural undamped frequency and the eigenvector of the system, respectively.

3.3. Modelling of damping for laminated composite plates

3.3.1 Scope of the study

Since there are many physical mechanisms for energy dissipation, it would be almost impossible to establish a complete characterization of damping for a composite material. However, it is necessary, for engineering applications, to describe the damping properties in the form of a reasonably accurate mathematical model which should be simple, yet representative of the behaviour of real materials. For laminated composite material, two levels of material damping studies should be realized; the micromechanical and macromechanical.

Figure 3.2 shows the input and output parameters and data which are necessary for the two studies. The input data for the macromechanical analysis are obtained from the results of the micromechanical analysis or from experimental measurements.

In the present work, the formulations of the two macromechanical damping models, namely, the Viscoelastic Damping (VED) model, and the Specific Damping Capacity (SDC) model, are derived from an application-oriented viewpoint.

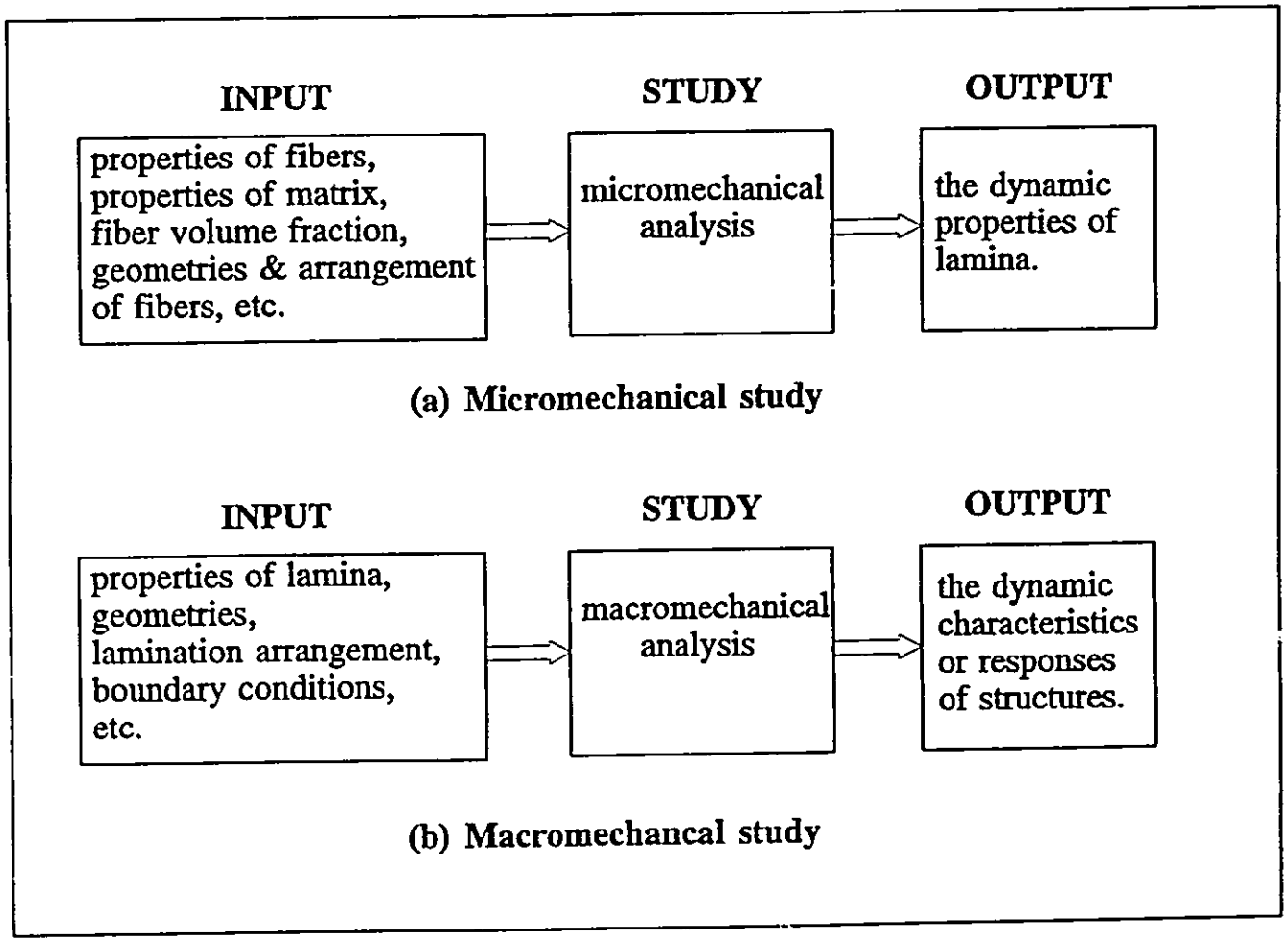

Figure 3.2 Input and output data of material damping studies for laminated composites

3.3.2 Viscoelastic Damping (VED) model

In this model, linear viscoelasticity will be assumed to be representative of the dynamic properties of the composites. According to the Correspondence Principle, the complex expressions of the engineering constants for transversely isotropic materials can be written in the following form:

$$\begin{aligned} E_L^* &= E_L(1 + i\eta_L) \ , \\ E_T^* &= E_T(1 + i\eta_T) \ , \\ G_{LT}^* &= G_{LT}(1 + i\eta_{G_{LT}}) \ , \\ G_{TT}^* &= G_{TT}(1 + i\eta_{G_{TT}}) \ , \\ \mu_{LT}^* &= \mu_{LT}(1 + i\eta_{\mu_{LT}}) \ , \end{aligned} \tag{3.19}$$

where η_L = damping along the longitudinal direction;

η_T = damping along the transverse direction;

$\eta_{G_{LT}}$ = shear damping relative to L-T plane;

$\eta_{G_{TT}}$ = shear damping relative to T-Z plane;

$\eta_{\mu_{LT}}$ = damping of Poisson's ratio;

i = $\sqrt{(-1)}$.

Equation (3.19) yields complex expressions for $[Q^*]$, $[\bar{Q}^*]$, $[A^*]$, $[B^*]$, $[D_b^*]$, $[D_s^*]$, and $[K^*]$. The complex stiffness $[K^*]$ will be written as follows:

$$[K^*] = [K_R] + i\,[K_I]\ , \tag{3.20}$$

where $[K_R]$ = storage stiffness matrix;

$[K_I]$ = damping stiffness matrix.

If there are no rigid body motion modes in the system, the matrix $[K_R]$ will be a real symmetric and positive definite one, but $[K_I]$ may be a semi-positive or positive definite real symmetric matrix.

For the free vibration problem, the discretized version of partial differential equation becomes:

$$[M]\{\ddot{x}\} + [K^*]\{x\} = \{0\}\ . \tag{3.21}$$

Equation (3.21) is converted to a complex eigenvalue problem by assuming a solution of the form

$$\{x\} = \{\phi^*\}^{(r)} \exp\left(i\omega^{*(r)}t\right)\ , \tag{3.22}$$

where $(\omega^{*(r)})^2$ and $\{\phi^*\}^{(r)}$ are the rth complex eigenvalue and eigenvector, respectively. They can be written in the form:

$$\begin{aligned} \omega^{*(r)} &= \omega^{(r)}\sqrt{1 + i\eta^{(r)}}\ , \\ \{\phi^*\}^{(r)} &= \{\phi_R\}^{(r)} + i\,\{\phi_I\}^{(r)}\ , \end{aligned} \tag{3.23}$$

where ω^* is the complex frequency factor, and $\eta^{(r)}$ is the loss factor in the rth mode. The complex eigenvalue problem is then formed from equation (3.21) by substituting equation (3.22) to obtain:

$$\left\{[K^*] - (\omega^{*(r)})^2 [M]\right\} \{\phi^*\} = \{0\}. \tag{3.24}$$

Expanding ω^* in Taylor series, the complex frequency factor can be written in the form as:

$$\omega^* = \omega \left[\left(1 + \frac{\eta^2}{8} - \frac{5\eta^4}{128} + \cdots \right) + i \left(\frac{\eta}{2} - \frac{\eta^3}{16} + \frac{7\eta^5}{256} - \cdots \right)\right] \tag{3.25}$$

providing that η is less than one. Note that the superscript (r) is dropped in equation (3.25) to simplify the notation.

While the real part of ω^* describes the natural frequency, the imaginary part is related to the modal damping. We define the generalized damped natural frequency as follows:

$$\omega_D = real\ (\omega^*) = \omega \left(1 + \frac{\eta^2}{8} - \frac{5\eta^4}{128} + \cdots \right), \tag{3.26}$$

where ω is the natural frequency. It should be noticed that ω in equation (3.23) is not necessarily equal to the natural frequency ω in equation (3.18) of the undamped system. They are generally close to each other in practice. Another form of ω_D for a single degree of freedom system can be written in the form:

$$\omega_D = \frac{\omega}{1 - \frac{\delta^2}{4\pi^2}}, \tag{3.27}$$

where δ is the logarithmic decrement. It is seen from equations (3.26) and (3.27) that ω_D increases with η or δ for the viscoelastically damped free vibrations. It decreases with

the damping ratio ξ for the viscously damped free vibrations. Figure 3.3 shows the curves of ξ and η vis ω_D/ω.

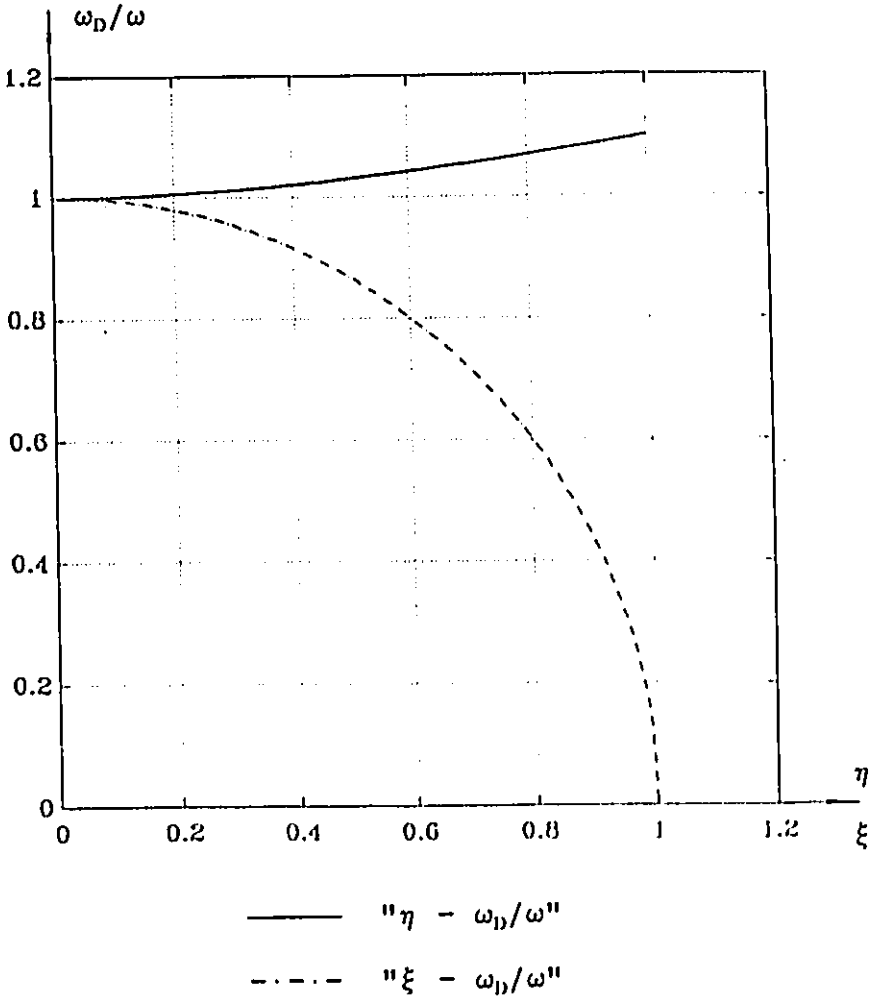

Figure 3.3 "η - ω_D/ω" and "ξ - ω_D/ω" curves.

3.3.3 Specific Damping Capacity (SDC) model

In this approach the internal damping behaviour of materials is quantified through the use of its experimentally determined hysteresis loop shown in Figure 2.4. In this model, the specific damping capacity (SDC) is defined as:

$$SDC = \psi = \frac{\Delta U}{U} , \tag{3.28}$$

where ΔU is the unit energy absorbed by the microscopically uniform material per unit volume per cycle of loading as depicted in Figure 2.4 b. U is the maximum strain energy per unit volume as shown in Figure 2.4 a.

Considering the mth lamina of an arbitrary laminate and assuming that it has unit width and length, one can obtain an expression for the strain energy in the form:

$$U_m = \frac{1}{2}\int_{z_m}^{z_{m+1}} \{\varepsilon\}_m^T \{\sigma\}_m \, dz = \frac{1}{2}\int_{z_m}^{z_{m+1}} \{\varepsilon\}_m^T [Q]_m \{\varepsilon\}_m \, dz . \tag{3.29}$$

Since the strain energy or dissipated energy is independent of the coordinate system, equation (3.29) is considered to be associated with the fibre-aligned coordinate system for convenience.

For a transversely isotropic lamina which exhibits a linear elastic stress-strain response, the strain energy can

be expressed in terms of seven components:

$$U_m = U_{11m} + U_{12m} + U_{21m} + U_{22m} + U_{44m} + U_{55m} + U_{66m} \ , \tag{3.30a}$$

where

$$\begin{aligned}
U_{11m} &= \frac{1}{2} \int_{z_m}^{z_{m+1}} (Q_{11}\varepsilon_1^2)_m \, dz \ , \\
U_{22m} &= \frac{1}{2} \int_{z_m}^{z_{m+1}} (Q_{22}\varepsilon_2^2)_m \, dz \ , \\
U_{12m} = U_{21m} &= \frac{1}{2} \int_{z_m}^{z_{m+1}} (Q_{12}\varepsilon_1\varepsilon_2)_m \, dz \ , \\
U_{44m} &= \frac{1}{2} \int_{z_m}^{z_{m+1}} (Q_{44}\gamma_{23}^2)_m \, dz \ , \\
U_{55m} &= \frac{1}{2} \int_{z_m}^{z_{m+1}} (Q_{55}\gamma_{13}^2)_m \, dz \ , \\
U_{66m} &= \frac{1}{2} \int_{z_m}^{z_{m+1}} (Q_{66}\gamma_{12}^2)_m \, dz \ .
\end{aligned} \tag{3.30b}$$

From the definition of SDC, it is obvious that the total energy dissipated in this lamina is given by the sum of the following seven components:

$$\Delta U_{11m} = \frac{1}{2}\int_{z_m}^{z_{m+1}} (\psi_{11}Q_{11}\varepsilon_1^2)_m \, dz \ ,$$

$$\Delta U_{22m} = \frac{1}{2}\int_{z_m}^{z_{m+1}} (\psi_{22}Q_{22}\varepsilon_2^2)_m \, dz \ ,$$

$$\Delta U_{12m} = \Delta U_{21m} = \frac{1}{2}\int_{z_m}^{z_{m+1}} (\psi_{12}Q_{12}\varepsilon_1\varepsilon_2)_m \, dz \ ,$$

$$\Delta U_{44m} = \frac{1}{2}\int_{z_m}^{z_{m+1}} (\psi_{44}Q_{44}\gamma_{23}^2)_m \, dz \ , \tag{3.31}$$

$$\Delta U_{55m} = \frac{1}{2}\int_{z_m}^{z_{m+1}} (\psi_{55}Q_{55}\gamma_{13}^2)_m \, dz \ ,$$

$$\Delta U_{66m} = \frac{1}{2}\int_{z_m}^{z_{m+1}} (\psi_{66}Q_{66}\gamma_{12}^2)_m \, dz \ ,$$

in which we define

$$\psi_{11} = \psi_L \ , \qquad \psi_{22} = \psi_T \ , \qquad \psi_{12} = \psi_{\mu_{LT}} \ ,$$
$$\psi_{44} = \psi_{G_{TT}} \ , \qquad \psi_{55} = \psi_{66} = \psi_{G_{LT}} \ . \tag{3.32}$$

The total energy dissipation for the mth lamina can be written in the following form:

$$\Delta U_m = \frac{1}{2}\int_{z_m}^{z_{m+1}} \{\varepsilon\}_m^T \, [Q_D]_m \{\varepsilon\}_m \, dz \ , \tag{3.33}$$

where

$$[Q_D] = \begin{bmatrix} \psi_{11}Q_{11} & \psi_{12}Q_{12} & 0 & 0 & 0 \\ \psi_{12}Q_{12} & \psi_{22}Q_{22} & 0 & 0 & 0 \\ 0 & 0 & \psi_{44}Q_{44} & 0 & 0 \\ 0 & 0 & 0 & \psi_{55}Q_{55} & 0 \\ 0 & 0 & 0 & 0 & \psi_{66}Q_{66} \end{bmatrix}. \qquad (3.34)$$

Equation (3.34) leads to a damping stiffness matrix $[K_D]$ which is a real symmetric positive (or semi-positive) definite matrix. It has the same band shape as that of [K]. These properties facilitate the implementation of the model to some existing commercial finite element programs. This result is different from Lin's (1984) formulation for $[K_D]$ which led to an unsymmetric matrix. It is known that the value of k_{ij} in [K] represents an internal force on the jth node when a unit displacement is imposed on the ith node. For a linear material, [K] should be symmetric, *i.e.* $k_{ij} = k_{ji}$, according to the Reciprocity Theorem. Consequently, one should expect a symmetric $[K_D]$.

In this model, it is assumed that the modal frequencies and mode shapes are the same as those of the associated undamped vibration system. Solving the real eigenvalue problem of equation (3.18), one obtains the specific damping capacity in the rth mode as given by:

$$\psi^{(r)} = \frac{\{\phi\}^{(r)T}\,[K_D]\,\{\phi\}^{(r)}}{\{\phi\}^{(r)T}\,[K]\,\{\phi\}^{(r)}}\,, \tag{3.35}$$

where $\{\phi\}^{(r)}$ is the rth mode shape of the system.

3.3.4 Comments on modelling methods

While the philosophy behind the VED model is clear, the underlying principles of the SDC model may be obscure. The definition of SDC provides a generalized and realistic description of material damping in cases where the mechanisms of damping are unknown or too complicated to represent. These two models are different in the mathematical treatment and need to be examined for both polymer-based and for metal-based composites.

Table 3.1 lists the damping coefficients used by other researchers as well as by the present author. It can be seen that the coefficients in the present models are more consistent and complete for implementation in the mathematical models. To the author's understanding, there is no substantial difference between using the damping parameters of ψ and η. The simple relationship between them is given in equation (2.20).

Five elastic constants have to be used for transversely isotropic materials and consequently there should

exist five damping coefficients to describe the damping properties. This study can be extended to most general cases of anelasticity problems according to the Correspondence Principle, in which all stiffness elements C_{ijkl} can be replaced by complex B^{*}_{ijkl}.

The most important feature of the present modelling approaches is that the damping terms are embedded in the matrices of $[K^{*}]$ and $[K_D]$, and are evaluated by the conventional finite element techniques. The implementation of these modelling approaches are straightforward.

However, it should be noted that material damping depends on the frequency and temperature for polymeric materials and on the stress level for metallic materials. A more general form of damping parameters can be assumed in the form:

$$\psi = \psi(\omega, T, \sigma) \ , \qquad or \qquad \eta = \eta(\omega, T, \sigma) \ ,$$

where ω = angular frequency;

T = temperature;

σ = stress tensor.

This assumption yields matrices $[K^{*}]$ and $[K_D]$ which are stress-level, frequency, and temperature-dependent.

Table 3.1 Damping coefficients corresponding to elastic constants of lamina

Adams (1973) (SDC)	Morison (1982) (SDC)	Lin (1984) (SDC)	Adams (1987) (SDC)	Sun (1987) (VED)	Present Author (VED)	Present Author (SDC)	Elastic Constants
ψ_L	ψ_{11}	ψ_1	ψ_L	η_L	η_L	$\psi_L(\psi_{11})$	$E_L(E_1)$
ψ_T	ψ_{22}	ψ_2	ψ_T	η_T	η_T	$\psi_T(\psi_{22})$	$E_T(E_2)$
-	ψ_{12}	-	-	$\eta_{\mu_{LT}}$	$\eta_{\mu_{LT}}$	$\psi_{\mu_{LT}}(\psi_{12})$	$\mu_{LT}(\mu_{12})$
-	-	ψ_{23}	ψ_{TT}	-	$\eta_{G_{TT}}$	$\psi_{G_{TT}}(\psi_{44})$	$G_{TT}(G_{23})$
ψ_L	ψ_{16}	ψ_{12}	ψ_{LT}	$\eta_{G_{LT}}$	$\eta_{G_{LT}}$	$\psi_{G_{LT}}(\psi_{55}, \psi_{66})$	$G_{LT}(G_{13}, G_{12})$

CHAPTER 4

THE MODIFIED MODAL STRAIN ENERGY METHOD AND ITS APPLICATION TO VISCOELASTICALLY DAMPED SYSTEMS

4.1. Statement of problem

The concise notion of complex modulus in viscoelastic theory provides a basic and mathematically consistent tool, and hence it is very useful in computations. As a result, the study of free vibrations based on this assumption involves solving a complex eigenvalue problem defined by equation (3.24), which is rewritten as:

$$[K^*]\{\phi^*\} = (\omega^*)^2 [M] \{\phi^*\}, \qquad (4.1\ a)$$

or as:

$$([K_R] + i[K_I])\{\phi^*\} = (\omega^*)^2 [M] \{\phi^*\}. \qquad (4.1\ b)$$

Both matrices $[K_R]$ and [M] are real symmetric and positive definite. $[K_I]$ is a real symmetric positive or semi-positive definite matrix. Moreover, both $[K_R]$ and $[K_I]$ are frequency-dependent.

Premultiplying both sides of equation (4.1) by the Hermitian transpose of $\{\phi^*\}$, one obtains Rayleigh's quotient:

$$(\omega^*)^2 = \frac{\{\phi^*\}^H [K^*] \{\phi^*\}}{\{\phi^*\}^H [M] \{\phi^*\}} , \qquad (4.2\ a)$$

which can be rewritten in the form:

$$(\omega^*)^2 = \frac{\{\phi^*\}^H [K_R] \{\phi^*\}}{\{\phi^*\}^H [M] \{\phi^*\}} + i \frac{\{\phi^*\}^H [K_I] \{\phi^*\}}{\{\phi^*\}^H [M] \{\phi^*\}} . \qquad (4.2\ b)$$

It can be shown that for any real symmetric matrix [A], the following relation holds:

$$\{\phi^*\}^H [A] \{\phi^*\} = \textit{real value} . \qquad (4.3)$$

This is because

$$\{\phi^*\}^H = \left(\{\phi_R\} + i\{\phi_I\} \right)^H = \{\phi_R\}^T - i\{\phi_I\}^T , \qquad (4.4)$$

and

$$\{\phi_R\}^T [A] \{\phi_I\} = \{\phi_I\}^T [A] \{\phi_R\} . \qquad (4.5)$$

Thus, for the complex symmetric matrix of [K^*], the following relationships can be obtained from equations (3.23) and (4.2)

$$\begin{aligned} \omega^2 &= \frac{\{\phi^*\}^H [K_R] \{\phi^*\}}{\{\phi^*\}^H [M] \{\phi^*\}} , \\ \omega^2 \eta &= \frac{\{\phi^*\}^H [K_I] \{\phi^*\}}{\{\phi^*\}^H [M] \{\phi^*\}} . \end{aligned} \qquad (4.6)$$

Eliminating ω^2 in equation (4.6) gives

$$\eta = \frac{\{\phi^*\}^H [K_I] \{\phi^*\}}{\{\phi^*\}^H [K_R] \{\phi^*\}} = \frac{U_I}{U_R} , \tag{4.7}$$

where U_I and U_R are the dissipated energy and strain energy, respectively. Note that the solution of the complex eigenvalue problem is needed to obtain η.

The Modal Strain Energy (**MSE**) method assumes that the damped system can be represented in terms of the real normal modes of the associated undamped system. Thus, the MSE method yields an approximate evaluation of the loss factor, or the modal damping, which is given by:

$$\hat{\eta} = \frac{\{\phi\}^T [K_I] \{\phi\}}{\{\phi\}^T [K_R] \{\phi\}} , \tag{4.8}$$

where $\{\phi\}$ is a real eigenvector which is the solution for:

$$[K_R] \{\phi\} = \omega^2 [M] \{\phi\} . \tag{4.9}$$

Since the MSE technique allows one to compute modal damping by a real, instead of a complex, eigenvalue solution, the following two advantages are gained over an exact solution:

a) The computational cost is greatly reduced;

b) The method can be easily implemented in existing commercial finite element programs.

However, it is important to assess the errors resulting from the approximate solution of the MSE method. To the author's knowledge, such an evaluation of the error in the

MSE method does not exist in the open literature. As will be demonstrated in details later in this chapter, large errors can be involved in the evaluation of the loss factor by the MSE method when the natural frequencies are not well separated, or when heavy non-proportional damping is encountered in the vibratory systems.

The errors associated with the approximate solutions for non-proportional damping were found to be significant, indicating the importance of conducting an adequate error analysis. However, this study has mainly been made on viscously damped systems.

The specific objectives of this chapter are:

a) to develop a Modified MSE method which provides a better approximation;

b) to propose numerical indices for the evaluation of the approximate methods;

c) to investigate the nature and magnitude of the errors inherent in both the MSE and the Modified MSE methods.

The numerical studies are to be conducted to illustrate the application of the proposed method and the proposed indices.

4.2. The Modified Modal Strain Energy method

Similar to the MSE technique, the proposed Modified MSE method also solves a real eigenvalue problem for the evaluation of modal damping. It is important to choose a real eigenvalue problem so that a proper real eigenvector can be used to obtain the approximate η in equation (4.7). In the MSE approach, η is evaluated using the real eigenvector $\{\phi\}$ which is independent of the damping stiffness matrix $[K_I]$. This may give rise to large errors in many cases.

The idea of the Modified MSE method is to define a real eigenvalue problem which takes the damping matrix $[K_I]$ into account. The influence of damping has been considered in terms of a weighted damping matrix, which actually results in a perturbation on the associated undamped system. The value of the weight is approximately related to the average over all modal damping. Consequently, the loss factor for the Modified MSE method is taken as:

$$\bar{\eta} = \frac{\{\bar{\phi}\}^T [K_I] \{\bar{\phi}\}}{\{\bar{\phi}\}^T [K_R] \{\bar{\phi}\}}, \tag{4.10}$$

where $\{\bar{\phi}\}$ is a real eigenvector which is associated with the eigenvalue problem:

$$\left([K_R] + \beta [K_I]\right)\{\bar{\phi}\} = \bar{\omega}^2 (1 + \beta \bar{\eta})[M] \{\bar{\phi}\}, \tag{4.11}$$

Here β is a real constant, calculated from:

$$\beta = \frac{trace[K_I]}{trace[K_R]} , \qquad (4.12)$$

where trace [A] for an (n×n) matrix is given by:

$$trace\ [A] = \sum_{i=1}^{n} A_{ii} = \sum_{i=1}^{n} \lambda_i , \qquad (4.13)$$

in which A_{ii} and λ_i are the ith diagonal term and the ith eigenvalue of [A], respectively.

By comparing equations (4.9) and (4.11) it can be seen that the MSE method is a special case of the Modified MSE method, *i e.* when $\beta = 0$, we have $\{\bar{\phi}\} = \{\phi\}$. The extra computational cost of the Modified MSE method over the MSE method is negligible compared to the total cost of the solution.

When $[K_I] = \alpha\ [K_R]$ where α is a constant, the system exhibits a proportional damping. In this case, all modes will be identical to the real eigenvectors of the undamped vibratory system. It will have the same loss factors, i.e., $\eta^{(i)} = \alpha$ (i=1,2,...,n). All motions of a proportionally damped system are exactly in phase or out of phase at resonance, resulting in modal displacements that simultaneously reach their extremes. For such a case, both the MSE and the Modified MSE methods render the exact solution for the eigenvector, *i e.*, $\{\phi^*\} = \{\phi\}$.

In the general case, which is normally a case of non-proportional damping, the eigenvector $\{\phi^*\}$ will be complex. The system modes must be described with phase angles as well as magnitudes. Any estimation of η using only a real eigenvector will give rise to an error. It is our objective to reduce this error by taking into account the effect of the damping matrix. Equation (4.12) for the calculation of β is basically an empirical formula. A mathematical rigorous analysis can be made to obtain the optimum value of β for the best estimation of error in η.

4.3. Proposed indices

4.3.1. Indices for classifying systems

As previously indicated, the Modified MSE method, as similar to the original MSE method, is an approximate technique which is developed to simplify the computations and to improve the accuracy. It is difficult to evaluate the errors by a strictly mathematical approach. Moreover, the conditions under which the error of approximation is acceptable have never been clearly specified. It is our objective here to identify these conditions and to propose practical indices to assess the accuracy of the approximate solutions.

Several indices are suggested. Each index takes into

account some particular aspect of the viscoelastically damped system. These are as follows:

a) Non-Proportionality Index (NPI)

It is defined as follows:

$$NPI = \frac{\|[NP]\|_f}{\|[K_R]\|_f} , \tag{4.14}$$

where $\|[\,]\|_f$ denotes the Frobenius norm, *i e.*,

$$\|[A]\|_f = \left[\sum_{i=1}^{n}\sum_{j=1}^{n} A_{ij}^2\right]^{1/2} , \tag{4.15}$$

and [NP] is the non-proportional matrix, defined by

$$[NP] = \begin{cases} [K_R] - \alpha[K_I] & \alpha \neq 0 , \\ [0] & \alpha = 0 , \end{cases} \tag{4.16}$$

The constant α is obtained by using the least square method for a minimum $\|[NP]\|_f$:

$$\alpha = \frac{\sum_{i=1}^{n}\sum_{j=1}^{n} (K_{R_{ij}} K_{I_{ij}})}{\sum_{i=1}^{n}\sum_{j=1}^{n} (K_{I_{ij}})^2} . \tag{4.17}$$

Four classes are suggested based on the values of the NPI:

i) Proportionally damped or undamped system,

NPI = 0;

ii) Lightly non-proportionally damped system, $0 < NPI \leq 0.1$;

iii) Moderately non-proportionally damped system, $0.1 < NPI \leq 0.5$;

iv) Heavily non-proportionally damped system, $NPI > 0.5$.

b) Damping Level Index (**DLI**)

It is defined as follows:

$$DLI = \frac{1}{n} \sum_{i=1}^{n} \overline{\eta}^{(r)} . \qquad (4.18)$$

Based on the DLI values, we proposed four classes:

i) Undamped system, DLI = 0;

ii) Lightly damped system, $0 < DLI \leq 0.02$;

iii) Moderately damped system, $0.02 < DLI \leq 0.2$;

iv) Heavily damped system, $0.2 < DLI \leq 1.0$.

c) Frequency Separation Index (**FSI**)

It is defined as follows:

$$FSI = \min \left[\frac{\overline{\omega}^{(r+1)} - \overline{\omega}^{(r)}}{\overline{\omega}^{(r)}} \right] \qquad r=1,2,....,n-1. \qquad (4.19)$$

Based on the FSI values, the vibratory system may belong to one of the following four classes:

i) Repeated frequency system, FSI = 0;

ii) Closely spaced frequency system, $0 < FSI \leq 0.02$;

iii) Moderately spaced frequency system, $0.02 < FSI \leq 0.1$;

iv) Well spaced frequency system, $FSI > 0.1$.

The ranges of the indices corresponding to individual classes are selected, for convenience, to characterize the systems. Each index is normalized to a relative value for the entire system. Sometimes, the first m ($m < n$) modes are of interest in an analysis for a large scale system. In this situation, the indices of the DLI and the FSI will be evaluated for those modes and considered as representatives of the entire system.

The computation of any index requires only the information of the known matrices and the results by the approximate methods, *e.g.*, $[K_R]$, $[K_I]$, $\bar{\omega}^{(r)}$ and $\bar{\eta}^{(r)}$. These indices are plausible because they provide reasonable identification of the system, and involve simple algebraic manipulations.

4.3.2 Overall Error Index

In the assessment of the accuracy of the approximate methods, the modal parameters are compared with the exact solutions. The absolute error associated with the rth modal parameter $y^{(r)}$, either damped natural frequency or loss factor, is defined as:

$$E^{(r)} = \hat{y}^{(r)} - y^{(r)} \ . \tag{4.20}$$

where $\hat{y}^{(r)}$ is the estimated parameter obtained by using an approximate method. For an n degree-of-freedom system, there will be n terms of $E^{(r)}$. It is convenient to describe them in a vectorial form {E}. Usually, the error $E^{(r)}$ varies from one mode to another. In order to evaluate the overall deviations as compared to the exact solutions, we define the Overall Error Index (OEI) as:

$$OEI(y) = \frac{\| \{E\} \|_1}{sum(y)} \times 100 \quad (\%), \tag{4.21}$$

in which $\| \{E\} \|_1$ is the first order norm:

$$\| \{E\} \|_1 = \sum_{r=1}^{n} | E^{(r)} | \ , \tag{4.22}$$

and

$$sum(y) = \sum_{r=1}^{n} y^{(r)} \ . \tag{4.23}$$

In definition of equation (4.21), the OEI is an overall relative error index, which can also be expressed as:

$$OEI(y) = \sum_{r=1}^{n} \left(W^{(r)}(y) \left| RE(y)^{(r)} \right| \right) \quad (\%), \tag{4.24}$$

where $RE(y)^{(r)}$ is the relative error associated with the rth mode parameter and is defined by:

$$RE(y)^{(r)} = \frac{\hat{y}^{(r)} - y^{(r)}}{y^{(r)}} \times 100 \quad (\%). \tag{4.25}$$

$W^{(r)}(y)$ is the weight associated with the rth mode and is given by:

$$W^{(r)}(y) = \frac{y^{(r)}}{sum(y)} . \tag{4.26}$$

Therefore, the OEI is equivalent to the weighted sum of the $RE(y)^{(r)}$. Small values for $y^{(r)}$ will have less contribution to the OEI. This is an appropriate treatment in the assessment of the overall error of modal damping, so that the contribution of large $RE(\eta)^{(r)}$ resulted from insignificant $\eta^{(r)}$ can be reduced (*i e.* when $\eta^{(r)} \approx 0$, $RE(\eta)^{(r)}$ might be enormous).

4.4. Typical examples

A computer simulation was carried out. Both the MSE and the Modified MSE methods were applied for the study of the multi degree-of-freedom systems shown in Figures 4.1 and 4.2.

These systems are chosen because their exact solutions can be obtained by solving the associated complex eigenvalue problem. The simulation results will also provide useful insight for the laminated plate problems.

Six cases were studied as shown in Table 4.1. Cases 32 and 62 have very closely spaced modal natural frequencies, FSI $\approx$ 0. Case 61 is associated with a moderately spaced frequency system. The other cases belong to well spaced frequency systems. The system configurations in Cases 33 and 63 were tailored to include more off-diagonal terms of $k^*_{ij}(i\neq j)$ in the complex stiffness matrix $[K^*]$. Since the maximum value of loss factor for viscoelastic materials is approximately equal to 1, the loss factor for each spring was assigned in the range $0 \leq \eta_i \leq 1.0$.

One of the significant characteristics of viscoelastic materials is that the stiffness and damping are dependent on both frequency and temperature. In the examples treated here, material data were used near a given natural frequency to be able to obtain the modes in the vicinity of that selected frequency. In such a case, the matrices were considered piecewise frequency independent. Under this consideration the assumption of frequency independence is adequate.

Table 4.2 shows Case 31 of the simulation results. The $\hat{\omega}_D$ and $\bar{\omega}_D$ used to determine the RE(y) were evaluated using the first two terms in equation (3.26). Usually, the estimation of modal damping is poorer than that of the modal frequency.

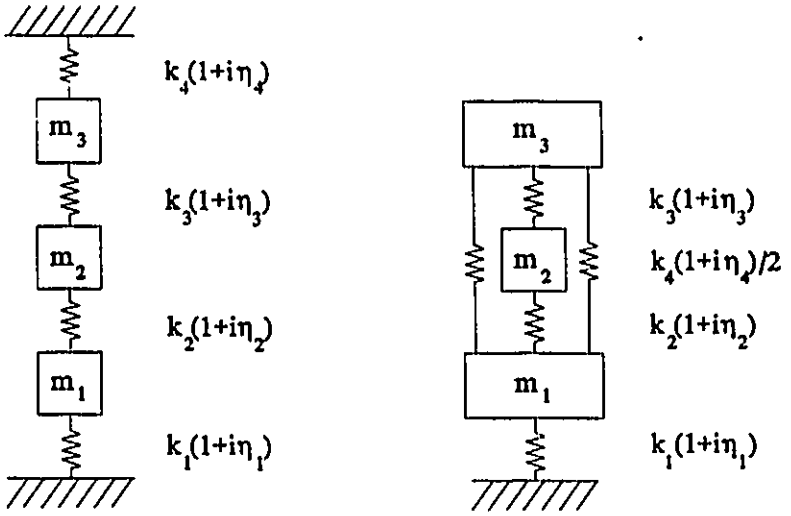

(a) (b)

Figure 4.1 Three-degree-of-freedom system

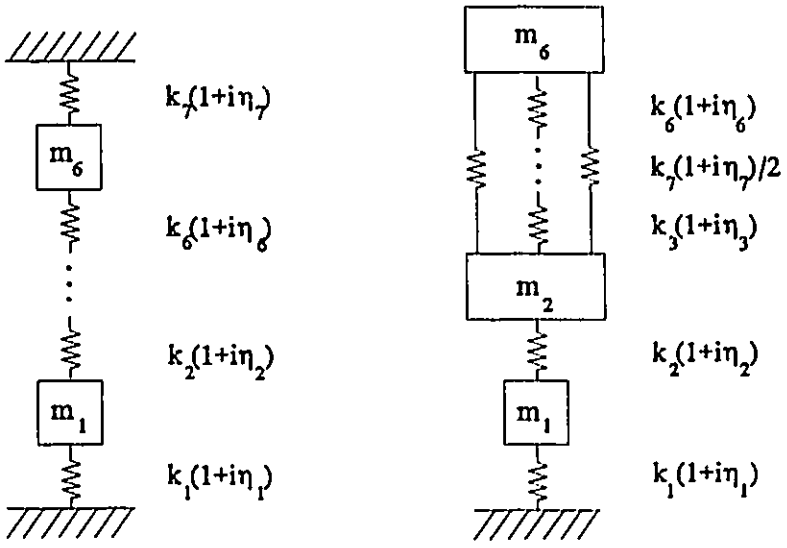

(a) (b)

Figure 4.2 Six-degree-of-freedom system

Table 4.1 Data of multi degree-of-freedom systems

Case Number	m_i (10^5 Ns^2/m), k_i (10^8 N/m)	$\omega^{(r)}$ (1/s)
Case 31 (Figure 4.1 a)	$m_1 = 3.0$, $m_2 = 3.0$, $m_3 = 3.0$. $k_1 = 4.0$, $k_2 = 4.0$, $k_3 = 4.0$, $k_4 = 4.0$.	$\omega^{(1)} = 27.95$, $\omega^{(2)} = 51.64$, $\omega^{(3)} = 67.47$.
Case 32 (Figure 4.1 a)	$m_1 = 3.0$, $m_2 = 0.3$, $m_3 = 3.0$. $k_1 = 4.0$, $k_2 = .04$, $k_3 = .04$, $k_4 = 4.0$.	$\omega^{(1)} = 16.23$, $\omega^{(2)} = 36.70$, $\omega^{(3)} = 36.74$.
Case 33 (Figure 4.1 b)	$m_1 = 3.0$, $m_2 = 4.0$, $m_3 = 5.0$. $k_1 = 6.0$, $k_2 = 5.0$, $k_3 = 4.0$, $k_4/2=1.5$.	$\omega^{(1)} = 18.31$, $\omega^{(2)} = 51.11$, $\omega^{(3)} = 73.28$.
Case 61 (Figure 4.2 a)	$m_1 = 3.0$, $m_2 = 3.0$, $m_3 = 3.0$, $m_4 = 3.0$, $m_5 = 3.0$, $m_6 = 3.0$. $k_1 = 4.0$, $k_2 = 4.0$, $k_3 = 4.0$, $k_4 = 4.0$, $k_5 = 4.0$, $k_6 = 4.0$, $k_7 = 4.0$.	$\omega^{(1)} = 16.25$, $\omega^{(2)} = 31.69$, $\omega^{(3)} = 45.53$, $\omega^{(4)} = 57.10$, $\omega^{(5)} = 65.80$, $\omega^{(6)} = 71.20$.
Case 62 (Figure 4.2 a)	$m_1 = 3.0$, $m_2 = 3.0$, $m_3 = 0.3$, $m_4 = 0.3$, $m_5 = 3.0$, $m_6 = 3.0$. $k_1 = 4.0$, $k_2 = 4.0$, $k_3 = .04$, $k_4 = .04$, $k_5 = .04$, $k_6 = 4.0$, $k_7 = 4.0$.	$\omega^{(1)} = 11.40$, $\omega^{(2)} = 19.75$, $\omega^{(3)} = 22.85$, $\omega^{(4)} = 23.00$, $\omega^{(5)} = 59.12$, $\omega^{(6)} = 59.12$.
Case 63 (Figure 4.2 b)	$m_1 = 1.0$, $m_2 = 2.0$, $m_3 = 3.0$, $m_4 = 4.0$, $m_5 = 5.0$, $m_6 = 6.0$. $k_1 = 8.0$, $k_2 = 7.0$, $k_3 = 6.0$, $k_4 = 5.0$, $k_5 = 4.0$, $k_6 = 3.0$, $k_7/2 = 2.0$.	$\omega^{(1)} = 11.35$, $\omega^{(2)} = 34.93$, $\omega^{(3)} = 41.75$, $\omega^{(4)} = 61.26$, $\omega^{(5)} = 85.72$, $\omega^{(6)} = 133.4$.

Table 4.2 Simulation results of Case 31

η_1, η_2, η_3, η_4	$\omega_D^{(1)}$	$\omega_D^{(2)}$	$\omega_D^{(3)}$	$\eta^{(1)}$	$\eta^{(2)}$	$\eta^{(3)}$
1.0,1.0,1.0,1.0	30.705	56.736	74.129	1.0	1.0	1.0,
	(2.395	2.395	2.395	0.0	0.0	0.0)
	[2.395	2.395	2.395	0.0	0.0	0.0]
0.3,0.6,0.3,0.6	28.880	52.872	68.970	0.430	0.450	0.454,
	(-0.781	0.142	0.302	4.651	0.0	-0.777)
	[-0.809	0.142	0.308	-0.050	0.0	-0.009]
0.4,0.6,0.6,0.4	28.608	53.142	69.958	0.425	0.500	0.572
	(-0.060	0.210	0.371	1.072	0.0	-0.156)
	[-0.060	0.210	0.374	-0.035	0.0	-0.011]
0.1,0.2,0.3,0.4	28.287	52.269	67.757	0.245	0.245	0.254
	(-0.427	-0.432	0.356	1.901	1.975	-1.458)
	[-0.428	-0.433	0.357	-0.034	0.061	-0.052]
0.2,0.3,.35,0.1	28.133	52.004	68.192	0.182	0.243	0.301
	(-0.240	0.029	0.061	1.406	-0.077	-0.140)
	[-0.235	0.029	0.062	-0.113	-.0005	-0.017]
0.6,0.3,.35,.12	28.798	52.262	68.264	0.331	0.346	0.332
	(-1.427	0.258	0.184	7.059	-1.039	-0.587)
	[-1.477	0.261	0.185	0.173	-0.130	-0.038]
1.0,1.0,0.0,0.0	29.211	57.326	67.037	0.472	0.120	0.824
	(-1.335	-7.104	3.792	5.989	318.0	-39.32)
	[-1.381	-6.880	4.988	-3.736	59.36	-14.15]
0.0,1.0,1.0,0.0	28.981	53.142	72.370	0.065	0.500	0.878
	(-3.309	0.210	1.721	125.2	0.0	-2.770)
	[-2.398	0.210	1.915	-23.84	0.0	-0.493]
0.6,0.4,0.2,0.0	28.724	53.118	67.307	0.279	0.275	0.319
	(-1.611	-1.690	1.370	7.438	8.902	-6.006)
	[-1.617	-1.696	1.383	-0.517	1.040	-0.810]
0.1,0.2,0.1,0.2	28.666	51.784	67.642	0.149	0.150	0.150
	(-0.142	0.002	0.003	0.593	0.0	-0.101)
	[-0.142	0.002	0.003	-0.0	0.0	-0.000]

Notes: Values in parentheses and bracket give the $RE(y)^{(i)}(\%)$ corresponding to the MSE and the Modified MSE methods, respectively.

The values of the OEI for six cases are listed in Tables 4.3-4.8. The various damping configurations were selected to simulate some coating schemes for viscoelastic layers on plates. In Table 4.3, for example, the locally distributed coating is simulated by $\{\eta_1, \eta_2, \eta_3, \eta_4\}$ = {1.0, 1.0, 0.0, 0.0}. The globally distributed coating is simulated using $\{\eta_1, \eta_2, \eta_3, \eta_4\}$ = {0.3, 0.6, 0.3, 0.6}. The values of the DLI are close to each other for both examples, but the NPI value for the former is higher than the latter.

The influence of the configurations of the systems on the estimated error is demonstrated schematically in Figure 4.3. The following two damping configurations were investigated:

a) Moderately non-proportionally damped system, η_1=0.001λ, η_2=0.002λ, η_3=0.001λ, η_4=0.002λ, (NPI=0.164 for Case 31, NPI=0.311 for Case 32);

b) Heavily non-proportionally damped system, η_1=0.001λ, η_2=0.001λ, η_3=0.0, η_4=0.0, (NPI=0.655 for Case 31, NPI=0.707 for Case 32);

where λ is an incremental factor. While the NPI has the same value in each case, the DLI is amplified by a factor λ.

One can draw the following conclusions from the numerical studies presented here:

a) If the system is lightly damped, *i e.*, DLI $\leq$ 0.02, and is associated with low non-proportionality, *i e.*, NPI $\leq$ 0.1, and with well

Table 4.3 Comparison of Overall Error Index (Case 31)

η_1,	η_2,	η_3,	η_4	OEI(ω_D) %		OEI(η) %		DLI	NPI
				MSE	Modified	MSE	Modified		
1.0,	1.0,	1.0,	1.0	2.395	2.395	0.0	0.0	1.0	0.0
0.3,	0.6,	0.3,	0.6	0.338	0.345	1.764	0.019	0.444	0.164
0.4,	0.6,	0.6,	0.4	0.256	0.257	0.364	0.014	0.498	0.091
0.1,	0.2,	0.3,	0.4	0.396	0.398	1.774	0.049	0.248	0.287
0.2,	0.3,	.35,	.12	0.084	0.084	0.436	0.035	0.242	0.151
0.6,	0.3,	.35,	.12	0.449	0.455	2.867	0.114	0.336	0.226
1.0,	1.0,	0.0,	0.0	4.561	5.008	51.77	14.50	0.451	0.655
0.0,	1.0,	1.0,	0.0	1.499	1.419	7.328	1.374	0.474	0.316
0.6,	0.4,	0.2,	0.0	1.530	1.540	7.376	0.789	0.291	0.447
0.1,	0.2,	0.1,	0.2	0.040	0.040	0.231	.0004	0.150	0.164

Table 4.4 Comparison of Overall Error Index (Case 32)

η_1,	η_2,	η_3,	η_4	OEI(ω_D) %		OEI(η) %		DLI	NPI
				MSE	Modified	MSE	Modified		
1.0,	1.0,	1.0,	1.0	2.395	2.395	0.0	0.0	1.0	0.0
0.3,	0.6,	0.3,	0.6	1.128	0.200	21.76	0.012	0.450	0.311
0.4,	0.6,	0.6,	0.4	0.148	0.147	0.052	0.006	0.467	.0097
0.1,	0.2,	0.3,	0.4	0.668	0.039	39.68	0.025	0.250	0.512
0.2,	0.3,	.35,	.12	0.081	0.010	12.02	0.227	0.215	0.237
0.6,	0.3,	.35,	.12	1.493	0.173	45.44	0.019	0.348	0.551
1.0,	1.0,	0.0,	0.0	3.851	1.067	66.66	0.007	0.500	0.707
0.0,	1.0,	1.0,	0.0	0.379	0.376	2.359	2.298	0.332	0.885
0.6,	0.4,	0.2,	0.0	1.577	0.173	66.17	0.029	0.300	0.705
0.1,	0.2,	0.1,	0.2	0.098	0.093	21.67	0.301	0.150	0.311

Table 4.5 Comparison of Overall Error Index (Case 33)

η_1,	η_2,	η_3,	η_4	OEI(ω_D) %		OEI(η) %		DLI	NPI
				MSE	Modified	MSE	Modified		
0.8,	0.7,	0.6,	0.5	0.579	0.573	0.587	0.014	0.669	0.089
0.1,	0.2,	0.3,	0.4	0.096	0.095	0.753	0.114	0.226	0.238
0.2,	0.3,	.35,	.12	0.150	0.151	0.524	0.055	0.243	0.213
0.6,	0.3,	.35,	.12	0.257	0.268	2.497	0.287	0.370	0.192
0.8,	0.1,	0.0,	0.6	1.617	1.648	10.26	2.895	0.392	0.570
1.0,	0.6,	0.2,	0.0	0.856	0.966	8.505	0.652	0.497	0.410
0.6,	0.0,	0.5,	0.4	0.734	0.756	3.816	0.426	0.379	0.408
1.0,	1.0,	0.0,	0.0	1.211	1.328	6.588	3.822	0.545	0.507
0.0,	1.0,	1.0,	0.0	4.556	4.865	26.84	3.612	0.420	0.465

Table 4.6 Comparison of Overall Error Index (Case 61)

η_1,	η_2,	η_3,	η_4,	η_5,	η_6,	η_7	OEI(ω_D) %		OEI(η) %		DLI	NPI
							MSE	Modified	MSE	Modified		
0.4,	0.6,	0.4,	0.6,	0.4,	0.6,	0.4	0.231	0.236	0.845	0.018	0.966	0.107
0.1,	0.2,	0.3,	0.4,	0.5,	0.6,	0.7	1.402	1.459	10.82	3.270	0.776	0.377
0.1,	0.2,	0.3,	0.4,	0.3,	0.2,	0.1	0.360	0.361	1.882	0.377	0.454	0.298
0.3,	0.2,	0.1,	0.4,	0.3,	0.2,	0.1	0.412	0.415	2.171	0.491	0.454	0.322
0.5,	0.0,	0.5,	0.0,	0.5,	0.0,	0.5	1.084	1.101	4.837	1.055	0.551	0.497
0.0,	0.5,	0.0,	0.5,	0.0,	0.5,	0.0	0.959	0.947	7.768	0.906	0.411	0.454
0.8,	0.4,	.65,	0.1,	0.4,	0.5,	0.2	1.134	1.144	5.876	2.578	0.844	0.311
0.8,	0.4,	.65,	0.1,	0.2,	0.5,	0.0	2.552	2.570	19.65	11.08	0.718	0.410
1.0,	1.0,	1.0,	0.0,	0.0,	0.0,	0.0	4.069	4.674	70.86	36.64	0.753	0.746
0.0,	0.0,	1.0,	1.0,	1.0,	0.0,	0.0	5.378	5.656	44.95	11.52	0.756	0.636

Table 4.7 Comparison of Overall Error Index (Case 62)

η_1,	η_2,	η_3,	η_4,	η_5,	η_6,	η_7	OEI(ω_D) %		OEI(η) %		DLI	NPI
							MSE	Modified	MSE	Modified		
0.4,	0.6,	0.4,	0.6,	0.4,	0.6,	0.4	0.247	0.249	0.574	0.036	0.974	0.090
0.1,	0.2,	0.3,	0.4,	0.5,	0.6,	0.7	1.714	0.287	41.23	1.119	0.796	0.498
0.1,	0.2,	0.3,	0.4,	0.3,	0.2,	0.1	0.138	0.140	0.524	1.199	0.422	0.144
0.3,	0.2,	0.1,	0.4,	0.3,	0.2,	0.1	0.143	0.055	13.45	1.619	0.443	0.186
0.5,	0.0,	0.5,	0.0,	0.5,	0.0,	0.5	0.837	0.856	3.441	0.840	0.545	0.652
0.0,	0.5,	0.0,	0.5,	0.0,	0.5,	0.0	0.772	0.746	4.968	1.499	0.425	0.326
0.8,	0.4,	.65,	0.1,	0.4,	0.5,	0.2	0.717	0.339	19.25	0.422	0.873	0.211
0.8,	0.4,	.65,	0.1,	0.2,	0.5,	0.0	1.050	0.600	31.76	1.316	0.752	0.299
1.0,	1.0,	1.0,	0.0,	0.0,	0.0,	0.0	4.404	1.543	79.67	4.207	0.857	0.707
0.0,	0.0,	1.0,	1.0,	1.0,	0.0,	0.0	0.437	0.451	9.468	10.01	0.670	0.990

Table 4.8 Comparison of Overall Error Index (Case 63)

η_1,	η_2,	η_3,	η_4,	η_5,	η_6,	η_7	OEI(ω_D) %		OEI(η) %		DLI	NPI
							MSE	Modified	MSE	Modified		
0.4,	0.6,	0.4,	0.6,	0.4,	0.6,	0.4	0.269	0.274	1.357	0.072	0.965	0.106
0.1,	0.2,	0.3,	0.4,	0.5,	0.6,	0.7	0.300	0.300	2.149	0.516	0.745	0.399
0.1,	0.2,	0.3,	0.4,	0.3,	0.2,	0.1	0.194	0.195	0.983	0.068	0.448	0.330
0.3,	0.2,	0.1,	0.4,	0.3,	0.2,	0.1	0.109	0.109	0.690	0.268	0.458	0.353
0.5,	0.0,	0.5,	0.0,	0.5,	0.0,	0.5	1.134	1.144	13.77	5.458	0.552	0.452
0.0,	0.5,	0.0,	0.5,	0.0,	0.5,	0.0	1.587	1.581	17.55	9.251	0.407	0.486
0.8,	0.4,	.65,	0.1,	0.4,	0.5,	0.2	0.410	0.422	3.345	0.558	0.868	0.305
0.8,	0.4,	.65,	0.1,	0.2,	0.5,	0.0	0.645	0.655	5.444	0.486	0.755	0.396
1.0,	1.0,	1.0,	0.0,	0.0,	0.0,	0.0	1.651	1.660	9.503	2.935	0.869	0.553
0.0,	0.0,	1.0,	1.0,	1.0,	0.0,	0.0	1.415	1.388	18.60	8.278	0.734	0.694

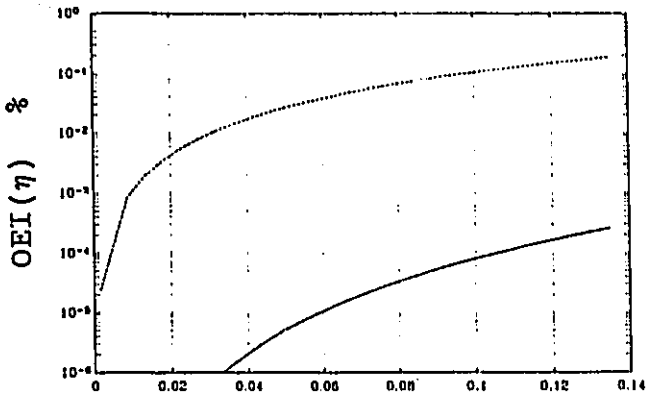

(a) Case 31, NPI = 0.164

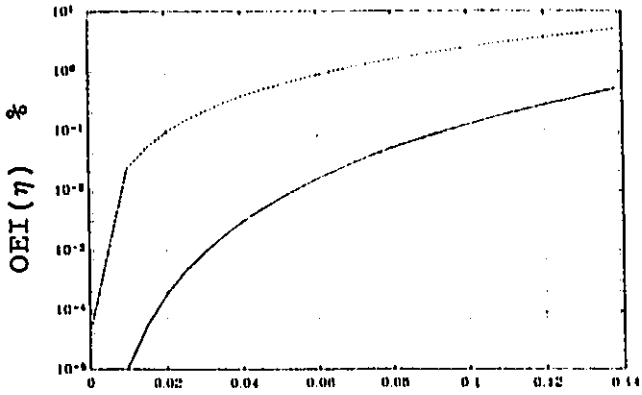

(b) Case 31, NPI = 0.655

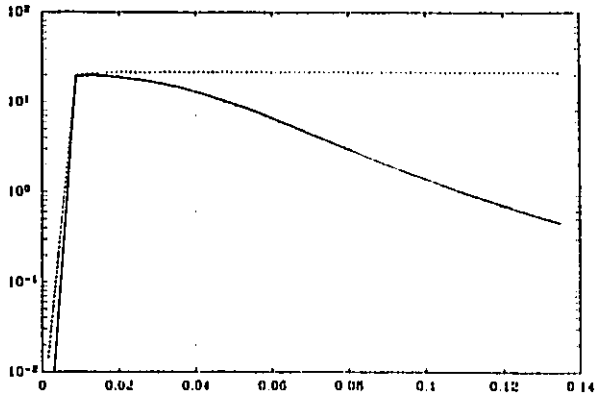

(c) Case 32, NPI = 0.311

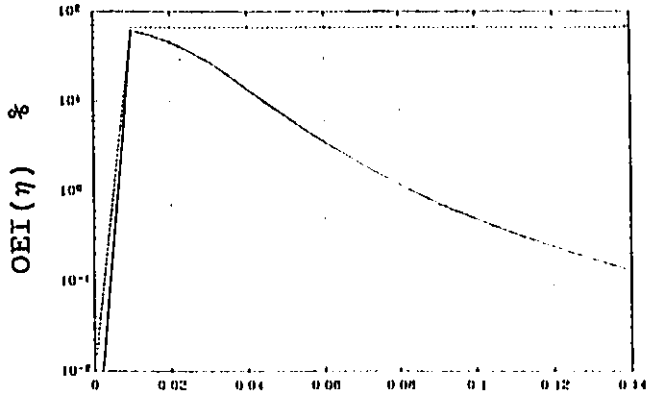

(d) Case 32, NPI = 0.707

——— The Modified MSE method

----- The MSE method

Figure 4.3 "DLI - OEI(η)" curves

spaced frequencies, *i e.*, FSI > 0.2, then each of the methods yields an error within an acceptable bound, < 1.0 %.

b) For most configurations as shown in Figure 4.3, the Modified MSE method gives a better estimation of η than the MSE method. When the error associated with the MSE method is exceedingly large, the Modified MSE method improves the accuracy appreciably.

c) Generally, the OEI will increase with the increment of the DLI as shown in Figure 4.3 a, b. Exceptions occur for a closely spaced frequencies as given by Figure 4.3 c, d, for FSI $\approx$ 0.

d) The non-proportionality of the system will have bad influence on the estimation of the accuracy as shown in Tables 4.3 to 4.8.

e) When the modal frequencies are too close, the accuracy may be reduced appreciably.

f) A large error occurs when the system is heavily damped, *i e.*, DLI > 0.2, and is associated with closely spaced modal frequencies, *i e.*, FSI < 0.02, and with a heavy non-proportionality, *i e.*, NPI > 0.5.

Three indices have been used to characterize the systems. When a system exhibits high damping and high non-

proportionality, the approximation solutions tend to deviate significantly from the exact. This is noticeable when the imaginary parts of the eigenvector $\{\phi^*\}$ become more prominent. To replace the complex eigenvector by a set of real eigenvectors, for the estimation of η, will generally cause large errors.

It is also noted that when modal frequencies of the systems are closely spaced, the estimation of the errors may become poor. The following comparison between Case 31, a well spaced frequency system, and Case 32, a closely spaced frequency system, demonstrates our observation.

The same damping configuration of the system is used for both cases. It is given by:

$$\{\eta_1,\ \eta_2,\ \eta_3,\ \eta_4\} = \{0.1,\ 0.2,\ 0.1,\ 0.2\}.$$

The exact solutions for the eigenvalues and eigenvectors are given by:

i) CASE 31:

$$\begin{bmatrix} \ddots & & \\ & (\omega_{ii}^*)^2 & \\ & & \ddots \end{bmatrix} = \begin{bmatrix} 783.4(1+0.149i) & & \\ & 2667(1+0.150i) & \\ & & 4555(1+0.150i) \end{bmatrix},$$

$$[\phi^*] = \begin{bmatrix} 0.714(\ 2.8°) & 0.986(174.4°) & 0.714(-177.2°) \\ 1.000(\ 0.0°) & 0.001(\ 1.3°) & 1.000(\ 0.0°) \\ 0.704(-2.8°) & 1.000(\ 0.0°) & 0.704(\ 177.2°) \end{bmatrix}.$$

ii) CASE 32:

$$\begin{bmatrix} \ddots & & \\ & (\omega_{ii}^{*})^2 & \\ & & \ddots \end{bmatrix} = \begin{bmatrix} 263.4(1+0.150i) & & \\ & 1348(1+0.101i) & \\ & & 1348(1+0.199i) \end{bmatrix},$$

$$[\phi^{*}] = \begin{bmatrix} 0.013(\ 6.2°) & 1.000(\ \ 0.0°) & 0.013(\ 84.9°) \\ 1.000(\ 0.0°) & 0.125(-173.0°) & 0.122(173.0°) \\ 0.012(-6.2°) & 0.013(\ 102.0°) & 1.000(\ \ 0.0°) \end{bmatrix}.$$

While Case 31 has distinct eigenvalues, Case 32 has two closely spaced eigenvalues. The complex mode shapes of Case 31 have phase angles close to 0° or 180°. However, this is not true for Case 32, in which the second and third modes have phase angles far from 0° or 180°. This indicates that closely spaced modal frequencies may lead to prominent imaginary part of the eigenvector $\{\phi^{*}\}$. Consequently, the estimation of η by a real eigenvector will carry a larger error in this case than in a well spaced frequency system.

4.5. Comments

The MSE method, as an approximation, has been in use for viscoelastically damped vibration analysis of the coated or sandwich structures. An overall error index (OEI) has been suggested for the first time to express the deviation of the MSE method from the exact solution.

The Modified MSE method has been developed and proposed. It was shown that the MSE method is a special case

of the Modified MSE method. By adding a weighted damping stiffness matrix $[K_I]$ in a real eigenvalue problem, the estimation of the modal damping is improved, especially for cases where the error inherent in the MSE method is exceedingly large. The Modified MSE method proposed here provides a positive approach to improve the approximate method especially if better β coefficient is used.

Indices (**NPI, DLI, FSI**) have been suggested for the first time to characterize a viscoelastically damped system. These indices serve to evaluate and compare the approximation methods relative to the exact solution.

Based on the present numerical studies, empirical rules have been obtained. If the system is lightly damped, *i e.*, DLI $\leq$ 0.02, and is associated with low non-proportionality, *i e.*, NPI $\leq$ 0.1, and with a well spaced frequencies, *i e.*, FSI > 0.2, both the MSE the Modified MSE methods are likely to give a good estimation of the modal damping, *i e.*, OEI(η) < 1.0 %. Generally, the OEI will be increased with the increment of the DLI and the NPI. When the modal frequencies are too close, the accuracy of the approximation to the corresponding modes is generally less.

CHAPTER 5

NUMERICAL STUDIES

The theoretical principles presented in Chapters 3 and 4 were converted into a finite element program capable of predicting both undamped and damped free vibrations of laminated composite plates. All computations were carried out using FORTRAN-77 in double precision on a Silicon-Graphics workstation.

The present program makes use of nine-node plate elements of the Lagrangian family, and four/eight-node plate elements of the Serendipity family. The selective integration scheme has been employed. For example, when a four-node element is used, the 2×2 Gauss rule is employed for membrane and flexure; while the 1×1 Gauss rule is employed for shear contributions. When an eight-node or nine-node element is used, the 3×3 and the 2×2 Gauss rule are applied respectively. The following relation is used for shear correction factors:

$$K_i K_j = \frac{5}{6} \qquad (i,j=1,2) \ .$$

In the numerical investigation conducted in this chapter, a full plate with 4×4 mesh configuration and 9-node plate elements was used. All plates were subjected to one of the following boundary conditions as illustrated in Figure 5.1:

a) BC-Free, a completely free plate;

b) BC-Clamped, a four-edge clamped plate;

c) BC-S1, a simply supported plate free of in-plane displacements normal to the boundary;

d) BC-S2, a simply supported plate free of in-plane displacements tangent to the boundary.

5.1. Undamped free vibrations

Two types of materials were chosen for the numerical studies of undamped free vibrations. They are characterized by the following dimensionless material properties:

i) Isotropic, typical of metallic materials:

$E_1/E_2 = 1.0$, $G_{12}/E_2 = 1/2(1 + \mu_{12})$, $\mu_{12} = 0.30$.

ii) Material 1, typical of graphite epoxy for the orthotropic:

$E_1/E_2 = 40$, $G_{12}/E_2 = 0.6$, $G_{23}/E_2 = 0.5$, $\mu_{12} = 0.25$.

In order to facilitate comparisons of the results and make them applicable for a wider class, the dimensionless fundamental frequency $\tilde{\omega}$ was used in the analysis. It is given by:

$$\tilde{\omega} = \omega a^2 \sqrt{\frac{\rho}{E_2 h^2}} \ . \qquad (5.1)$$

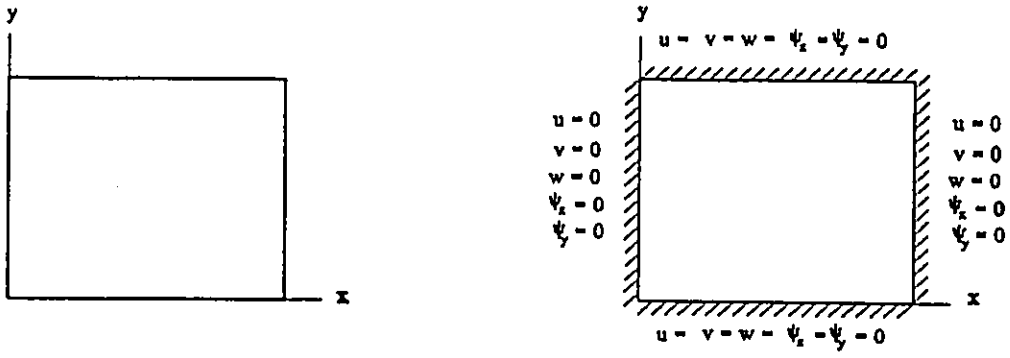

(a) BC-Free (b) BC-Clamped

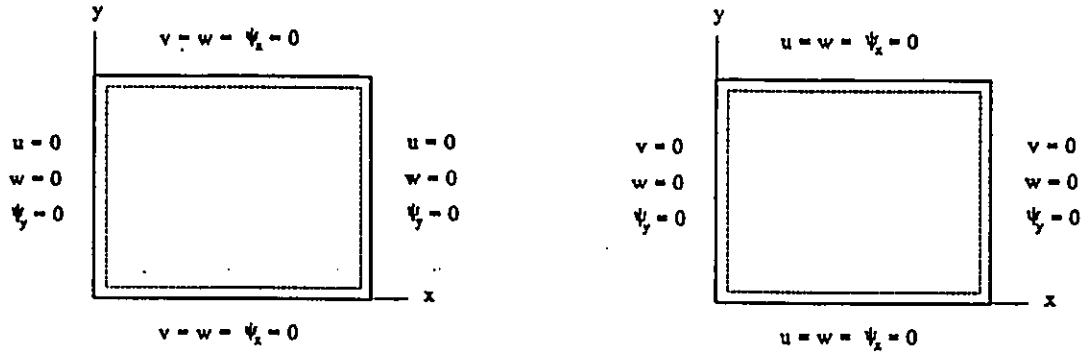

(c) BC-S1 (b) BC-S2

Figure 5.1 Boundary conditions of plates

Since ω is proportional to $\sqrt{(E_2/\rho)}$, the expression for $\bar{\omega}$ is independent of the values of the elastic modulus E_2 and the mass density ρ. Therefore, E_2 and ρ are set to unity in this study for convenience in the computations.

The results of the free vibrations of a four-layer, antisymmetric angle-ply, [45°/-45°/45°/-45°] square plate are given in Table 5.1, together with the results reported by Reddy (1980), Kant (1989) and the closed form solution by Bert and Chen (1978). It can be seen from Table 5.1 that the strategy developed by the present author gives considerably accurate results.

Figures 5.2 - 5.16 show the mode shapes of the plates for the Isotropic and Material 1 with various lamination arrangements and boundary conditions, while the geometry of the plates is unchanged. The fibres of orthotropic or 0° layers are aligned along a horizontal direction as shown in Figure 3.1. The values in brackets are the dimensionless frequencies. The values in parentheses are the numbers of transverse vibration waves along the horizontal and the vertical directions, respectively. In the transverse vibration modes, the fine solid lines represent the nodal lines. In the in-plane vibration modes, the dotted lines display vibration shapes of the corresponding fine solid lines.

The natural modes of the plates are normally influenced by the material properties, the boundary conditions, the lamination arrangements and the geometry.

Table 5.1. Dimensionless fundamental frequencies, $\tilde{\omega}$, of a simply supported square plate; a/h = 10, Material 1, stacking sequence: [45°/-45°/45°/-45°], BC-S1, NDFPN = 5.

m	n	Reddy(1979) Half Plate 2 × 2 8-Node	Kant(1989) Full Plate 4 × 4 9-Node	Present Author Full Plate 4 × 4 9-Node	Exact Bert and Chen(1978)
1	1	18.26(-1.08)	18.45(-0.054)	18.47(0.054)	18.46
In-plane*				34.57	
1	2	35.59(2.065)	34.54(-0.946)	35.02(0.430)	34.87
2	2	---	49.99(-1.049)	50.65(0.257)	50.52
1	3	54.37(0.184)	53.87(-0.737)	55.48(2.230)	54.27
2	3	70.32(4.690)	65.08(-3.112)	67.77(0.893)	67.17
In-Plane				73.01	
1	4	79.32(5.367)	75.25(-0.004)	77.26(2.630)	75.28
3	3	99.60(20.23)	81.99(-1.026)	83.01(0.205)	82.84
2	4	---	85.05(-0.258)	84.98(-.340)	85.27

Notes: FOST for all FEM solutions.

NDFPN = Number of degrees of freedom per node, 5,
= $(u, v, w, \psi_x, \psi_y)$.

m, n = The number of transverse vibration waves along horizontal and vertical directions, respectively.

* = In-plane vibration modes.

Values in parentheses represent percentage errors with respect to the exact solution.

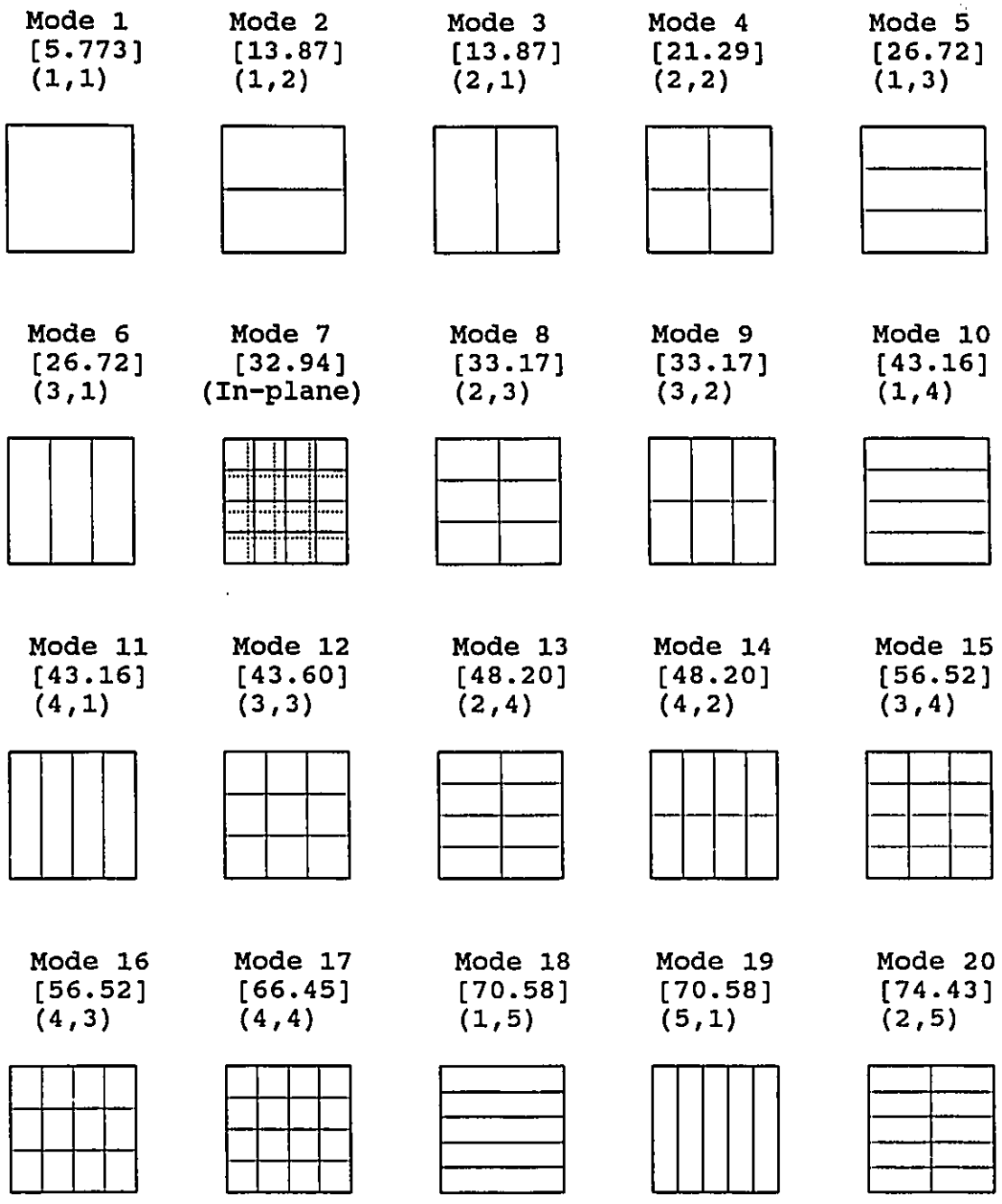

Figure 5.2 Mode shapes of an isotropic plate, BC-S1

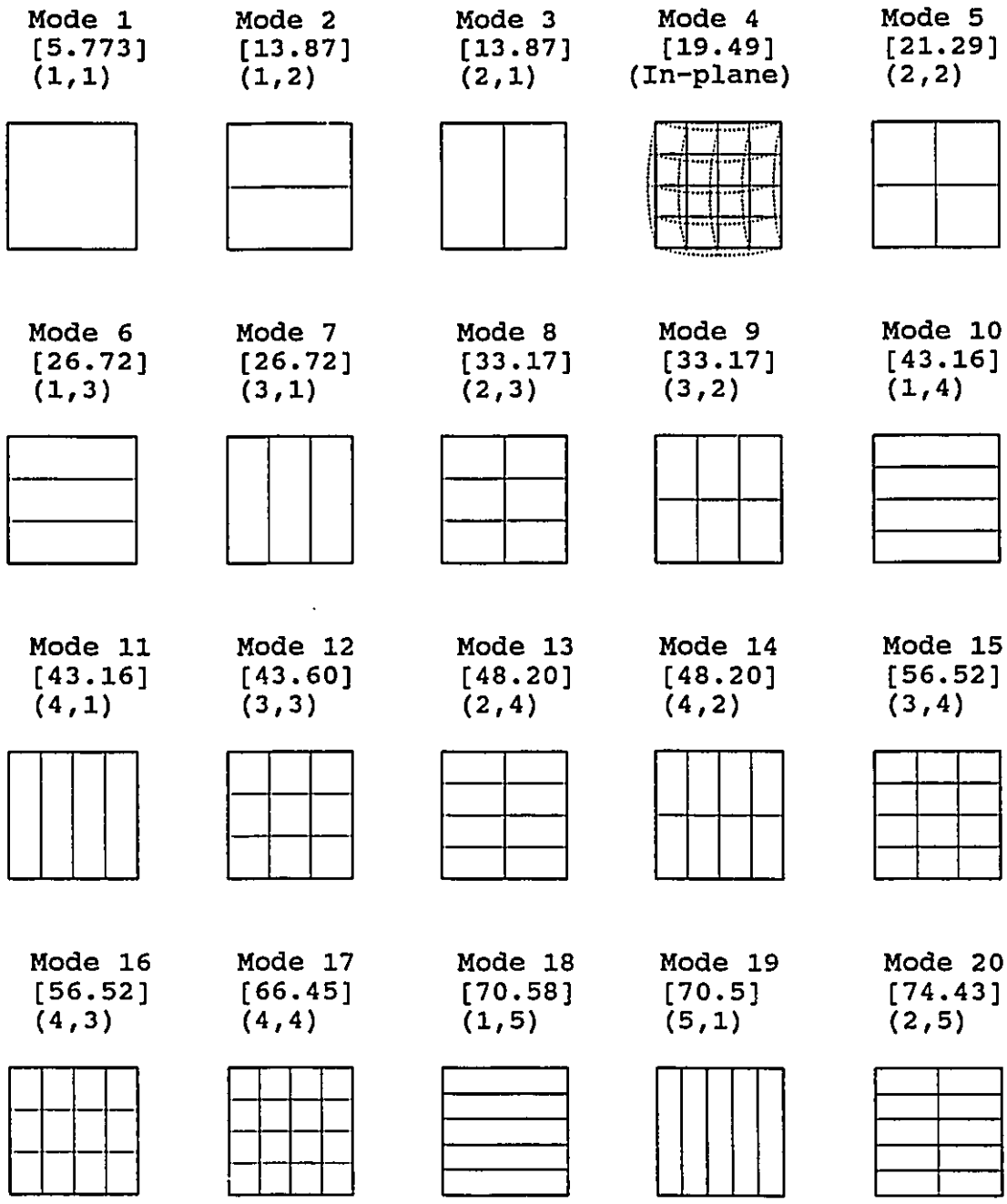

Figure 5.3 Mode shapes of an isotropic plate, BC-S2

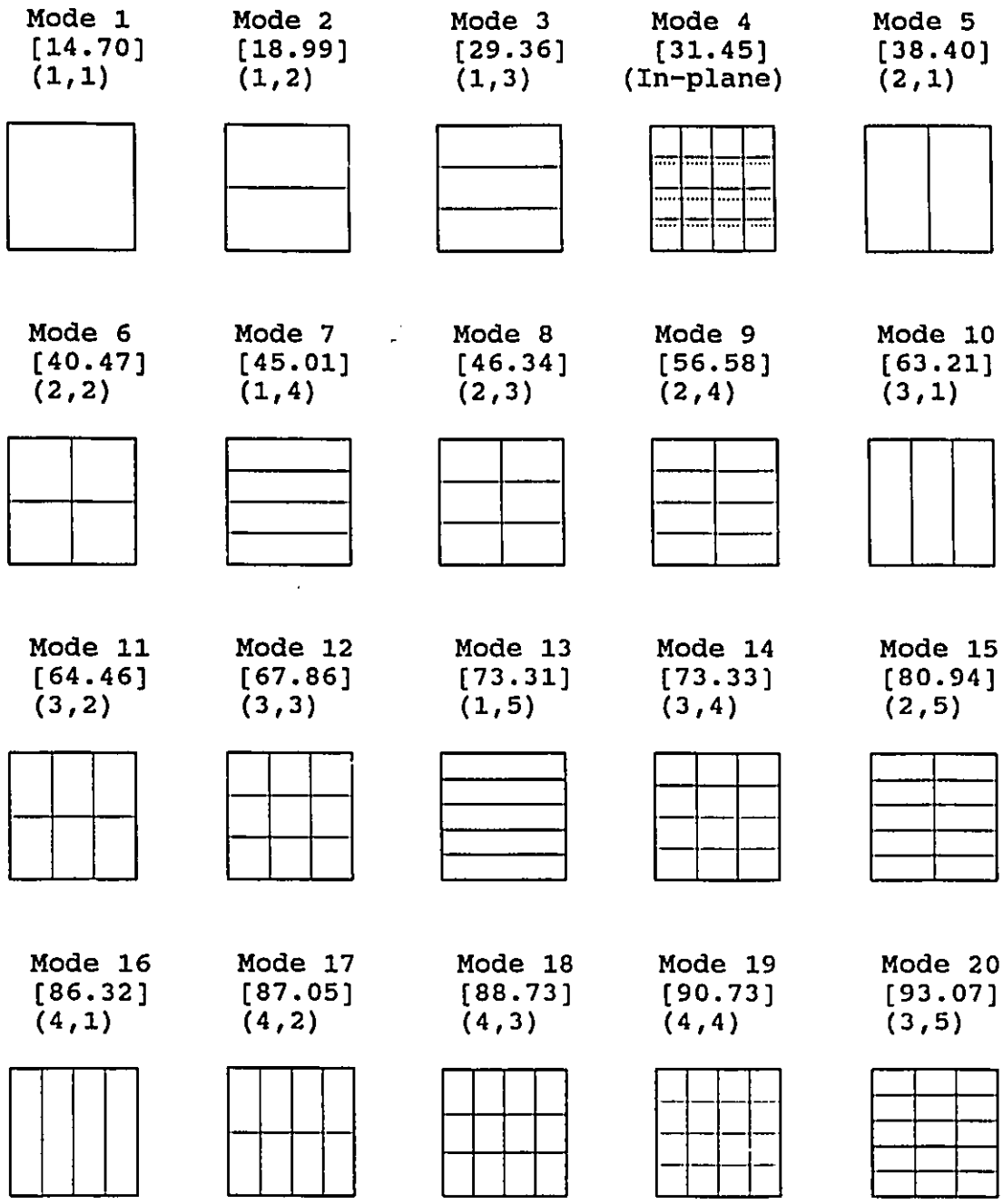

Figure 5.4 Mode shapes of an orthotropic plate, BC-S1

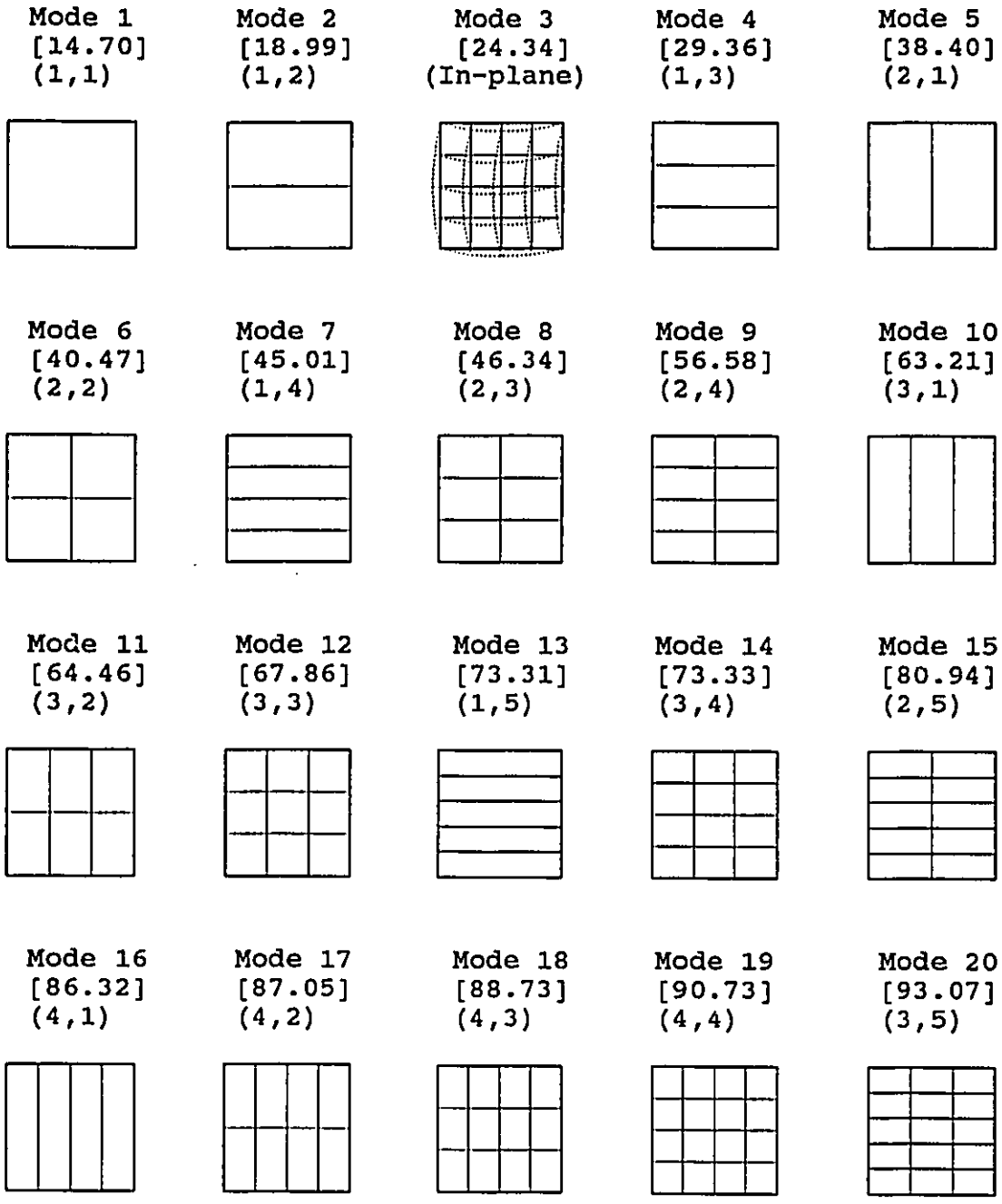

Figure 5.5 Mode shapes of an orthotropic plate, BC-S2

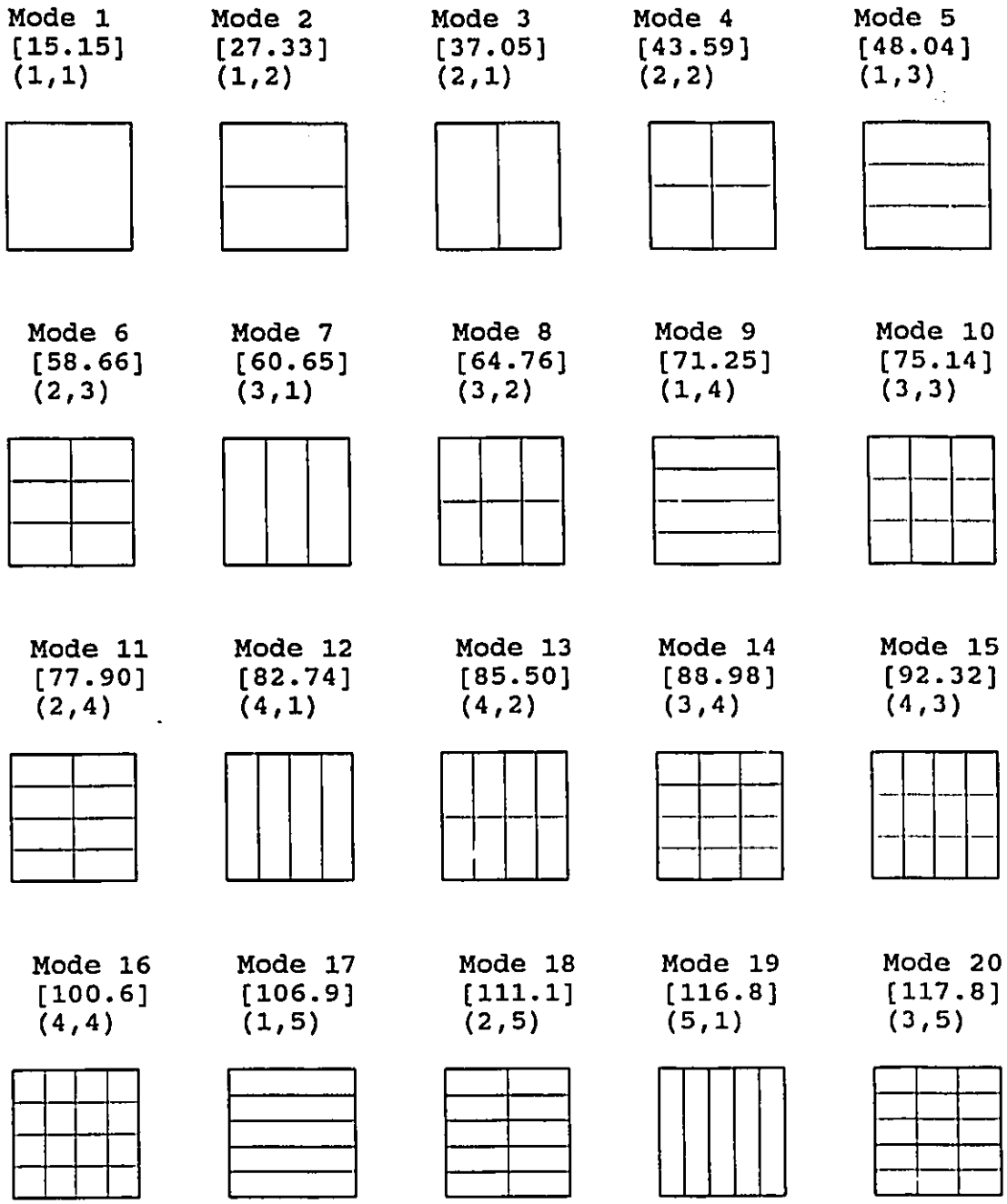

Figure 5.6 Mode shapes of a [0°/90°/90°/0°], BC-S1

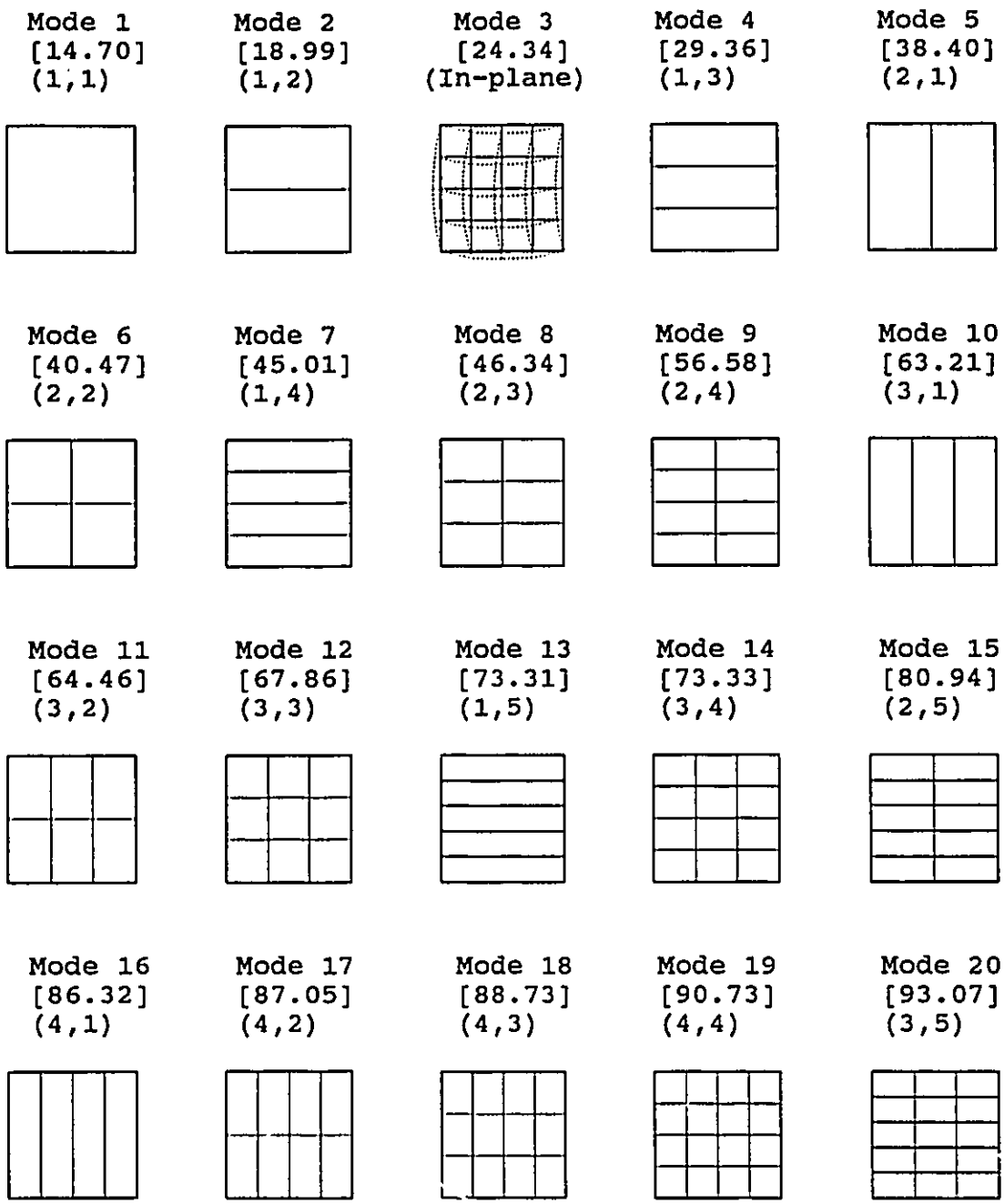

Figure 5.7 Mode shapes of a [0°/90°/90°/0°], BC-S2

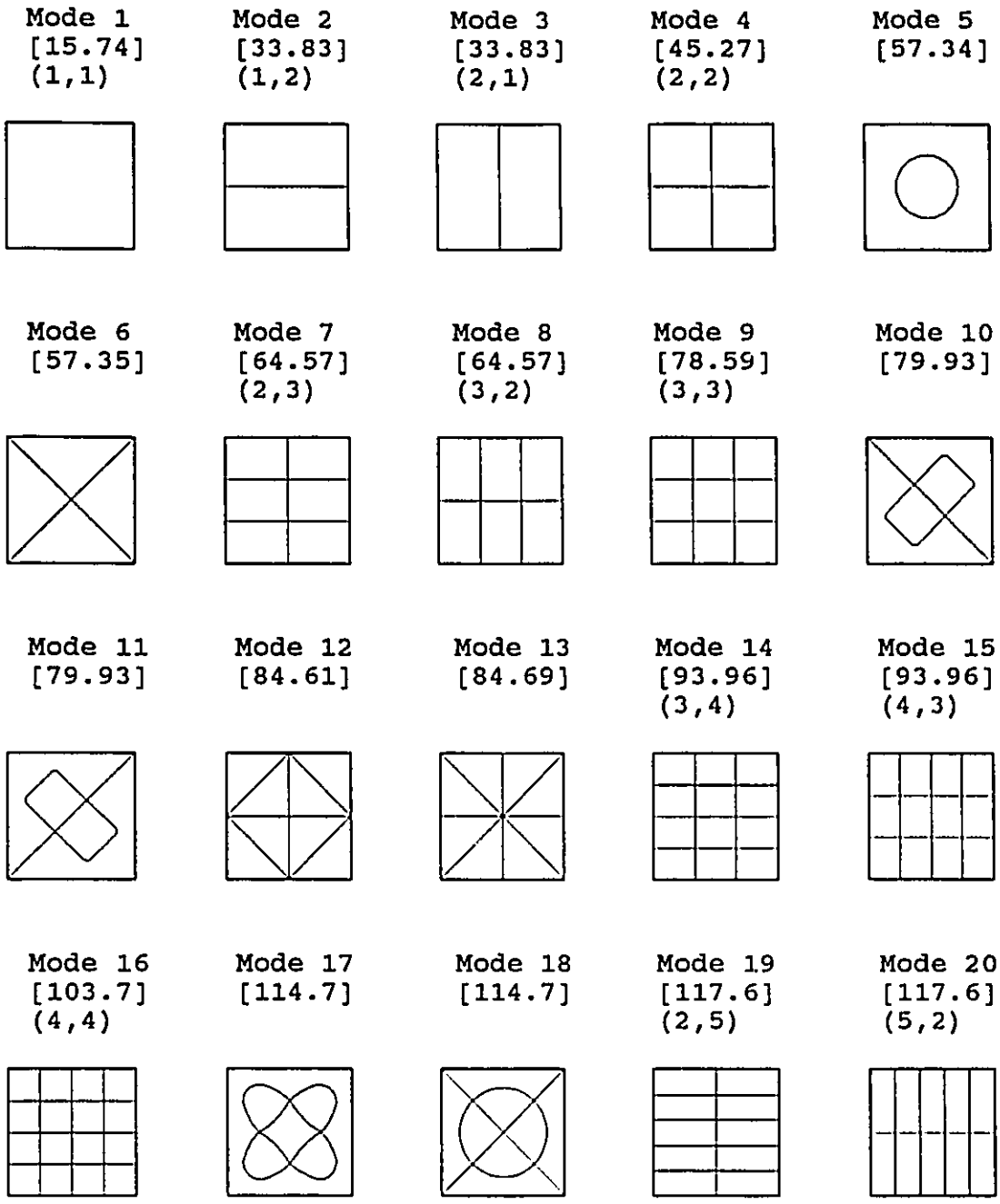

Figure 5.8 Mode shapes of a [0°/90°/0°/90°], BC-S1

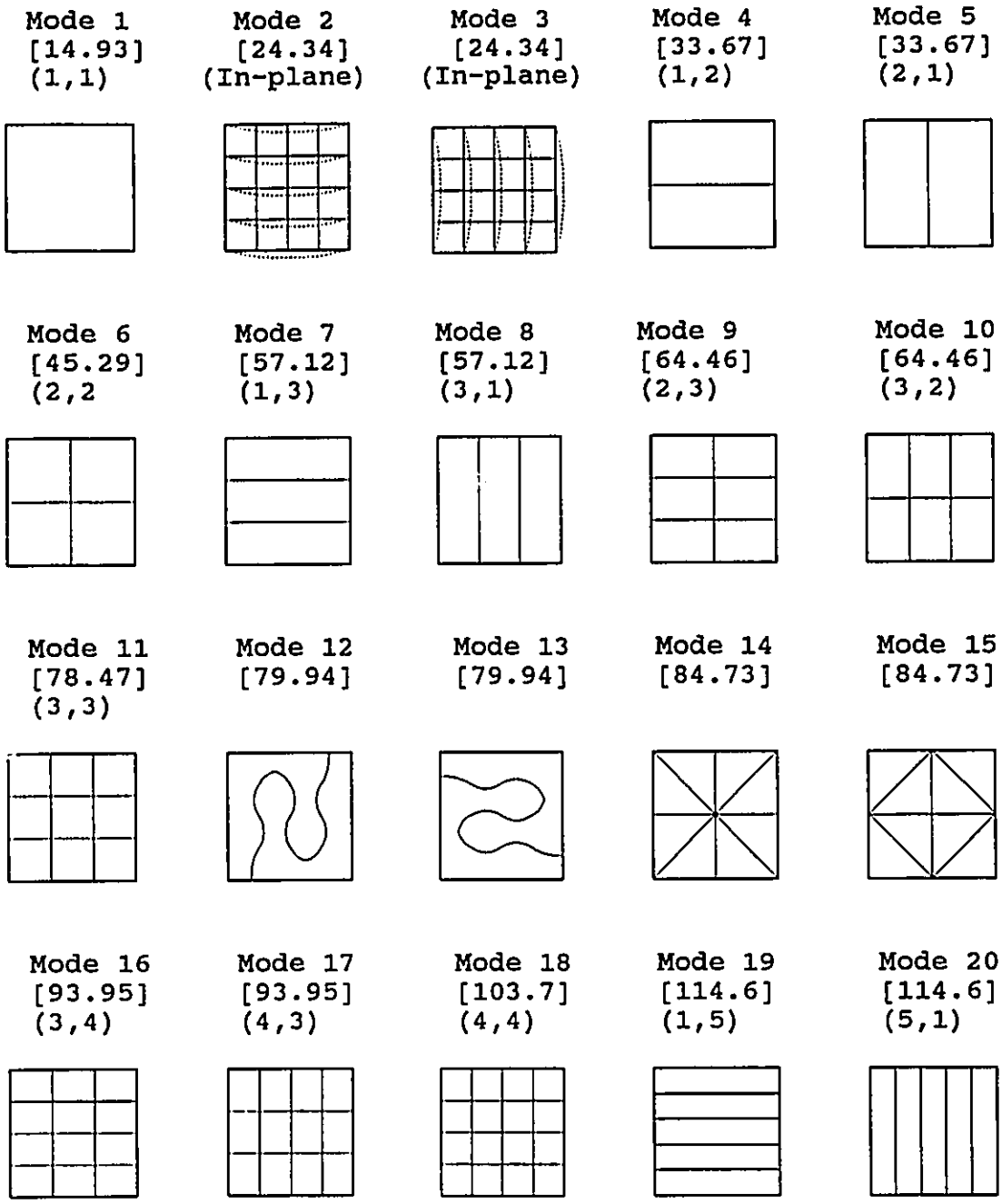

Figure 5.9 Mode shapes of a [0°/90°/0°/90°], BC-S2

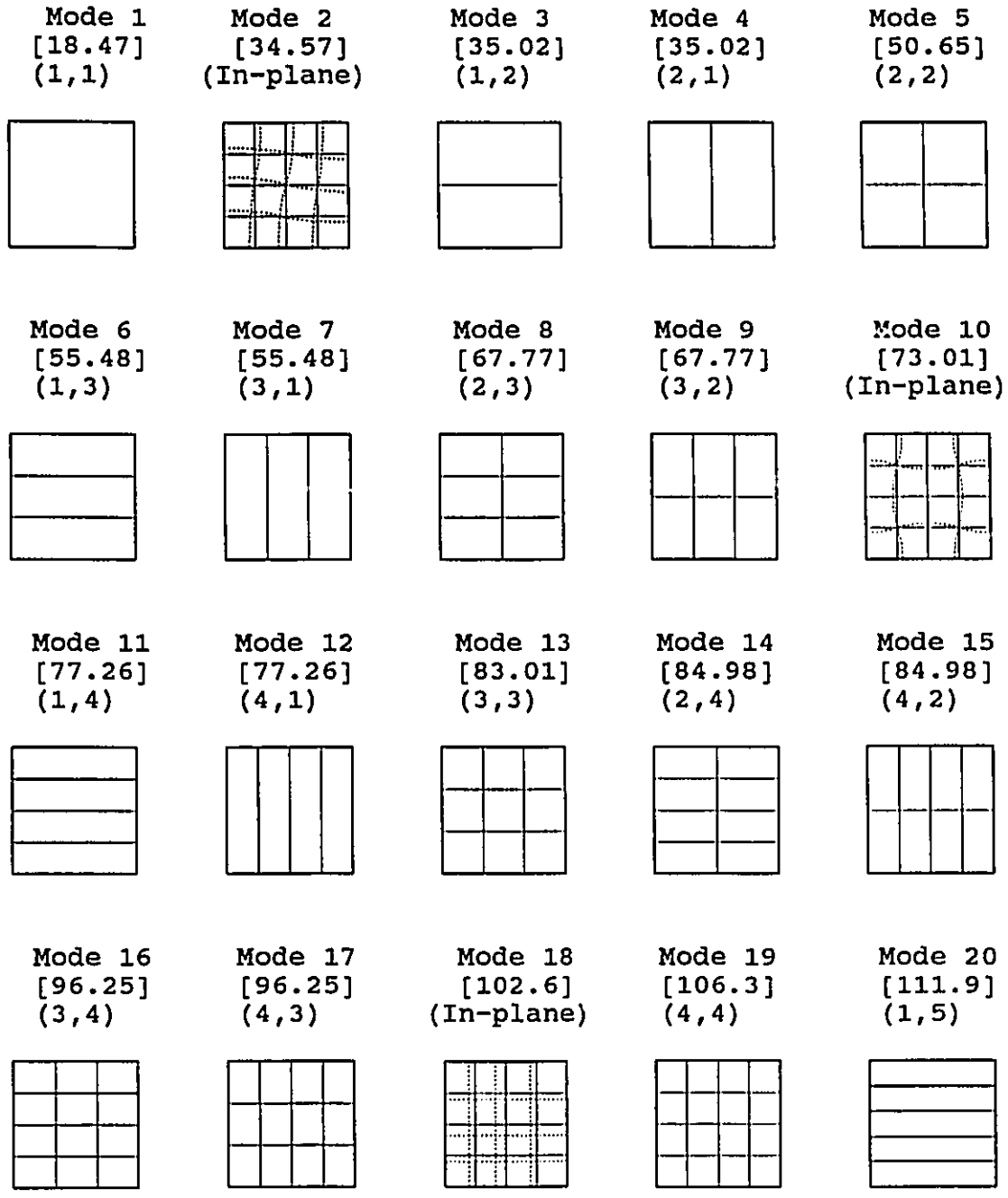

Figure 5.10 Mode shapes of a [45°/-45°/45°/-45°], BC-S1

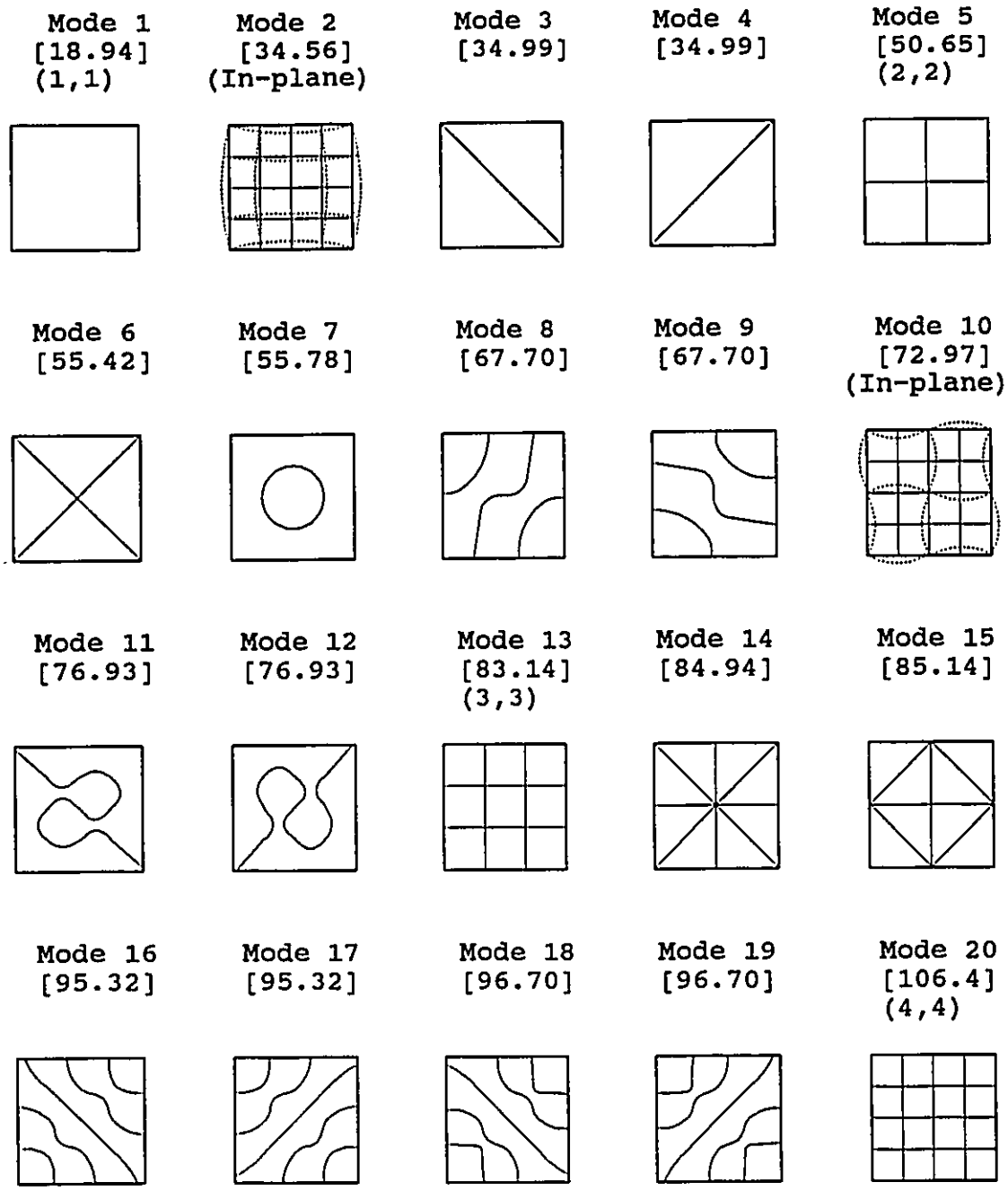

Figure 5.11 Mode shapes of a [45°/-45°/45°/-45°], BC-S2

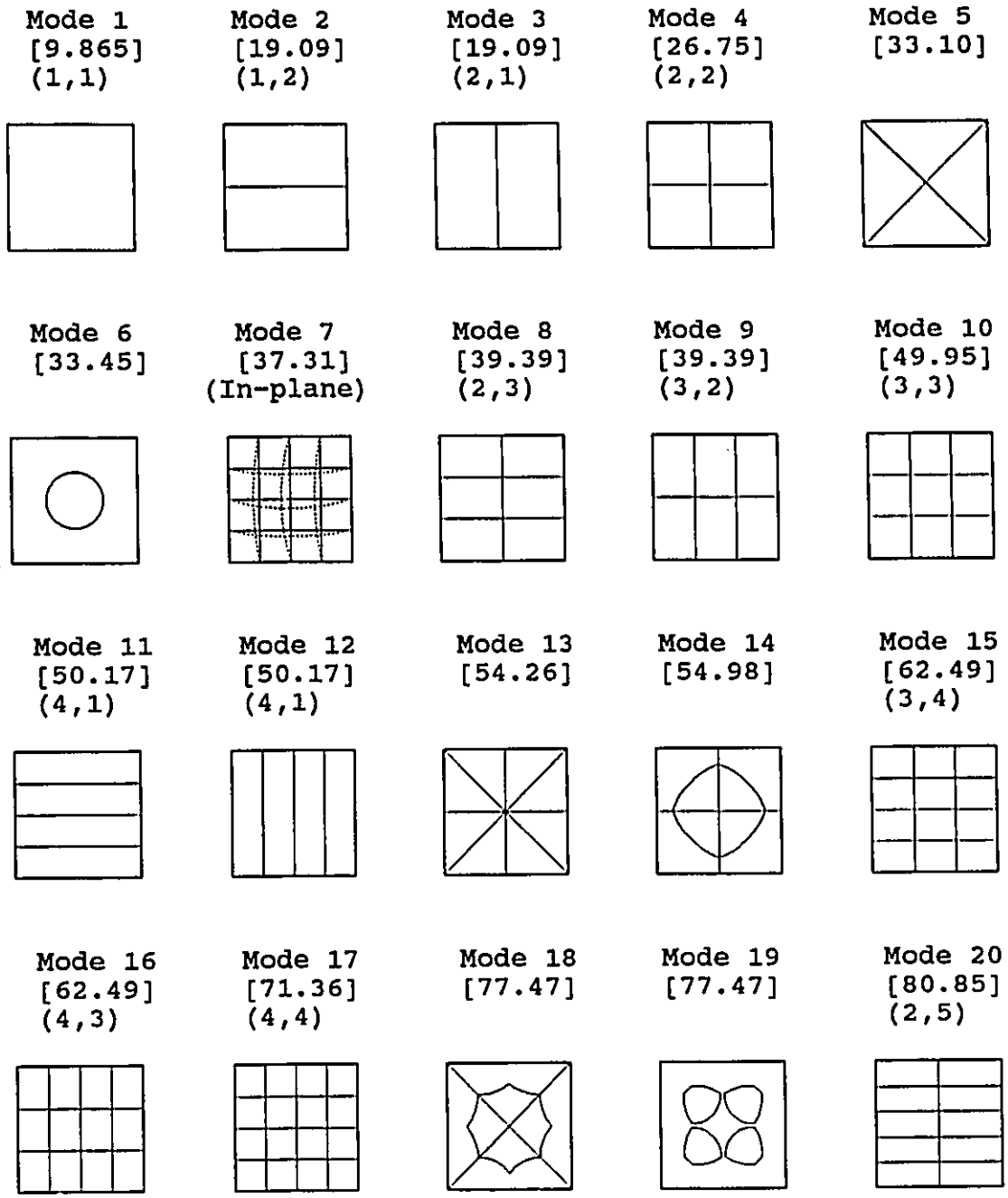

Figure 5.12 Mode shapes of an isotropic plate, BC-Clamped

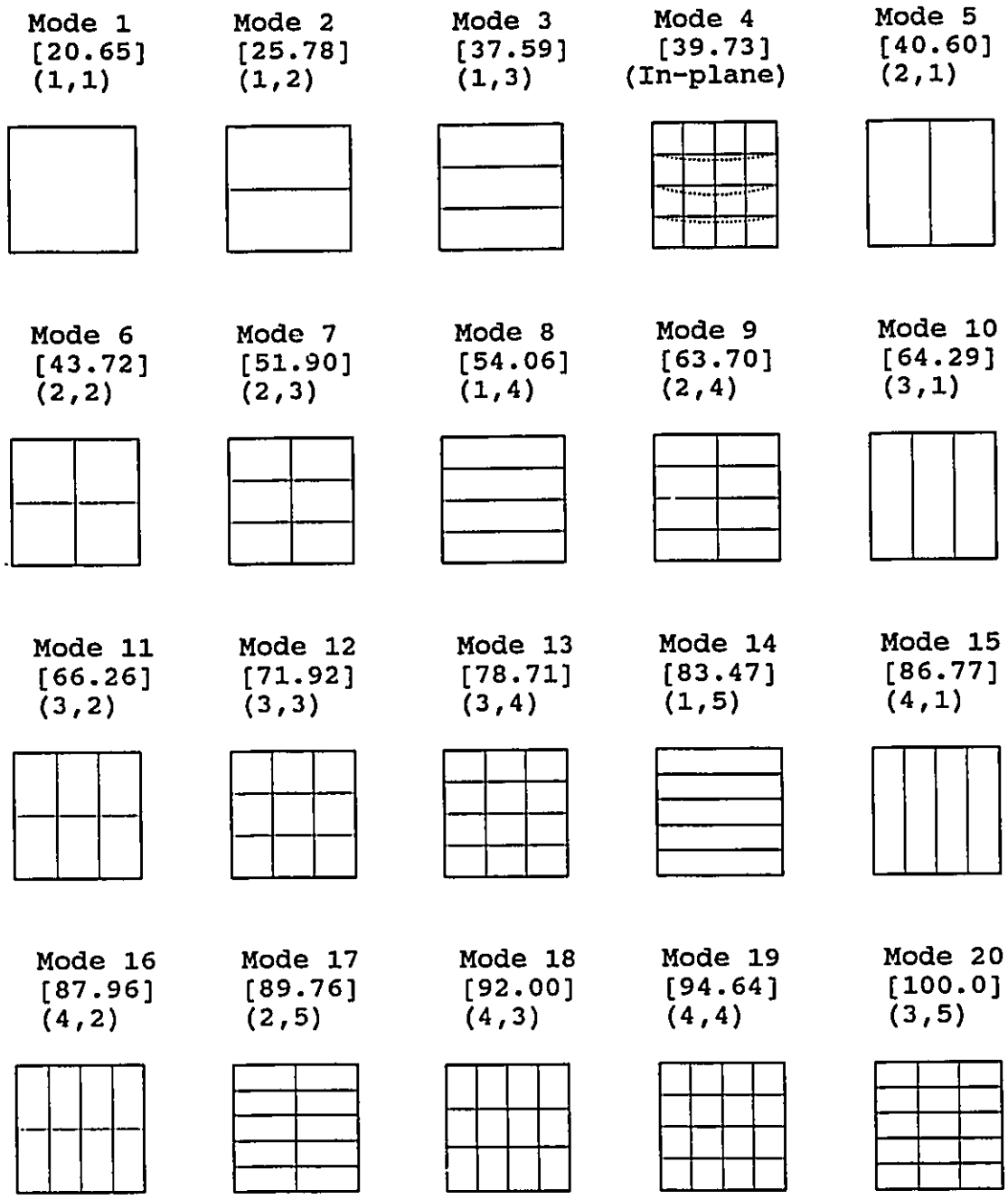

Figure 5.13 Mode shapes of an orthotropic plate, BC-clamped

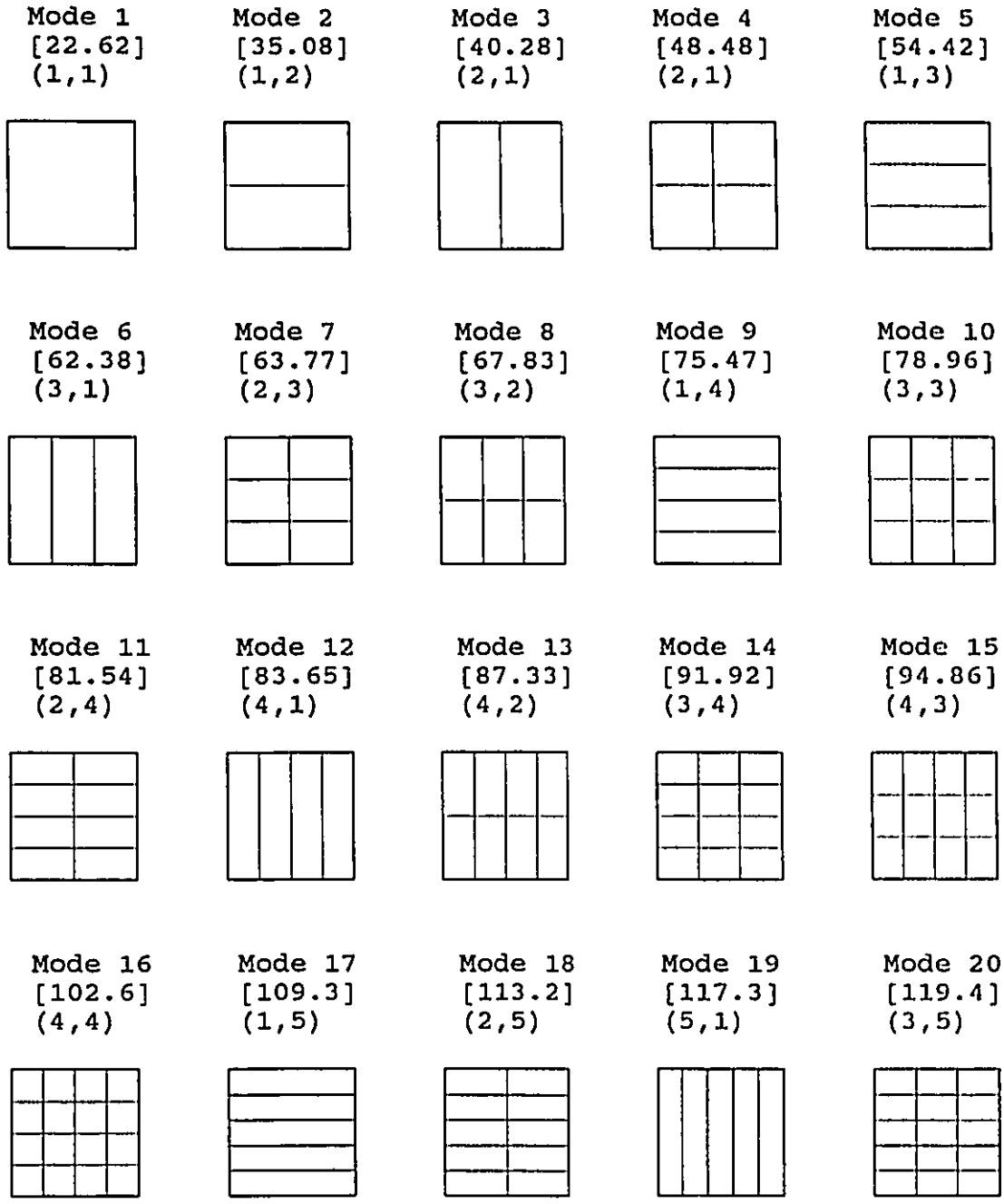

Figure 5.14 Mode shapes of a [0°/90°/90°/0°], BC-Clamped

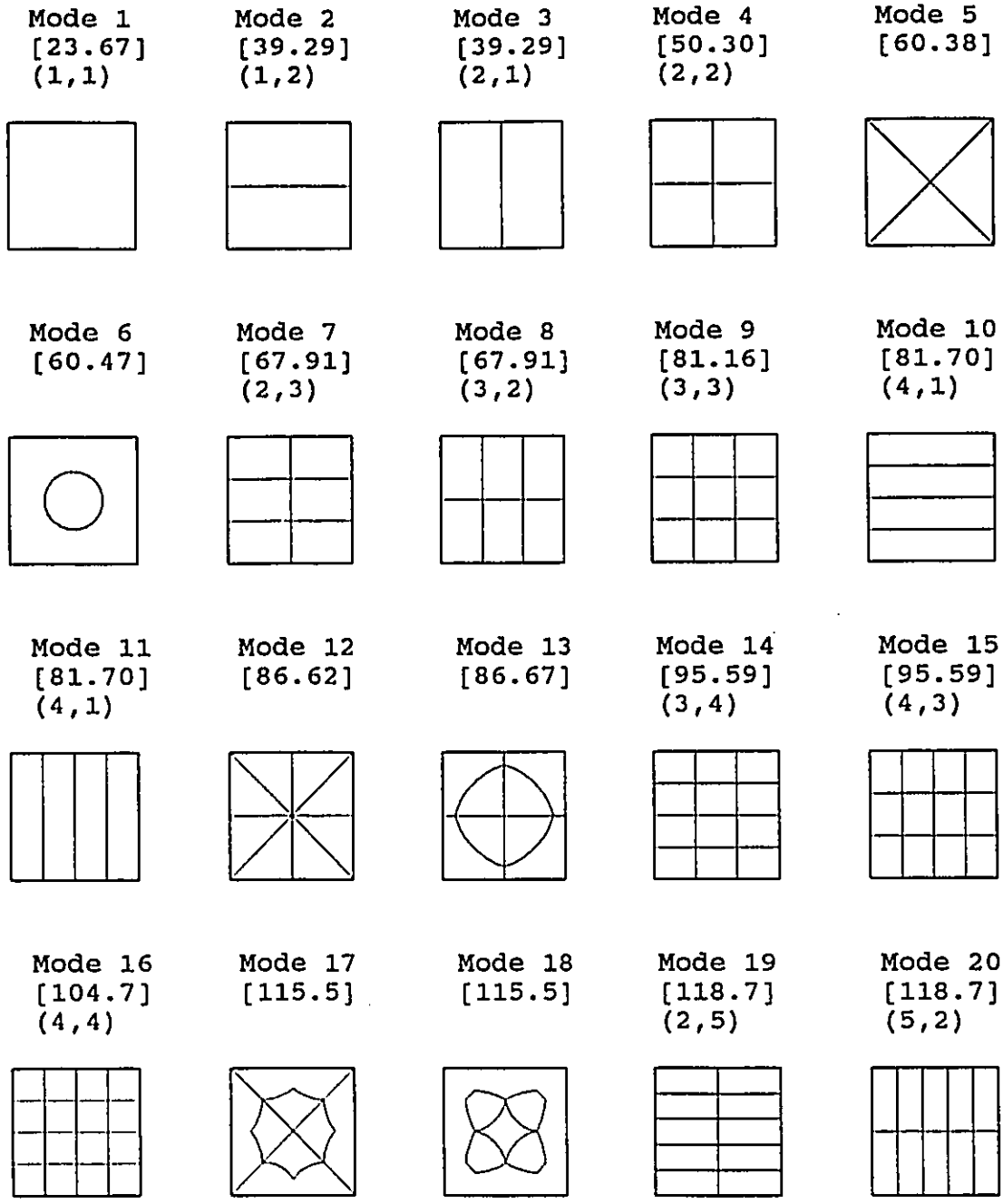

Figure 5.15 Mode shapes of a [0°/90°/0°/90°], BC-Clamped

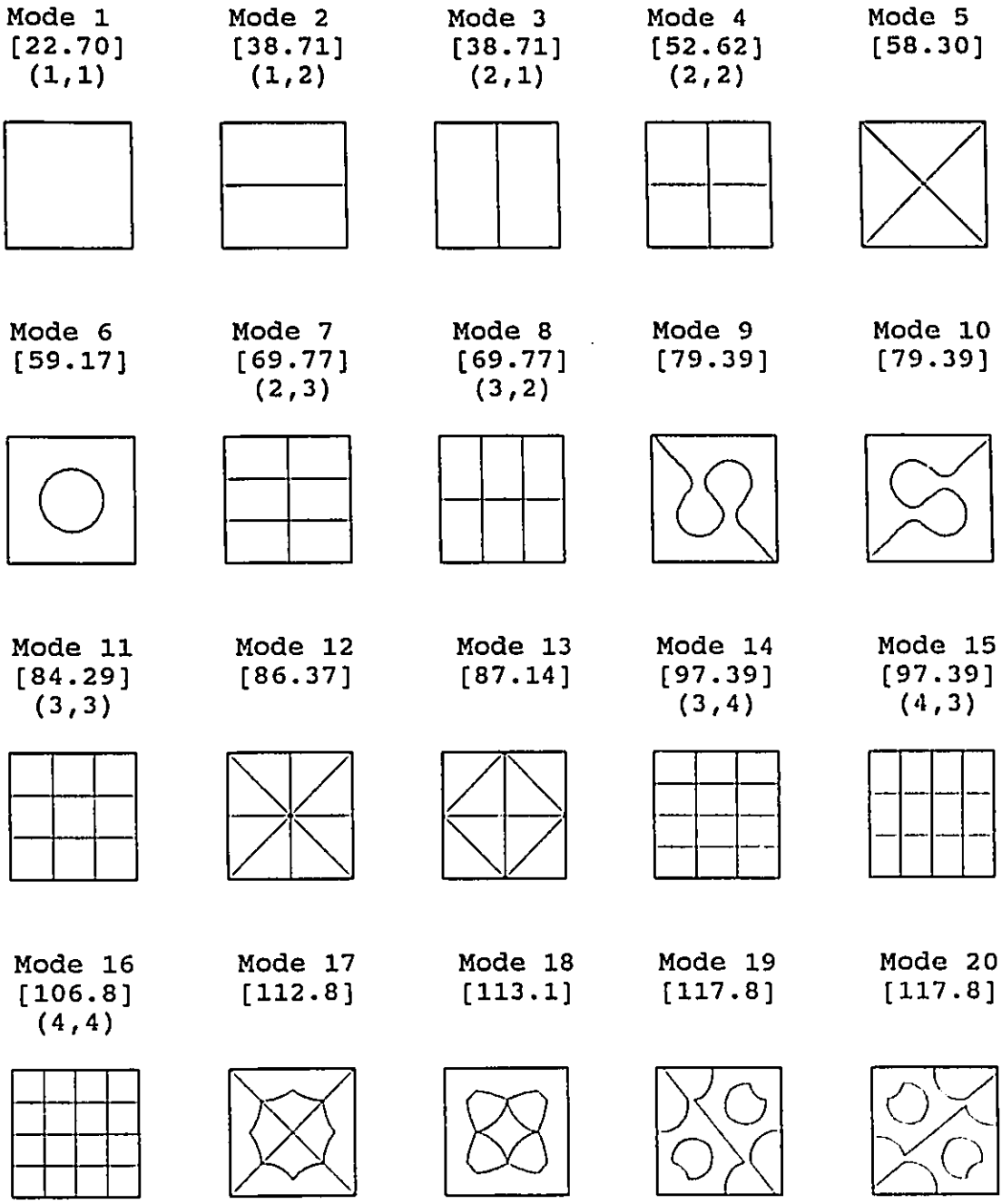

Figure 5.16 Mode shapes of a [45°/-45°/45°/-45°], BC-Clamped

The mode shapes of laminated plates differ from those of isotropic plates in the following aspects:

i) directional preference;

ii) shift of the in-plane vibration mode;

iii) variation of mode shapes.

The directional preference manifests itself when the plate exhibits more tendency to form vibration modes along a particular direction than along other directions. This becomes pronounced in the case of orthotropic plates. As shown in Figure 5.4, one notices that each of the (1,2) and the (1,3) modes has frequency lower than the (2,1) mode. In contrast, an isotropic plate, as shown in Figure 5.2, has the same frequency for both the (2,1) and the (1,2) modes. The degree of directional preference is influenced by the lamination of the plate. A four-layer [0°/90°/90°/0°] plate as shown in Figure 5.6 exhibits less degree of directional preference than an orthotropic plate, while a four-layer [0°/90°/0°/90°] plate as shown in Figure 5.8 does not exhibit directional preference. This can be explained by comparing the structural properties, the boundary conditions, and the dimensions of the plate in the x and y directions. If all remain unchanged when x is exchanged with y, the plate will not show directional preference as shown in the case of a [0°/90°/0°/90°] plate. This indicates that it is also possible to obtain mode shapes for laminated plates without directional preference. In this case, there may exist two possible mode shapes for the same frequency.

In addition to the transverse vibration modes, three in-plane vibration modes for the four-layer [45°/-45°/45°/-45°] plate were obtained as shown in Figure 5.10. These in-plane vibrations are reported here in Table 5.1 for the first time. While the first in-plane vibration mode is the seventh fundamental frequency, $\tilde{\omega}$ = 32.94, for the isotropic plate shown in Figure 5.2, it shifts to be the fourth, $\tilde{\omega}$ = 31.45, for the orthotropic plate shown in Figure 5.4, and to be the second, $\tilde{\omega}$ = 34.57, for the [45°/-45°/45°/-45°] plate shown in Figure 5.10.

The fundamental frequencies of the in-plane vibration modes for the above three cases are almost equal. The change of the order of the in-plane vibration modes relative to the other modes is mainly due to the remarkable shifts of some bending modes. For instance, the nondimensional fundamental frequency corresponding to the (1,2) mode of the isotropic plate is 13.87 as shown in Figure 5.2, while for the four-layer [45°/-45°/45°/-45°] plate this frequency shifts to a much higher value of 35.02 as shown in Figure 5.10. As a result, the first in-plane vibration becomes a low vibration mode which is associated with the second natural frequency of the laminated plate. Since the first in-plane vibration mode of a laminated plate may often shift to a relative low order, it is important for the structural designer to evaluate both the in-plane and the bending vibration modes.

The mode shapes of a laminated plate are influenced by the lamination of the plate. This is demonstrated in Figure 5.17, which shows the contours of the first mode of a four-layer $[\theta/-\theta/]_s$, free-free rectangular plate. The intersections between shaded and unshaded areas form the nodal lines. The mode shape varies with the lamination angle θ for this symmetric angle-ply plate. In this particular case, each mode shape contains a two fold symmetry; the axis of the symmetry rotates from the horizontal direction as lamination angle θ increases. This can be a useful property for structure designers to control the dynamic property of a system.

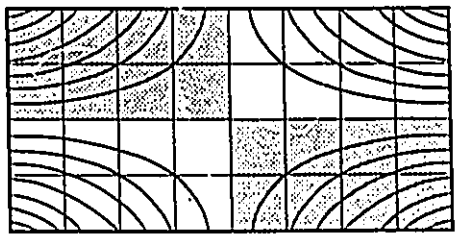

(a) θ = 0°, $\bar{\omega}$ = 9.278

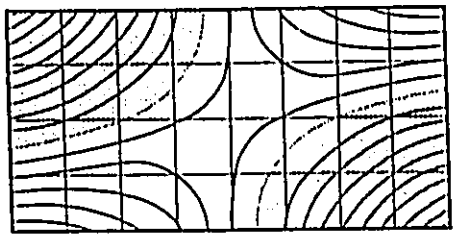

(b) θ = 15°, $\bar{\omega}$ = 13.77

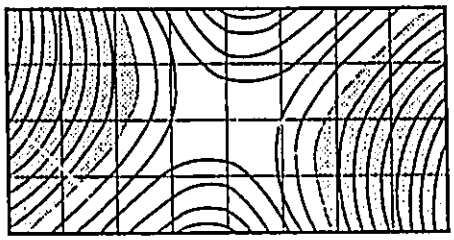

(c) θ = 30°, $\bar{\omega}$ = 14.35

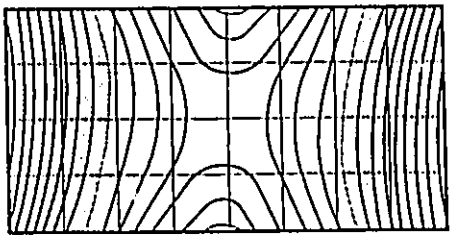

(d) θ = 45°, $\bar{\omega}$ = 9.481

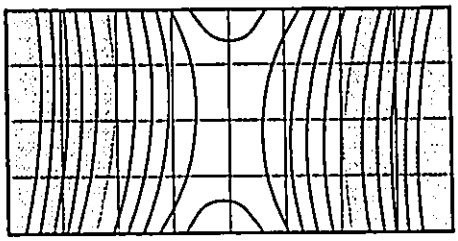

(e) θ = 60°, $\bar{\omega}$ = 7.081

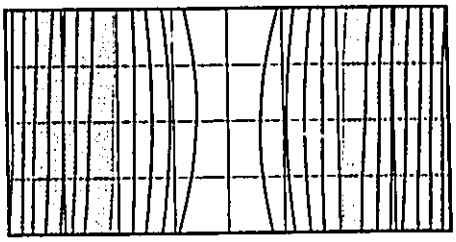

(f) θ = 75°, $\bar{\omega}$ = 6.369

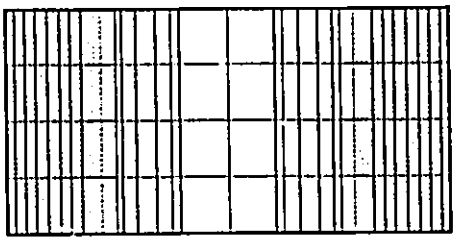

(g) θ = 90°, $\bar{\omega}$ = 6.260

a/b =2

a/h =10

BC-Free

Material 1

Figure 5.17 Contours of a 4-layer $[\theta/-\theta]_s$ free-free rectangular plate of the first mode

5.2 Damped free vibrations

In this section, the available published results are used to assess, compare and evaluate the modelling methods on polymer-matrix and metal-matrix composite materials. Finally, the parametric studies are conducted on modal frequency and damping for the laminated plates.

5.2.1 Application of damping models to polymer-matrix composites

The data of polymer-matrix composite plates, which are used in the present investigation, are listed in Table 5.2. The data for Plates 761 and 734 are mainly taken from the paper by Lin, *et al.* (1984) and Ni and Adams (1984 a). Both plates were made of glass fibre in epoxy resin matrix. We have assumed $G_{TT} = G_{LT}/2$ in the present simulation, since the value of G_{TT} was not reported by Lin or Ni. It is noted that the final results are only changed by less than 4% when G_{TT} is set equal to G_{LT}. The fact that the final results are found to be insensitive to the value of G_{TT} is due to the condition a/h > 100 for thin plates which is satisfied in the present simulation. In this case the transverse strain energy constitutes a very small portion of the total strain energy of the plates.

The data for Plates GFRP, glass fibre, and CFRP, carbon fibre, are based on Alam and Asnani's paper(1986). They did not provide the dimensions of the plates. Instead, they gave the dimensional ratios:

$$a/b = 4, \quad \text{and} \quad a/h = 150.$$

Altering a, b, and h, while keeping their ratios unchanged, it was found that the fundamental frequencies were changed but the modal damping remained unchanged. Therefore, the comparison will be confined only to modal damping.

Both of the VED and the SDC damping models are employed in the present simulation. The Modified MSE method proposed in Chapter 4 has been applied to solve the modal damping in the VED model. Tables 5.3 and 5.4 list the natural frequencies and damping of an orthotropic $[0°]_8$ plate and an eight-layer $[0°/90°]_{2s}$ plate, respectively. These results are compared with both the experimental results and the predictions from Lin *et al.* (1984) who used an unsymmetric damping matrix in the SDC model while the symmetric damping matrix developed in Chapter 3 was used in the present simulation. Despite this difference, both approaches gave predictions that are in reasonable agreement with the experimental results. Comparing the results obtained by using the VED and the SDC models in Tables 5.3 and 5.4, it was found that the difference between the two models is insignificant. This indicates that both modelling methods will yield close results if the system is lightly damped.

Table 5.2 The data of polymer-based composite plates the

Plate Number	Plate 761	Plate 734	Plate GFRP	Plate CFRP
Stacking Sequence	$[0°]_8$	$[0°/90°]_{2s}$	$[\theta/-\theta/\theta/-\theta]$	$[\theta/-\theta/\theta/-\theta]$
Boundary Conditions	BC-Free	BC-Free	BC-S2	BC-S2
a (mm)	182.75	227.0	1500	1500
b (mm)	182.75	270.0	375	375
h (mm)	1.64	2.05	10.0	10.0
E_L (GPa)	42.62	34.49	55.0	211.0
E_T (GPa)	12.50	9.40	18.3	5.3
G_{LT}(GPa)	5.71	4.49	9.10	2.60
G_{TT}(GPa)	2.855	2.245	4.55	1.30
μ_{LT}	0.30	0.30	0.25	0.25
ρ (kg/m^3)	1971.0	1813.9	1993.0	1524.0
ψ_L (%)	0.87	0.87	0.0	0.0
ψ_T (%)	5.05	4.75	50.0	50.0
$\psi_{G_{LT}}$ (%)	6.91	6.13	50.0	50.0
$\psi_{G_{TT}}$ (%)	6.91	6.13	50.0	50.0
$\psi_{\mu_{LT}}$ (%)	0.0	0.0	0.0	0.0

Table 5.3 Comparisons of natural frequencies and damping of an orthotropic $[0°]_8$ square plate.

	Mode Number	1	2	3	4	5	6
Frequency (Hz)	Exp.(Lin)	78.1	131.2	211.5	246.0	287.1	362.6
	SDC (Lin)	88.08	130.7	222.2	246.1	297.8	374.4
	SDC(Present)	87.86	127.4	218.2	238.2	292.3	364.3
	VED(Present)	88.09	127.7	218.7	238.2	292.6	365.0
Damping (%)	Exp.(Lin)	6.0	4.8	5.8	1.3	2.8	4.0
	SDC (Lin)	5.99	4.44	5.40	0.93	2.80	4.34
	SDC(Present)	6.73	5.19	6.11	0.93	3.15	4.95
	VED(Present)	6.75	5.03	6.14	1.01	3.04	5.09

Notes: NPI = 0.615,
DLI = 0.042, (on the first twelve modes).
FSI = 0.089, (on the first seven modes).

Table 5.4 Comparisons of natural frequencies and damping of a 8-layer $[0°/90°]_{2s}$ square plate.

	Mode Number	1	2	3	4	5	6
Frequency (Hz)	Exp.(Lin)	62.2	131.4	159.2	180.5	200.1	326.7
	SDC (Lin)	66.42	131.6	164.5	189.8	208.9	347.2
	SDC(Present)	66.29	126.2	159.9	183.7	205.9	336.7
	VED(Present)	66.43	126.3	160.0	184.0	206.1	337.2
Damping (%)	Exp.(Lin)	6.7	2.8	1.9	4.9	3.2	5.8
	SDC (Lin)	7.16	2.47	1.62	4.87	3.73	5.09
	SDC(Present)	5.91	2.39	1.31	4.17	3.20	4.26
	VED(Present)	5.93	2.22	1.49	4.21	3.22	4.38

Notes: NPI = 0.324,
DLI = 0.026, (on the first twelve modes),
FSI = 0.068, (on the first seven modes).

Tables 5.5 and 5.6 show the modal damping associated with the first fundamental frequency of four-layer angle-ply $[\theta/-\theta/\theta/-\theta]$ plates. This investigation is performed because the material damping of those plates is high as noted in Table 5.2. These values are not based on a true material. They were selected by Alam and Asnani (1986) to determine the damping effectiveness of the layer plates for various fibre orientations. The results of the present simulation are compared with the solutions of Alam and Asnani. The modal damping of the layered plates, with respect to the fibre orientations, was computed using the present finite element method and was found to be consistent with the results given by Alam and Asnani. The maximum modal damping is obtained for $\theta = 0°$, *i e.*, when the plate is completely orthotropic.

5.2.2. Application of damping models to metal-matrix composites

In this section the newly developed damping models are tested for metal-matrix composites. Kinra *et al.* (1991, a) studied experimentally the dynamic behaviour of a cantilever beam made of P55Gr/6061Al, graphite fibre/aluminum matrix composite. The mechanical properties of a unidirectional lamina of the beam were given by:

Table 5.5 Comparison of modal damping ψ (%) of a $[\theta/-\theta/\theta/-\theta]$ rectangular (GFRP) plate at the first mode.

	Angle θ	0°	15°	30°	45°	60°	75°	90°
GFRP	VED (Alam)	48.2	44.2	33.4	20.3	9.95	4.03	2.16
	VED(Present)	50.7	47.5	37.9	25.1	13.9	6.48	3.66
	SDC(Present)	48.2	44.4	34.1	21.6	11.3	4.77	2.20
	NPI	.075	.112	.222	.335	.501	.676	.742
	DLI	.422	.348	.271	.208	.184	.191	.200
	FSI	.208	.205	.210	.197	.157	.115	.101

Note: The DLI is calculated on the first twelve modes, and the FSI is on the first two modes.

Table 5.6 Comparison of modal damping ψ (%) of a $[\theta/-\theta/\theta/-\theta]$ rectangular (CFRP) plate at the first mode.

	Angle θ	0°	15°	30°	45°	60°	75°	90°
CFRP	VED (Alam)	42.9	23.1	8.15	3.43	2.20	2.12	2.20
	VED(Present)	44.2	25.7	10.3	4.86	3.33	4.93	2.87
	SDC(Present)	42.9	24.6	9.67	4.49	3.17	4.81	2.86
	NPI	.638	.757	.864	.874	.922	.977	.991
	DLI	.348	.220	.108	.079	.086	.106	.219
	FSI	.611	.651	.521	.281	.097	.006	.007

Note: The DLI is calculated on the first twelve modes, and the FSI is on the first two modes.

E_L = 158.4 GPa, ψ_L = 0.0040,

E_T = 36.5 GPa, ψ_T = 0.0155,

G_{LT} = 16.2 GPa, $\psi_{G_{LT}}$ = 0.032,

μ_{LT} = 0.33, ρ = 2.43 kg/m^3.

Kinra *et al.* applied the Classical Laminated Plate Theory (**CLPT**), and the SDC damping model to predict the flexural damping of the beam. In that analytical solution, the mechanical quantities G_{TT} and $\psi_{G_{TT}}$ were neglected and hence their values were not reported by Kinra. In the present simulation using finite element analysis, we assumed $G_{TT} = G_{LT}/2$, $\psi_{G_{TT}} = \psi_{G_{LT}}$, and $\psi_{\mu_{LT}} = 0$.

The geometries of each specimen, *i e.*, the length (l), width (w) and height (h), in the experiments of Kinra *et al.* (1991, a) were given by:

l = 13.03 - 15.47 cm,

w = 0.955 - 1.217 cm,

h = 0.203 - 0.211 cm.

However, the geometry of the beam was not specified by Kinra *et al.* in their predictions. We assigned the following data for the present analysis:

l = 14 cm,

w = 1.2 cm,

h = 0.21 cm.

As will be shown later, these data are adequate and valid for the comparison.

In the present finite element analysis, the 9-node plate elements and 14×1 mesh configurations were used for the analysis of the four-layer $[\theta/-\theta/-\theta/\theta]$ beam. The numerical studies showed that if we double the thickness of the beam the modal damping changes only very little, *i e.*, < 2%. This is mainly because the beam is long, l/h > 60, and has low anisotropic ratio, *i e.*, $E_L/E_T < 5$. The results indicate that the geometry we used is appropriate for the comparison.

Table 5.7 lists the flexural damping of the first mode which is associated with various ply-angles for the beam predicted by the present SDC and VED models, together with the experimental and theoretical results from Kinra *et al.* (1991, a). These results are also shown in Figure 5.18. As can be seen from the Table and the Figure, there is a good agreement between the present results and Kinra's results. Both the SDC and the VED models applied here give close predictions because of the small damping present in the structure. The maximum modal damping is observed at $\theta \approx 48°$, while the minimum damping is obtained when the fibres in the beam are unidirectional and along the longitudinal direction of the beam, *i e.*, $\theta = 0°$. The natural frequencies of the first mode were found to vary with the ply-angle θ as shown in Figure 5.19. This figure indicates that the natural frequency, or the stiffness, of the beam decreases as θ increases.

Table 5.7 Comparison results of modal damping ψ (%) of a $[\theta/-\theta]_s$ cantilevered beam at the first mode.

Angle θ	0°	15°	30°	45°	60°	75°	90°
Exp. (Kinra)	0.40	1.04	1.96	2.32	2.67	2.19	1.55
SDC (Kinra)	0.40	1.08	1.96	2.61	2.36	1.80	1.55
SDC (Present)	0.45	1.04	1.85	2.48	2.31	1.81	1.60
VED (Present)	0.41	1.02	1.87	2.54	2.34	1.79	1.55
NPI	.584	.502	.356	.366	.404	.491	.555
DLI	.013	.013	.017	.022	.021	.020	.020

Notes: The DLI is calculated on the first twelve modes, and FSI > 0.1 on the first two modes.

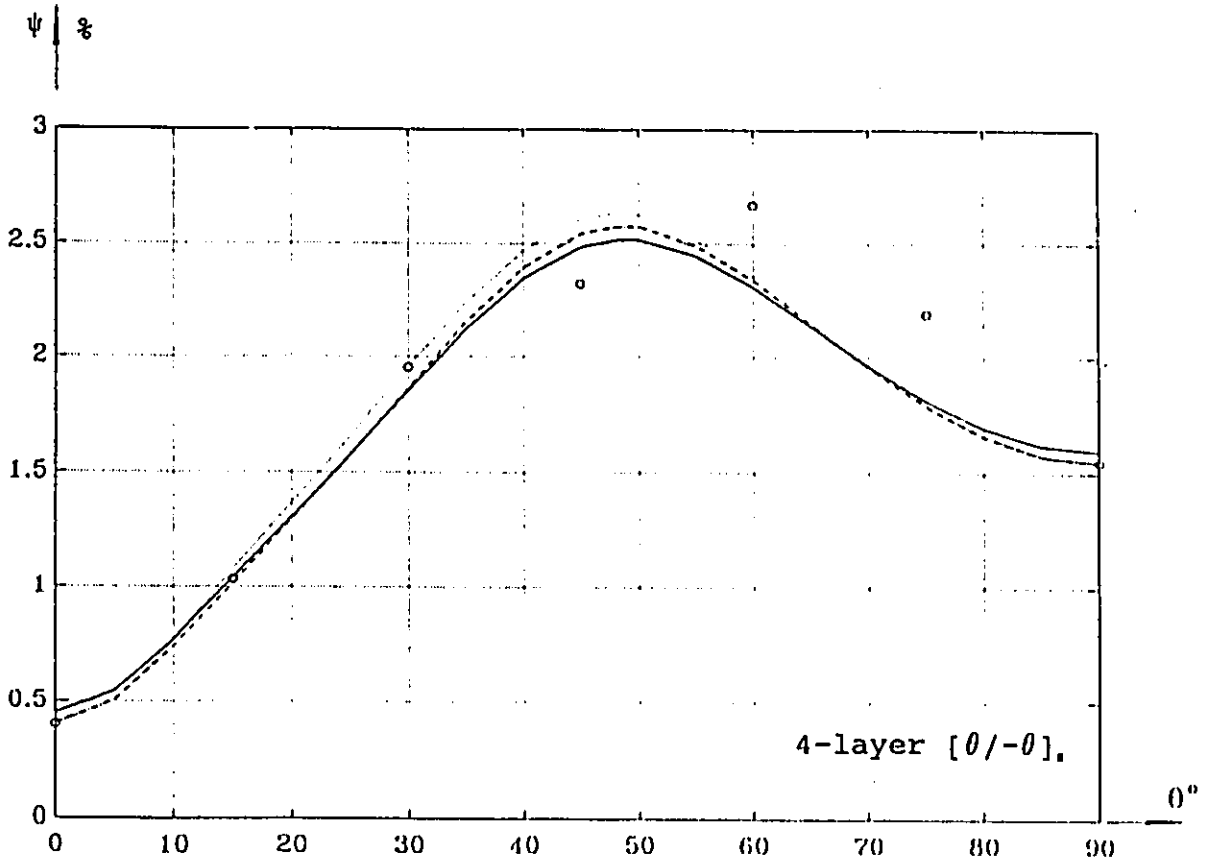

° ° Experiment (Kinra, 1991)
..... CLPT (Kinra, 1991)
——— The SDC model
—·—·— The VED model

Figure 5.18 Modal damping of the first mode vs. the ply-angle for a cantilever beam

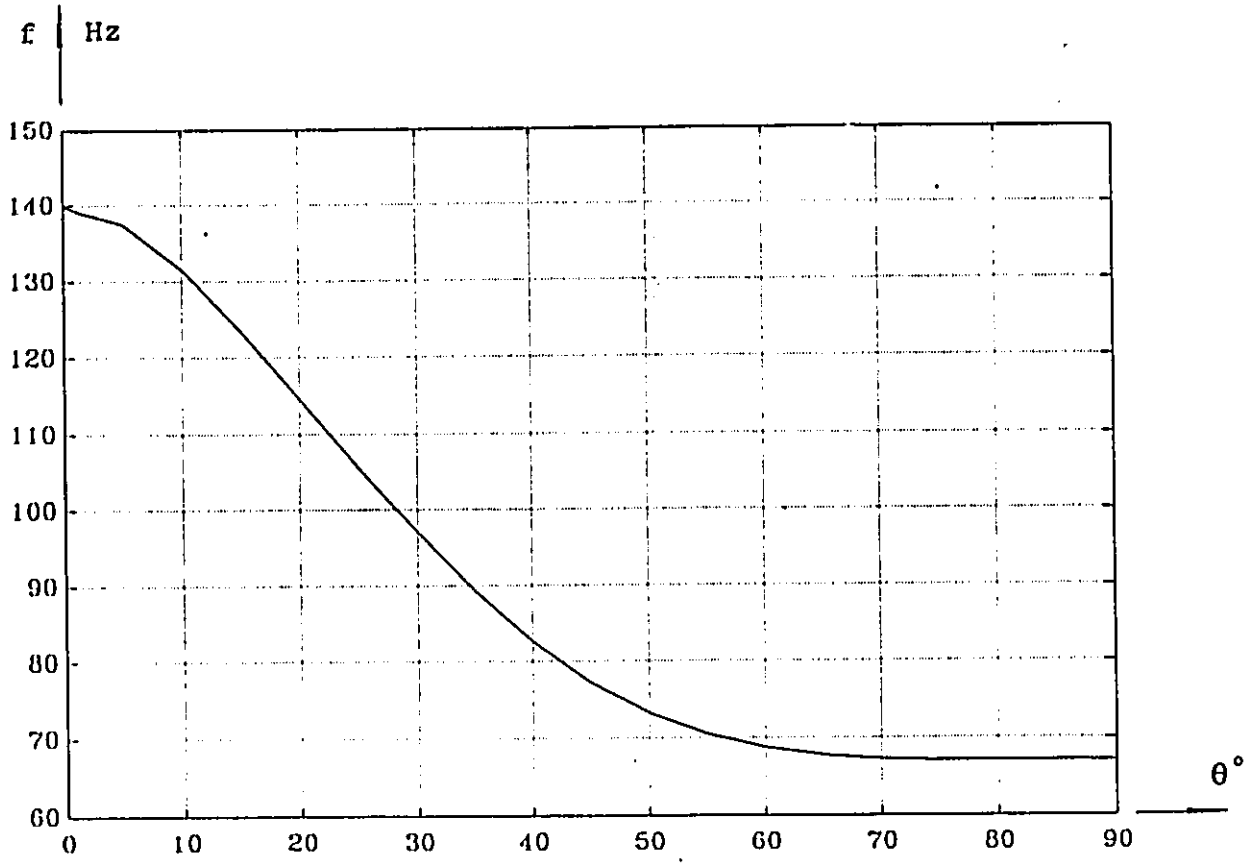

Figure 5.19 The fundamental frequency of the first mode vs. the ply-angle for a cantilever beam

5.2.3. Comments on selection of damping models

Two approaches, the SDC and the VED damping models, were used in the present study. Both models have been developed to include additional terms for the construction of the matrices in more complete forms. The experimental data available in the literature were used to test the present models for both polymer-matrix and metal-matrix composites. The damping data, however, indicate that the structures are not heavily damped, *i e.*, DLI $\leq$ 0.1. For the lightly damped systems, one can make the following conclusions:

a) There is no significant difference in the values of the natural frequencies, modal damping, and mode shapes by using the SDC model or the VED model.

b) The predictions of both modelling methods are in reasonable agreement with the experiments, showing that both methods are appropriate for the prediction of modal damping of polymer-matrix and metal-matrix composites, as long as the damping is low in the system.

It has been noted from the present numerical simulations that the differences between the results of two damping models become appreciable for heavily damped systems. Experimental data for heavily damped systems are needed to test which damping model is more appropriate under these

conditions.

In fact, light damping has been implied by the SDC model, because it utilises the mode shapes of the associated undamped system to evaluate the modal damping. There is no such restriction in the VED model. Consequently, the VED model is likely to be more appropriate in comparison with the SDC model for general applications.

5.2.4. Parametric studies

In this section parametric studies are conducted to investigate the effects on modal damping of side-to-thickness ratio, the principal moduli ratio, the total number of layers, and the angle of fibre orientation of the angle-ply plates. A square plate made of Material 1 as specified in Section 5.1 is used for this investigation. In addition to the mechanical properties introduced previously the following damping properties are assumed:

$$\psi_L = \psi_{\mu_{LT}} = 0.01, \quad \psi_T = \psi_{G_{LT}} = \psi_{G_{TT}} = 0.1 \ .$$

Figure 5.20 and 5.21 present the results of non-dimensional frequency and damping of the first mode vibration vs. the side-to-thickness ratio respectively. The non-dimensional frequency increases as the ratio a/h increases, but modal damping decreases as the ratio increases. However, they become less sensitive to a/h as it gets larger. They

approach constant values for high values of a/h, *i e.*, >50, which corresponds to a typical thin plate. It is known that the solutions using the CLPT, which can give rather good predictions for a thin plate or a long beam, are not influenced by the variation of a/h. Since the FSDT is used in the present study, the results will have better accuracy of predictions comparing to the CLPT. The CLPT solutions are likely to yield higher values for the natural frequencies, and lower values for the modal damping as shown in Figures 5.20 and 5.21. The main reason for this deviation is that the CLPT does not take into consideration the transverse shearing deformation, whose effects on both the natural frequency and the modal damping cannot be neglected for thick plates or short beams.

The ratio a/h = 10 was used in the following parametric studies as shown in Figures 5.22 to 5.27. Figures 5.22 and 5.23 show the variation of modal frequency and damping with the degree of material anisotropy. For the four-layer plates under the present investigation, selection of materials with high principal moduli ratio can be an efficient way to increase the damping of the structure.

The natural frequency and modal damping may vary as the number of layers is changed as shown in Figures 5.24 and 5.25. However, these variations tend to be insignificant as the number of layers exceeds six.

The non-dimensional frequency and damping of the first

vibration mode for different ply-angles have also been studied. The maximum damping is obtained for $\theta = 0°$ as shown in Figure 5.27, *i e.*, for the orthotropic plates; while the maximum natural frequency occurs for $\theta = 45°$. The natural frequency and damping are seen to change substantially for different boundary conditions. Figure 5.26 shows the dependence of the nondimensional frequency $\tilde{\omega}$ on the ply-angle θ for free, clamped and simply supported plates. Figure 5.27 shows the dependence of modal damping on the ply-angle for the same types of support.

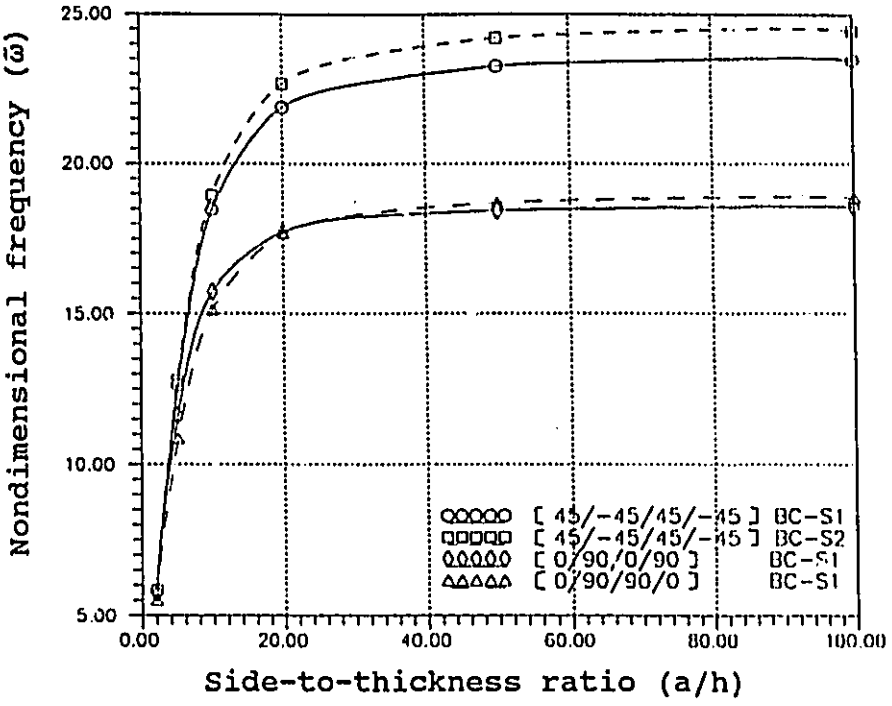

Figure 5.20 Nondimensional frequency of the first mode vs. the side-to-thickness ratio

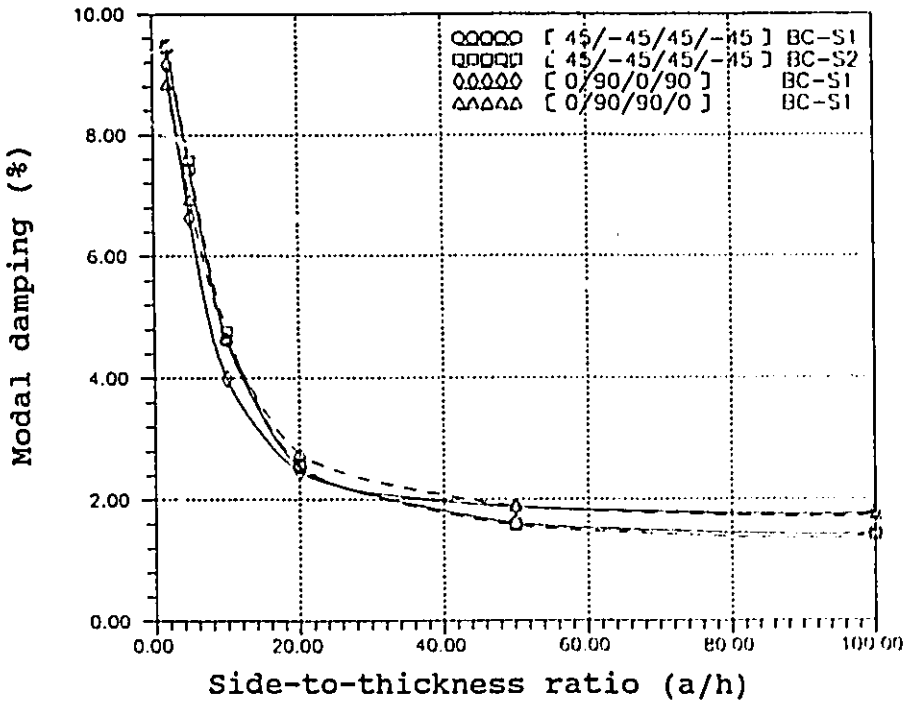

Figure 5.21 Damping of the first mode vs. the side-to-thickness ratio

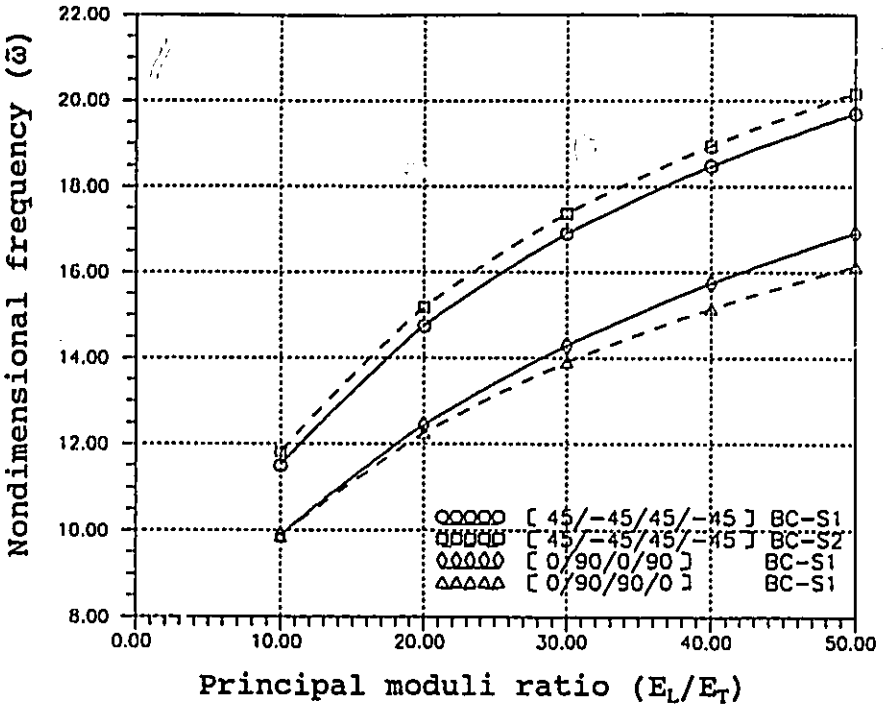

Figure 5.22 Nondimensional frequency of the first mode vs. the principal moduli ratio

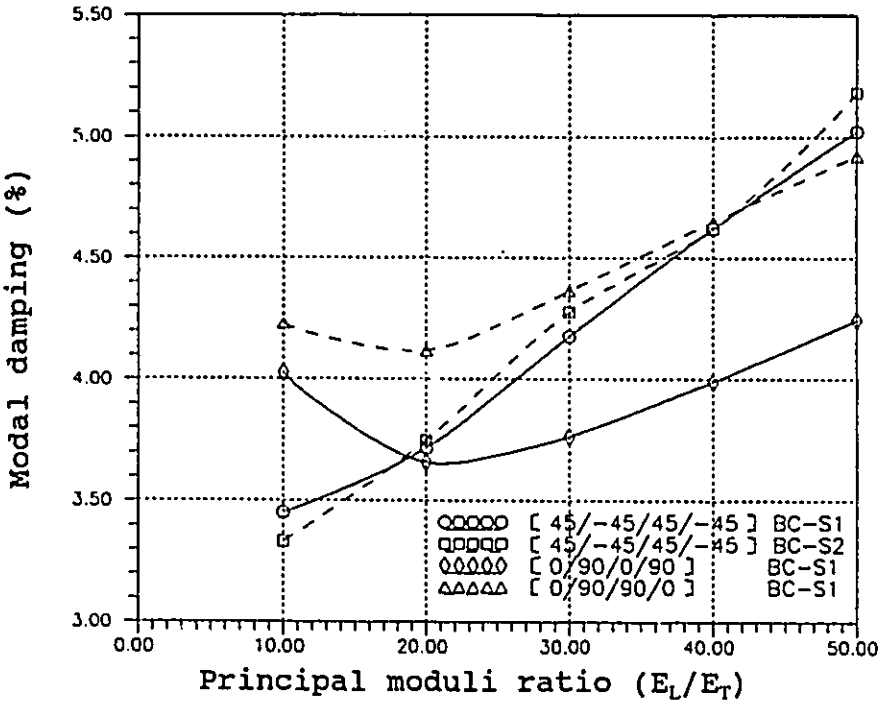

Figure 5.23 Damping of the first mode vs. the principal moduli ratio

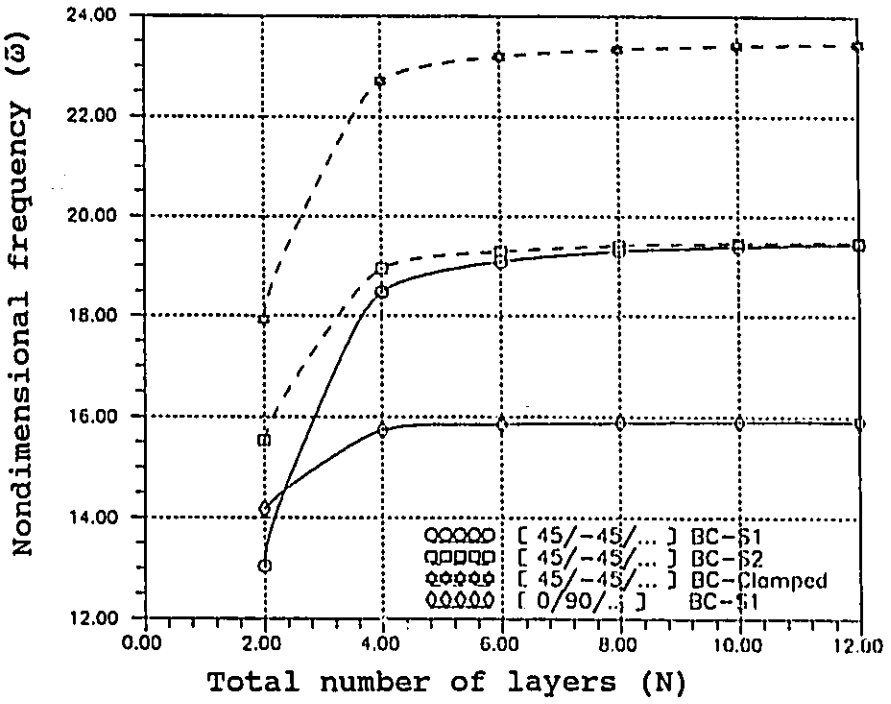

Figure 5.24 Nondimensional frequency of the first mode vs. the total number of layers

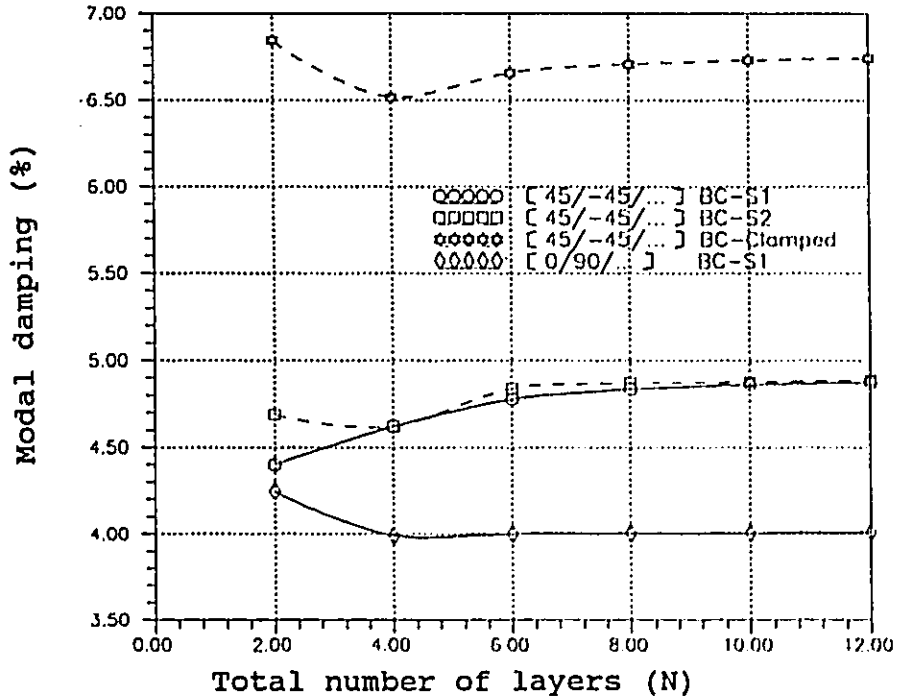

Figure 5.25 Damping of the first mode vs. the total number of layers

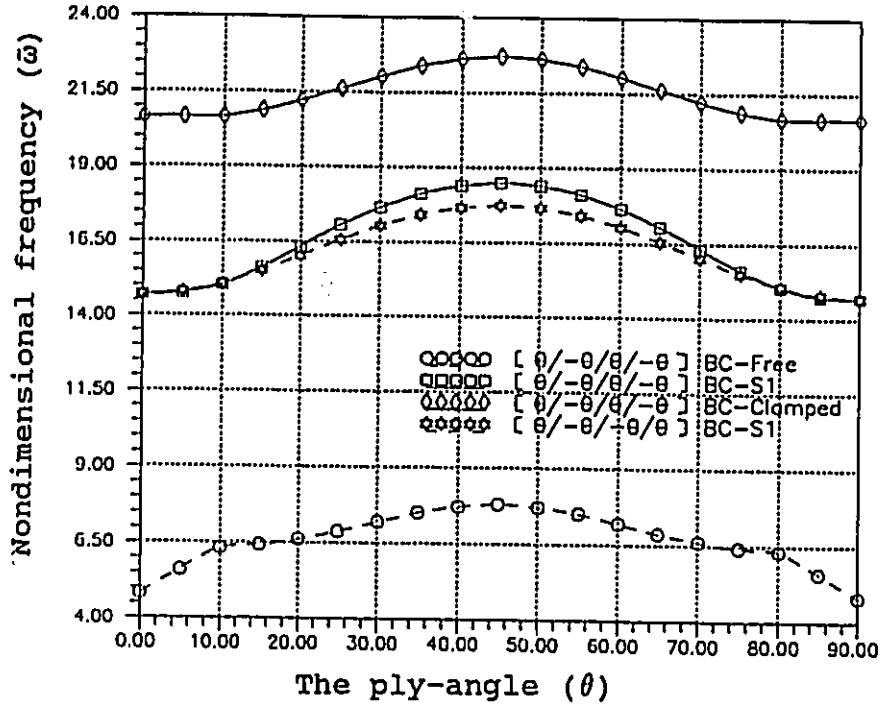

Figure 5.26 Nondimensional frequency of the first mode vs. the ply-angle

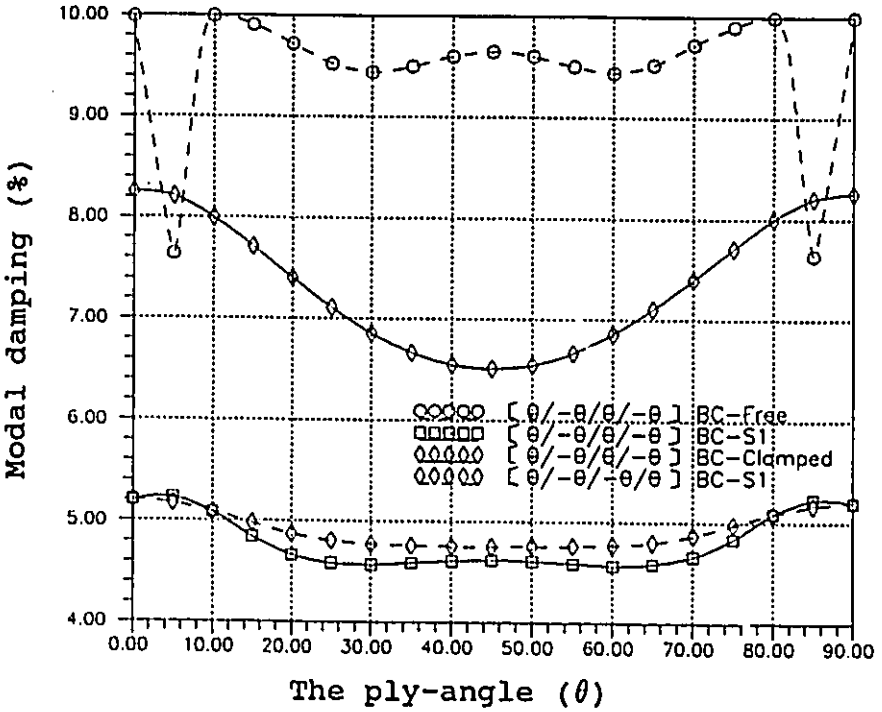

Figure 5.27 The damping of the first mode vs. the ply-angle

CHAPTER 6

SUMMARY

6.1 Summary and Conclusions

The available theories of laminated composite plates have been reviewed. Various kinematic models and solutions were compared and their advantages and disadvantages were highlighted for practical applications. The selection of a proper model is problem-dependent and quite often a compromise has to be made between solution accuracy and computational cost.

A literature review has also been presented for damped vibration analysis of layered fibre-reinforced composites. Material damping was briefly examined for two groups of composites; metal-matrix and polymer-matrix. The various mathematical treatments of damping in macromechanical analysis were described. One approach assumes viscoelasticity for the polymer-matrix composites. As a result, a complex eigenvalue problem is encountered in solving the damped free vibrations. Several methods for the solution of this problem were outlined. The shortcomings of each method were pointed out.

For laminated composite materials, material damping studies were identified in two levels. The input and output data corresponding to micromechanical and macromechanical

analyses were defined. In the present work, the damping study of composites was approached through macromechanical analysis. Two damping models, namely, the Viscoelastic Damping (**VED**) and the Specific Damping Capacity (**SDC**) models, were developed. While these two models are in principle based on the existing ideas, further development has been made in the present derivation. According to the Corresponding Principle (Schaper, 1974), the present formulations tend to provide better construction of the matrices $[K^*]$ and $[K_D]$, which describe the physical systems more completely. An important feature of the present SDC model is that the damping is described by a symmetric matrix $[K_D]$, which has the same band shape as that of the stiffness matrix [K] so that it is easily evaluated by conventional finite element techniques. In addition, since symmetry is a property for a linear system, the symmetric damping matrix $[K_D]$ is more physically justifiable than the unsymmetric one which was used in previous studies.

Because of its economical computational cost, the Modal Strain Energy (**MSE**) method is widely used for the analysis of viscoelastically damped vibrations of coated and sandwich structures. The present work is the first attempt to investigate the validity of applying this approximate method. Several indices, namely, Non-Proportionality Index (**NPI**), Damping Level Index (**DLI**), and Frequency Separation Index (**FSI**), have been proposed in order to characterize a damped system, and an Overall Error Index (**OEI**) has also been

suggested to measure the solution accuracy of the approximate method. It was shown here in the present work that a large error, *i e.*, OEI > 10%, can affect the analysis when the MSE method is applied to heavily non-proportional damping systems.

For a better evaluation of modal damping, the Modified MSE method was developed, in which the MSE method can be included as a special case. Instead of neglecting the damping stiffness matrix $[K_I]$ in the determination of the eigenvectors as was the case for the MSE method, we have considered the influence of this matrix by adding the weighted $[K_I]$ to form a real eigenvalue problem. With such a modification the estimation of the modal damping is often improved, especially when the error resulting from the use of the MSE method is exceedingly large. Though better values of the coefficient β may be possible using more sophisticated mathematical analysis, the Modified MSE method provides a positive approach to improve the approximation. It is believed that an identification of the error inherent in the MSE or the Modified MSE methods is difficult to obtain using strictly mathematical approaches. The validity and the risk of applying approximation methods can be quantized by the indices proposed in the present work.

Based on the numerical studies of multi degree-of-freedom systems, empirical rules have been obtained for the application of the Modified MSE method to the viscoelastically damped vibration analysis. If the system is lightly damped, *i*

e., DLI $\leq$ 0.02, and is associated with lightly non-proportionality, *i e.*, NPI $\leq$ 0.1, and with well spaced frequencies, *i e.*, FSI > 0.2, both the MSE and the Modified MSE methods are likely to give a good estimation of the modal damping, *i e.*, OEI(η) < 1.0 %.

Numerical studies were conducted on the damped and undamped free vibrations of laminated plates. For undamped free vibrations, fairly accurate results of the transverse vibration modes were obtained by the present routine and in-plane vibration modes were reported for the first time. Three significant aspects of the vibration of laminated plates have been described; the directional preference, the shift of the in-plane vibration modes and the variation of mode shapes. It was pointed out that the first in-plane vibration mode might shift to a very low order fundamental frequency due to the lamination of the plates.

Experimental data reported in open literature for damped free vibrations in both polymer-matrix and metal-matrix composites were used in the present finite element analysis to test and compare the damping models. The results from both the VED and SDC modelling methods are in satisfactory agreement with the experimental results. Both methods were found to be valid as long as the damping is low in the systems. Under this condition, no significant differences of natural frequencies, modal damping and mode shapes are found between the two models. Since a small damping is implied in the SDC model, the

VED model is considered to be more appropriate for more general applications though this needs to be tested by experimental data on highly damped systems.

The parametric studies conducted on the modal frequencies and damping have been reported with respect to the side-to-thickness ratio, the principal moduli ratio, the total number of layers, and the ply-angle of laminated plates.

6.2. Suggestions for future work

The present modelling methods were verified by comparing theoretical prediction with the experimental data in the literature. The selection of a particular damping model for a particular application still needs further study for heavily damped composite structures.

In this work, the emphasis was placed on the free vibration analysis to obtain the modal parameters and the mode shapes. The mode shapes in the present analysis were all expressed in real eigenvectors. It will be interesting to model the response of the system in terms of these modes. The question may arise; "Are these mode shapes still valid in predicting the responses of the laminated plates?".

The Modified Modal Strain Energy method provides a means to obtain better approximations of modal damping. The solution accuracy is dependent on the proper choice of a constant β which was obtained mainly on empirical basis. By

trying other values for β, it was found that the errors can be minimized. However, an expression of such an optimum value of β which can be applied a wide class is yet to be found.

REFERENCES

(Theories of laminated plates)

Barker, R.M., *et al.*, 1972, "Three-dimensional finite-element analysis of laminated composites", *Comput. Struct.*, **2**, pp. 1031-1029.

Bert, C.W., and Mayberry, B.L., 1969, "Free vibrations of unsymmetrically laminated anisotropic plates with clamped edges", *J. Compos. Mater.*, **3**, pp. 282-293.

Bert, C.W., and Chen, T.L., 1983, "Effect of shear deformation on vibration of antisymmetric angle-ply laminated rectangular plates", *Int. J. Solids Struct.*, **14**, pp. 456-473.

Bert, C.W., 1984, "A critical evaluation of new plate theories applied to laminated composites", *Compos. Struct.*, **2**, pp. 329-347.

Bhimaraddi, A., and Stevens, L.K., 1984, "A higher order theory for free vibration of orthotropic, homogeneous, and laminated rectangular plates", *J. Appl. Mech.*, **51**, pp. 195-198.

Chaudhuri, R.A., 1986, "An equilibrium method for prediction of transverse shear stresses in a thick laminate plate", *Comput. Struct.*, **23**, pp. 136-146.

Chow, T.S., 1971, "On the propagation of flexural waves in an orthotropic laminated plate and its response to an impulsive load", *J. Compos. Mater.*, **5**, pp. 219-221.

Craig, T.J., and Dawe, D.J., 1986, " Flexural vibration of symmetrically laminated composite rectangular plates including transverse shear effects", *Int. J. Solids Struct.*, **22**, pp. 155-169.

Dawe, D.J., Craig, T.J., 1986, "The vibration and stability of symmetrically-laminated composite rectangular plate subject to in plane stresses", *Compos. Struct.*, **5**, pp. 281-307.

Di Sciuva, M., 1986, "Bending, vibration and buckling of simply supported thick multilayered orthotropic plates: an evaluation of a new displacement model", *J. Sound Vib.*, **105**, pp. 425-442.

Engblom, J.J., and Ochoa, O.O., 1986, "Finite element formulation including interlaminar stress calculations", *Comput. Struct.*, **23**, pp. 241-249.

Fan, J., and Ye, J., 1989, "Exact solutions of axisymmetric vibration for laminated circular plates", *ASCE J. Eng. Mech.*, **116**, pp. 920-927.

Hinton, E., 1977, "Flexure of composite laminates using the thick finite stripe method", *Comput. Struct.*, **7**, pp. 217-220.

Hoa, S.V., *et al.*, 1985, "Analysis of filament wound vessel using finite elements", *Compos. Struct.*, **3**, pp. 1-18.

Hughes, T.J.R., *et al.*, 1978, "Reduced and selective integration techniques in finite element analysis of plates", *Nuclear Eng. Design*, **46**, pp. 203-222.

Jones, *et al.*, 1984, "Analysis of multi-layer laminates using three-dimensional super-elements", *Int. J. Numer. Mech. Eng.*, **20**, pp. 583-587.

Kamal, K., Durvasula, S. 1986 a, "Some studies on free vibration of composite laminates", *Compos. Struct.*, **5**, pp. 177-202.

Kamal, K., and Durvasula, S., 1986 b, "Macromechanical behaviour of composite laminates", *Compos. Struct.*, **5**, pp. 309-318.

Kant, T, *et al.*, 1988, "Finite element transient dynamic analysis of isotropic and fibre reinforced composite plates using a higher-order theory", *Compos. Struct.*, **9**, pp. 319-342.

Kant, T., and Mallikarjuna, T.K., 1989, "A higher-order theory for free vibration of unsymmetrically laminated composite and sandwich plates - Finite element evaluations", *Comput. Struct.*, **32**, pp. 1125-1132.

Krishna Murty, A.V., 1987, "Flexure of Composite Plates", *Compos. Struct.*, **7**, pp. 161-177.

Kwon, Y.W., and Akin, J.E., 1987, "Analysis of layered composite plates using a high-order deformation theory", *Comput. Struct.*, **27**, pp. 619-623.

Lajczok, M.R., 1986, "New approach in the determination of interlaminar shear stresses from the results of MSC/NASTRAN", *Comput. Struct.*, **24**, pp. 651-656.

Lo, K.H., Christensen, R.M., and Wu, E.M., 1977, "A high-order theory of plate deformation, part 1. homogeneous plates, part 2. laminated plates", *J. Appl. Mech.*, **44**, pp. 663-676.

Mallick, P.K., 1988, *Fiber-Reinforced Composites, Materials, Manufacturing, and Design*, Marcel Dekker, Inc., pp. 73.

Mau, S.T., Pian, T.H., and Tong, P., 1972, "Finite element solutions for thick plates", *J. Compos. Mater.*, **6**, pp. 304-311.

Mau, S.T., Pian, T.H., and Tong, P., 1973, "Vibration analysis of laminated plates and shells by a hybrid stress element", *AIAA J.*, **11**, pp. 1450-1452.

Mau, S.T., 1973, "A refined laminated plate theory", *J. Appl. Mech.*, **40**, pp. 606-607.

Mawenya, A.S., Davies, J.D., 1974, "Finite element bending analysis of multilayer plates", *Int. J. Numer. Methods Eng.*, **8**, pp. 215-225.

Mindlin, R.D., 1951, "Influence of rotatory inertia and shear on flexural motions of isotropic, elastic plates", *J. Appl. Mech.*, **18**, pp. 31-38.

Murakami, H., 1986, "Laminated composite plate theory with improved in-plane responses", *J. Appl. Mech.*, **53**, pp. 661-666.

Noor, A.K., 1975, "Stability of multilayered composite plates", *Fibre Sci. Tech.*, **8**, pp. 81-89.

Noor, A.K., Burton, W.S., 1989 a, "Stress and free vibration analyses of multilayered composite plates", *Compos. Struct.*, **11**, pp. 183-204.

Noor, A.K., Burton, W.S., 1989 b, "Assessment of shear deformation theories for multilayered composite plates", *Appl. Mech. Rev.*, **42**, pp. 1-12.

Owen, D.R.J., Li, Z.H., 1987 a, "A refined analysis of laminated plates by finite element displacement methods - I. Fundamentals of static analysis", *Comput. Struct.*, **26**, pp. 907-914.

Owen, D.R.J., Li, Z.H., 1987 b, "A refined analysis of laminated plates by finite element displacement methods - II. Vibration and stability", *Comput. Struct.*, **26**, pp. 915-923.

Pagano, N.J., 1969, "Exact solutions for composite laminates in cylindrical bending", *J. Compos. Mater.*, **3**, pp. 398-411.

Pagano, N.J., 1970, "Exact solutions for rectangular bidirectional composites and sandwich plates", *J. Compos. Mater.*, **4**, pp. 20-34.

Panda, S.C., Natarajan, R., 1976, "Finite element analysis of laminated shells of revolution", *Comput. Struct.*, **6**, pp. 61-64.

Panda, S.C., Natarajan, R., 1979, "Finite element analysis of laminated composite plates", *Int. J. Numer. Meth. Eng.*, **14**, pp. 69-79.

Pryor, C.W. Jr. and Barker, R.M., 1971, "A finite-element analysis including transverse shear effects for applications to laminated plates", *AIAA J.*, **9**, pp. 912-917.

Putcha, N.S., Reddy, J.N., 1986, "A refined mixed shear flexible finite element for the nonlinear analysis of laminated plates", *Comput. Struct.*, **22**, pp.529-538.

Reddy, J.N., 1979, "Free vibration of antisymmetric, angle-ply laminated plates including transverse shear deformation by the finite element method", *J. Sound Vib.*, **66**, pp. 567-576.

Reddy, J.N., 1980 , "A penalty plate-bending element for the analysis of laminated anisotropic composite plate", *Int. J. Numer. Meth. Eng.*, **15**, pp. 1187-1206.

Reddy, J.N., and Chao, W.C., 1981, "A comparison of closed-form and finite-element solutions of thick, laminated, anisotropic rectangular plates", *Nuclear Eng. Design*, **64**, pp. 153-167.

Reddy, J.N., 1984, "A simple higher-order theory for laminated composite plates", *J. Appl. Mech.*, **51**, pp. 745-752.

Reddy, J.N., 1989, "On the generalization of displacement-based laminated theories", *Appl. Mech. Rev.*, **42**, pp. S213-S222.

Reddy, J.N., 1990, "A review of refined theories of laminated composite plates", *Shock Vib. Digest*, **22**, pp. 3-17.

Reissner, E., 1945, "The effect of transverse shear deformation on the bending of elastic plates", *J. Appl. Mech.*, **12**, pp. 69-77.

Ren, J.G., and Hinton, E., 1986, "The finite element analysis of homogeneous and laminated composite plate using a simple higher order theory", *Commu. Appl. Numer. Meth.*, **2**, pp. 217-228.

Senthilnathan, N.R., *et al.*, 1988, "Vibration of laminated orthotropic plates using a simplified higher-order deformation theory", *Compos. Struct.*, **10**, pp. 211-219.

Sivakumaran, K.S., 1989, "Free vibration of annular and circular asymmetric composite laminates", *Compos. Struct.*, **11**, pp. 205-226.

Spiker, R.L., and Munir, N.I., 1980, "Comparison of hybrid-stress element through-thickness distributions corresponding to a high-order plate theory", *Comput. Struct.*, **11**, pp. 579-586.

Spiker, R.L., 1984, "An invariant eight-node hybrid-stress element for thin and thick multilayer laminated plates", *Int. J. Numer. Meth. Eng.*, **20**, pp. 573-582.

Srinivas, S., et al., 1970 a, "Bending, vibration and buckling of simply supported thick orthotropic rectangular plates and laminates", *Int. J. Solids Struct.*, **6**, pp. 1463-1481.

Srinivas, S., et al., 1970 b, "An exact analysis for vibration of simply supported homogeneous and laminated thick rectangular plates", *J. Sound Vib.*, **12**, pp.187-199.

Srinvas, S., 1973, "A refined analysis of composite laminates", *J. Sound Vib.*, **30**, pp. 495-507.

Stein, M., 1986, "Nonlinear theory for plates and shells including the effects of transverse shearing", *AIAA J.*, **24**, pp. 1537-1544.

Sun, C.T., Whitney, J.M., 1973, "Theories for the dynamic response of laminated plates", *AIAA J.*, **11**, No. 2, pp. 178-183.

Toledano, A., and Murakami, H., 1987, "A high-order laminated plate theory with improved in-plane responses", *Int. J. Solids Struct.*, **23**, pp. 111-131.

Tsay, C.S., Reddy, J.N., 1978, "Bending, stability and free vibration of thin orthotropic plates by simplified mixed finite elements", *J. Sound Vib.*, **59**, pp. 307-311.

Vinson, J.R., and Sierakowski, R.L., 1986, *The Behavior of Structures Composed of Composite Materials*, Martinus Nijhoff Publishers.

Weeton, J.W., Peters, D.M., and Thomas, K.L., 1987, *Engineers' Guide to Composite Materials*, ASME.

Whitney, J.M., and Pagano, N.J., 1970, "Shear deformation in heterogeneous anisotropic plates", *J. Appl. Mech.*, **37**, pp. 1031-1036.

Whitney, J.M., Sun, C.T., 1973, "A higher order theory for extensional motion of laminated composites", *J. Sound Vib.*, **30**, pp. 85-97.,

Whitney, J.M., 1973, "Shear correction factors for orthotropic laminates under static load", *J. Appl. Mech.*, **40**, pp. 302-304.

Whitney, J.M., 1987, *Structural Analysis of Laminated Anisotropic Plates*, Technomic Publishing Co., Inc.

Yang, Pp.C., Norris, C.H. and Stavsky, Y., 1966, "Elastic wave propagation in heterogeneous plates", *Int. J. Solids Struct.*, **2**, pp. 665-684.

Zienkiewicz, O.C., *et al.*, 1971, "Reduced integration technique in general analysis of plates and shells", *Int. J. Numer. Mech. Eng.*, **3**, pp. 275-290.

REFERENCES

(Damping of composites)

Adams, R.D., *et al.*, 1969, "The dynamic properties of unidirectional carbon and glass fiber reinforced plastics in torsion and flexure", *J. Compos. Mater.*, **3**, pp. 594-603.

Adams, R.D., 1972, "The damping characteristics of certain steels, cast irons and other metals", *J. Sound Vib.*, **23**, pp. 199-216.

Adams, R.D., and Bacon, D.G.C., 1973, "Effect of fiber orientation and laminate geometry on the dynamic properties of CFRP", *J. Compos. Mater.*, **7**, pp. 402-428.

Adams, R.D., 1987, "Damping properties analysis of composites", Reinhart, T.J., (eds.), *Engineering Materials Handbook*, Vol.1, *Composites*, ASM International, pp. 206-217.

Alam, N., and Ashani, N.T., 1986, "Vibration and damping analysis of fibre reinforced composite material plates", *J. Compos. Mater.*, **20**, pp. 3-18.

Bellos, J. and Inman, D.J., 1990, "Frequency response of nonproportionally damped, lumped parameter, linear dynamic systems", *J. Vib. Acous.*, **112**, pp. 194-200.

Bert, C.W., 1973, "Material damping: An introductory review of mathematical models, measures and experimental techniques", *J. Sound Vib.*, **29**, pp.129-153.

Bert, C.W., 1980, "Composite materials: A survey of the damping capacity of fiber reinforced composites", *Damping Applications for Vibration Control*, Torvik, P.J., (ed.), ASME, **AMD-38**, 1980.

Brockman, R.A., 1984, "On vibration damping analysis using the finite element method", *Vibration Damping 1984 Workshop Proceedings*, Rogers, L., (ed.), 1984.

Crawley, E., *et al.*, 1983, "Experimental measurement of passive material and structural damping for flexible space structures", *Acta Astronautical*, **10**, No.5-6, pp. 381-393.

Crawley, E.F., 1984, "Experimental measurement of material damping for space structures", *Vibration Damping 1984 Workshop Proceedings*, Rogers, L., (ed.), 1984.

Creama, L.B., Castellani, A., and Polcaro, V.F., 1991, "Low temperature effect on damping coefficients of aerospace materials", *Composite Material Technology - 1991-*, Hui, D., and Kozik, T.J., (eds.), 1991, ASME **PD -37**, pp. 33-36.

Deonath, N.R and Rohatgi, P.K., 1981, "Damping capacity, resistivity, thermal expansion and machinability of aluminum alloy-mica composites", *J. Mater. Sci.*, **16**, pp.3025-3032.

Gibson, R.F., Chaturvdei, S.K., and Sun, C.T., 1982, "Complex moduli of aligned discontinuous fiber-reinforced polymer composites", *J. Mater. Sci.*, **17**, pp. 3499-3509.

Golla, D.F. and Hughes, P.C., 1985, "Dynamics of viscoelastic structures - A time-domain finite element formulation", *J. Appl. Mech.*, **52**, pp. 897-906.

Goodman, L.E., 1988, "Material damping and slip damping", *Shock and Vibration Handbook, Harris*, C.M., (eds.), McGraw-Hill Book, pp. (36) 1-28.

Hashin, Z., 1970, "Complex moduli of viscoelastic composites - I. General theory and application to particulate composites", *Int. J. Solids Struc.*, **6**, pp. 539-552.

Hwang, S.J., and Gibson, R.F., 1991, "The effects of three-dimensional states of stress on damping of laminated composites", *Compos. Sci. Tech.*, **41**, pp. 379-393.

Johnson C.D., and Kienholz, D.A., 1982, "Finite element prediction of damping in structures with constrained viscoelastic layers", *AIAA J.*, **20**, pp. 1248-1290.

Jones, D.I.G., 1986, "The impulse response function of a damped single degree of freedom system", *J. Sound Vib.*, **106**, pp. 353-356.

Joseph, J.A., (ed.), 1974, *MSC/NASTRAN Applications Manual*, Vol., Sec. 7.2.6.2.

Kinra, V.K., *et al.*, 1991 a, "On the influence of ply-angle on damping and modulus of elasticity of a metal-matrix composite", *Matall. Trans.*, **22 A**, pp. 645-651.

Kinra, V.K., *et al.*, 1991 b, "Damping in metal-matrix composites: Theory and experiment", *Composite Material Technology -1991-*, Hui, D., and Kozik, T.J., (eds.), 1991, ASME, **PD-37**, pp. 25-31.

Lazan, B.J., 1959, "Energy dissipation mechanisms in structures, with particular reference to material damping", *Structural Damping*, Ruzicka, J.E., (ed.), ASME, 1959.

Lazan, B.J., 1965, "Damping studies in materials science and materials engineering", *Internal Friction, Damping, and Cyclic Plasticity*, ASTM, pp. 1-20.

Lee, H.J., 1987, *Determination of the complex modulus of a solid propellant and random vibration analysis of layered viscoelastic cylinders with finite element*, Ph.D. these, Virginia Polytechnic Institute and State University.

Lesieutre, G.A., *et al.*, 1991, "Improved composite material damping using high damping graphite fibers", *Composite Material Technology - 1991*, Hui, D., and Kozik, T.J., (eds.), ASME, **PD-37**, pp. 21-24.

Liao, D.X., Sung, C.K., and Thompson, B.S., 1986, "The optimal design of symmetric laminated beams considering damping", *J. Compos. Mater.*, **20**, pp. 485-501.

Lin, D.X., Ni, R.G., and Adams, R.D., 1984, "Prediction and measurement of the vibrational damping parameters of carbon and glass fibre-reinforced plastics plates", *J. Compos. Mater.*, **18**, pp. 132-152.

Maymon, G., *et al.*, 1977, "Influence of moisture absorption /elevated temperature on the dynamic behaviour of resin matrix composites: Preliminary results", *Advanced Composite Materials - Environmental Effects*, Vinson, J.R., (ed.), ASTM, STP 658, pp. 221-233.

McLean, D., and Read, B.W., 1975, "Storage and loss moduli in discontinuous composites", *J. Mater. Sci.*, **10**, pp.481-492.

Morison, W.D., 1982, "The prediction of material damping of laminated composites", *Can. Aeronaut Space J.*, **28**, pp. 72-382.

Nashif, A.D., Jones, D.I.G., and Henderson, J.P, 1985, *Vibration Damping*, John Wiley & Sons, Inc.

Nelson, D.J. and Hancock, J.W., 1979, "Interfacial slip and damping in fibre reinforced composites", *J. Mater. Sci.*, **13**, pp. 2429-2440.

Ni, R.G., and Adams, R.D., 1984 a, "The damping and dynamic moduli of symmetric laminated composite beams - Theory and experimental results", *J. Compos. Mater.*, **18**, pp. 104-121.

Ni, R.G., and Adams, R.D., 1984 b, "A rational method for obtaining the dynamic mechanical properties of lamina for predicting the stiffness and damping of laminated plates and beams", *Compos.*, **15**, pp. 193-199.

Prater, G. Jr., and Singh, R., 1986, "Quantification of the extent of non-proportional viscous damping in discrete vibratory systems", *J. Sound Vib.*, **104**, pp. 109-125.

Rawal, S.P., Misra, M.S. and Rath, B.B., 1985, "Introduction: material damping-How to define it?", *Role of Interfaces on Material Damping*, Rath, B.B. and Misra, M.S., (eds.), pp. 1-4.

Rehfield, L.W. and Briley, R.P., 1978, "A comparison of environmental effects of dynamic behaviour of graphite/epoxy composites with aluminum alloys", ASME paper 78-WA/Aero-10.

Roylance, D. and Roylance, M., 1976, "Influence of outdoor weathering on dynamic mechanical properties of glass/epoxy laminate", *Environmental Effects on Advanced Composite Materials*, ASTM, STP 602.

Schapery, R.A., 1974, "Stress analysis of viscoelastic composite materials", *Mechanics of Composite Materials*, **2**, Sendeckyj, G.P. (ed.), pp. 85-168.

Shen, S., and Stevens, K.K., 1984, "A perturbation method for analysis of free-layer damping treatments", *Vibration Damping 1984 Workshop Proceedings*, Rogers, L., (ed.), 1984, IDC 1-16.

Singh, S.S., Rohatgi, P.K., and Keshavram, B.N., 1991, "Vibrational damping behavior of composite materials", *Composite Material Technology - 1991-*, Hui, D., and Kozik, T.J., (eds.), ASME, pp. 1-5.

Soni, M.L. and Bogner, F.K., 1982, "Finite element vibration analysis of damping structures", *AIAA J.*, **20**, pp. 700-707.

Sun, C.T., *et al.*, 1985, a, "Internal material damping of

polymer matrix composites under-axis loading", *J. Mater. Sci.*, **20**, pp. 2575-2685.

Sun, C.T., *et al.*, 1985, b, "Internal damping of short-fiber reinforced polymer matrix composites", *Comput. Struct.*, **20**, pp. 391-401.

Sun, C.T., *et al.*, 1987, "Prediction of material damping of laminated polymer matrix composites", *J. Mater. Sci.*, **22**, pp. 1006-1012.

Sun, C.T., Sankar, B.V., and Rao, V.S., 1990, "Damping and vibration control of unidirectional composite laminates using add-on viscoelastic materials", *J. Sound Vib.*, **139**, pp. 277-287.

Varschavsky, A., 1972, "The matrix fatigue behavior of fibre composites subjected to repeated tensile loads", *J. Mater. Sci.*, **7**, pp. 159-167.

Weiss, H.J., 1977, "The effect of axial residual stress on the mechanical behaviour of composites", *J. Mater. Sci.*, **4**, pp. 797-909.

Wolfenden, A., and Wolla, J.M., 1991, "Dynamic mechanical properties", *Metal Matrix composites: Mechanisms and Properties*, Everett, R.K., and Arsenault, R.J., (eds.) 1991, Academic Press.

Xiao, *et al.*, 1988, "Finite element analysis of modal parameters of anisotropic laminated plates", *J. Vib., Acous., Stress, Reliability Design*, **110**, pp. 473-477.